Investigation of Low Temperature Cracking in Asphalt Pavements National Pooled Fund Study – Phase II

Task 2 Report

Prepared by:

Mihai Marasteanu
Eyoab Zegeye Teshale
Ki Hoon Moon
Mugur Turos
University of Minnesota

William Buttlar
Eshan Dave
Sarfraz Ahmed
University of Illinois

November 2010

Prepared for:

Minnesota Department of Transportation
Research Services of MS 330
395 John Ireland Boulevard
St.Paul, MN 55155

TABLE OF CONTENTS

LIST OF TABLES

LIST OF FIGURES

1. INTRODUCTION

In this task, the research team tested and analyzed nine asphalt mixtures used in field studies with respect to their low temperature cracking resistance. The tests consisted of Indirect Tensile (IDT) creep and strength tests, as well as Semi-Circular Bend (SCB) and Disc-Shaped Compact Tension (DCT) tests. The set of mixtures included Recycled Asphalt Pavement (RAP) mixtures, Poly-Phosphoric Acid (PPA) modified mixtures, and polymer modified mixtures (SBS, and Elvaloy).The mixtures are described in Table 1.

Table 1. Asphalt Mixtures used in Task 2

Location	Construction date	Binder Grade	Asphalt modifiers	RAP
MnRoad 33	September 2007	PG 58-34	PPA	-
MnRoad 34	September 2007	PG 58-34	SBS+PPA	-
MnRoad 35	September 2007	PG 58-34	SBS	-
MnRoad 77	September 2007	PG 58-34	Elvaloy+PPA	-
MnRoad 20	August 2008	PG 58-28	-	30% Non-Fractioned
MnRoad 21	August 2008	PG 58-28	-	30% Fractioned
MnRoad 22	August 2008	PG 58-34	-	30% Fractioned
Wisconsin 9.5 mm SMA	2008	PG 64-22	-	-
NYS Typical Mix	2008	PG 64-22	-	-

The experimental variables considered in the experimental work and analyses were test temperature, asphalt mixture conditioning, and mixture air voids content. Two test temperatures were selected based on the asphalt binder used, as follow:

- PGLT (abbreviated as PG)
- PGLT+ 10°C (abbreviated as PG+10)

where PGLT is the binder PG low temperature limit.

Two levels of air voids were considered in the preparation of laboratory cylinders from the loose mix collected at the job sites: 4% and 7%, which represent the design air voids and typical field compaction levels, respectively. The asphalt mixture samples with 7% air voids were also long term aged according to AASHTO R30-02 (1). Note that for the NY's mixture, it was not possible to compact specimens to achieve 4% air voids.

In summer of 2010, cores were also obtained from the MnRoad sites described in Table 1, and tested following the same methods used for the loose mix laboratory prepared specimens. At the time of this report, the cores from Wisconsin and New York have not been delivered to the UMN laboratory. Table 2 describes the experimental plan pursued in Task 2, and the shadowed cells indicate the data missing from the experimental layout.

Table 2. Laboratory experimental layout

Test Device	Temp	Mix Conditioning	MN/Road Test Section				WI		NYS	
			33, 34, 35, 77		20, 21, 22					
			Air Voids, %							
			4	7	4	7	4	7	4	7
SCB	PGLT	None	xxx	xxx	xxx	xxx	xxx	xxx	xxx	xxx
	PGLT+10ºC	None	xxx	xxx	xxx	xxx	xxx	xxx	xxx	xxx
	PGLT	5 days@85ºC		xxx		xxx		xxx		xxx
	PGLT	Field cores		xxx		xxx		xxx		xxx
DC(T)	PGLT	None	xxx	xxx	xxx	xxx	xxx	xxx	xxx	xxx
	PGLT+10ºC	None	xxx	xxx	xxx	xxx	xxx	xxx	xxx	xxx
	PGLT	5 days@85ºC		xxx		xxx		xxx		xxx
	PGLT	Field cores		xxx		xxx		xxx		xxx
IDT	PGLT	None	xxx	xxx	xxx	xxx	xxx	xxx	xxx	xxx
	PGLT+10ºC	None	xxx	xxx	xxx	xxx	xxx	xxx	xxx	xxx
	PGLT	5 days@85ºC		xxx		xxx		xxx		xxx
	PGLT	Field cores		xxx		xxx		xxx		xxx

Subtask on Physical Hardening

This task also includes a subtask dealing with physical hardening effects in the asphalt binders used to prepare the mixtures in Table 1. A protocol to simplify the measurements of physical hardening and to adjust S and m values based on such protocol based on climatic condition is proposed in this subtask. In addition, glass transition measuring techniques were used to quantify the effect of isothermal storage on dimensional stability of asphalt mixtures. A separate report is provided for this work.

2. EXPERIMENTAL WORK

As stated in the introduction, two sets of material were investigated. The first set consists of laboratory prepared specimens following a statistically designed test matrix and using asphalt mixtures obtained from nine different test sections, as described in Table 1. The second set consists of field cores taken from the field sections.

Preparation of laboratory compacted asphalt mixture specimens

Approximately 200 kg of loose asphalt mixture from each source, described in Table 1, were delivered to University of Minnesota (UMN) research team. All gyratory specimens were compacted in the UMN pavement laboratory and then distributed to Illinois (UIUC) and Wisconsin (UWM) research teams. Half of the 7% air voids cylinders were conditioned for 5 days at 85℃, according to AASHTO R30-02 protocol. The IDT, SCB and DCT specimens were obtained by cutting the gyratory cylinders as shown in Figures 1, 2, and 3.

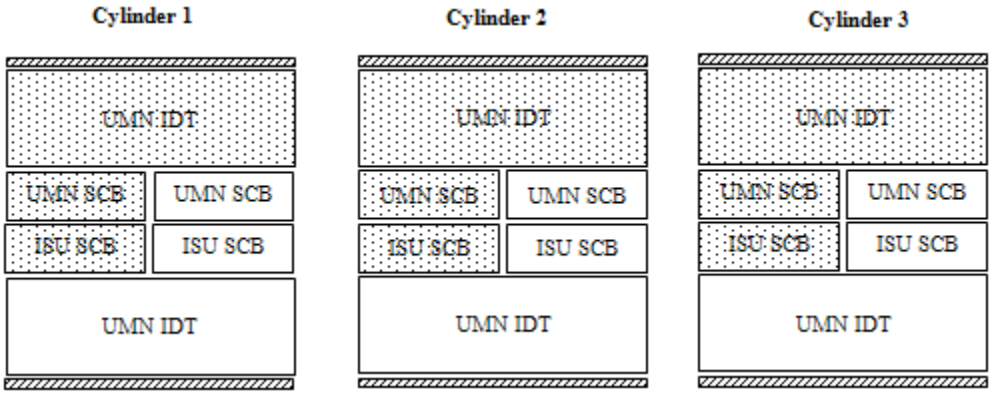

Figure 1. Non-conditioned specimens used at UMN

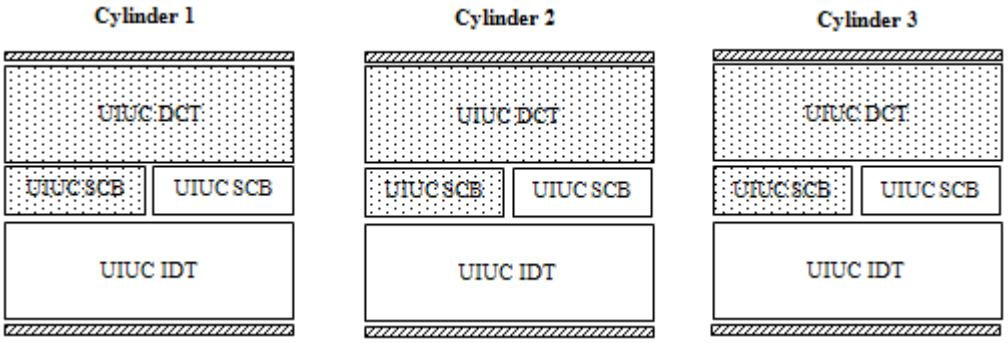

Figure 2. Non-conditioned specimens, used at UIUC

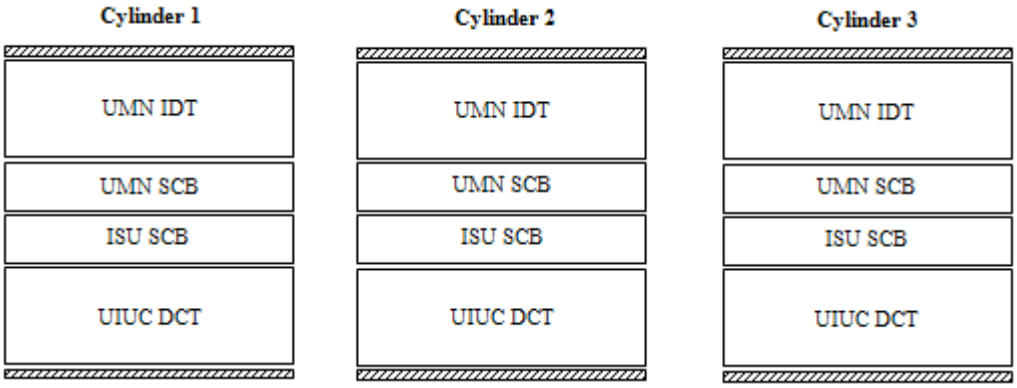

Figure 3. Conditioned specimens

The dotted surfaces in Figure 1 and Figure 2 represent the specimens tested at PGLT, while the blank surfaces represent the specimens tested at PGLT+10˚C. All conditioned specimens were tested at PGLT temperature.

For three randomly selected mixtures, a fourth cylinder was gyratory compacted and utilized to prepare DCT specimens to be tested at UMN. Similarly, three mixtures were randomly selected and utilized to prepare SCB specimens to be tested at UIUC.

Preparation of field cored asphalt mixture test samples

Field cores were taken from cells 20, 21, 22, 33, 34, 35, and 77 at the MnROAD facility. The cores were taken from MnROAD in June 2010, approximately 2 and 3 years after the constructions of the cells 33, 34, 35, 77 and cells 20, 21, and 22, respectively. Eleven cylindrical field cores, for each mixture, sampled from between wheel paths, approximate offset 6 ft. of the pavement test sections, were delivered to UMN. The thickness of the cores ranged from 100 mm to 150 mm (4" to 6"). The cells from which the samples were collected had several layers, but only the top layers were made of the mixtures of interest to this research study. Therefore the bottom layers were cut and discarded (see Figure 4). In addition, the upper 5 mm (0.20") was also cut and discarded (see Figure 4). The cylindrical cores were then cut into IDT, SCB, and DCT test specimens and distributed to the research teams.

Figure 4. Sample preparation for field cores

The air voids for the field cores were obtained in a previous study carried out at UMN (2); the air void content of 145 field cores, extracted from various cells at MnROAD, were

determined according AASHTO T166. The air void content for the mixtures in Task 2 are presented in Table 3.

Table 3. Air void content for field cores.

Field cores air void content		
Cell	Mean	CV
20	6.0	0%
21	5.1	2%
22	5.7	2%
33	5.3	1%
34	5.9	2%
35	6.4	2%
77	5.1	13%

Specimens identification system

The following labeling system was developed for the identification of the testes specimens:

- The first term of each label indicates the specimen geometry and the test type
- The term in second column indicates the source of the mixture
- The third term represents the air void content. As it is shown in Table 2, samples compacted at 4% air void content were tested only at one level of mix conditioning. On the other hand, samples with 7 % void content were tested at both conditioned and non conditioned levels.
- Finally, the fourth column indicates the test temperature in absolute value.

Testing Methods and Test Results

The test methods used to determine the low temperature fracture properties of the asphalt mixtures and the test results are presented in the next paragraphs.

Disc-shaped Compact Tension (DCT)

The Disc-Shaped Compact Tension test (DCT) was developed as a practical method for the determination of low-temperature fracture properties of cylindrically-shaped asphalt concrete test specimens. The DCT's advantages include easy specimen fabrication, from both field and gyratory samples, and it is a standard fracture test configuration (3; 4). The specimen configuration is shown in Figure 5. The DCT specimen are placed in a controlled chamber and conditioned for a minimum of 2 hours at the desired temperature. The test is performed under tensile loading and the crack mouth opening displacement (CMOD) is measured with a clip-on gage at the face of the crack mouth. After temperature conditioning, the specimens are inserted in loading fixtures, subjected to a preload, no greater than 0.2 kN, and then tested with a constant CMOD of 1mm/min (0.017 mm/s or 0.00067 in/s). The test is completed when the post peak level has reduced to 0.1 kN.

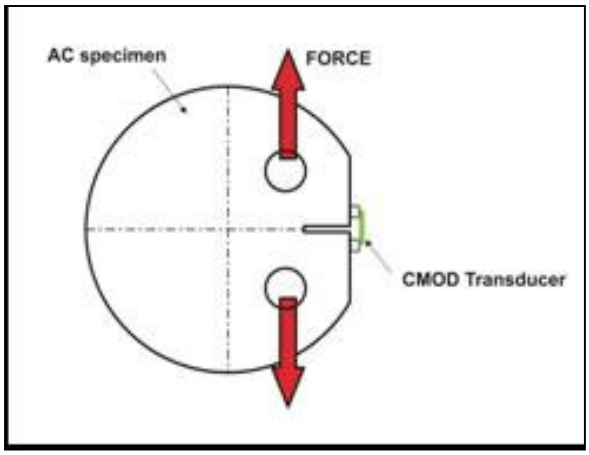

Figure 5. DCT test scheme

Typical plots of Load vs.CMOD are shown in Figure 6. The fracture energy is calculated by determining the area under the Load-CMOD curve normalized by the initial ligament length and thickness.

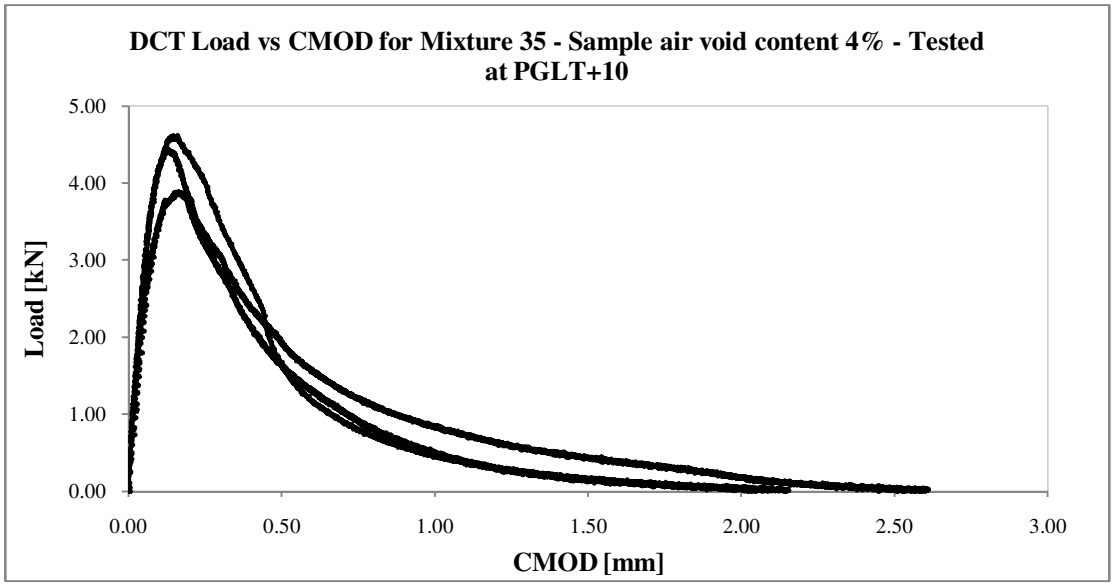

Figure 6. Typical Load-CMOD plots from DCT tests of three replicates

DCT test results for laboratory compacted and field samples

Table 4 to

Table 6 , show DCT data obtained at UIUC for the laboratory compacted specimens. The fracture energy was obtained from the average of the three test replicates. In some cases, due to fabrication or testing errors, only two replicates were considered. The shaded cells represent test results which were discarded from the analysis.

Table 4. DCT test results for specimens with 4% air void content

Mixture Identification	Void [%]	Temp [˚C]	G_f [J/m^2]	Mean G_f [J/m^2]	COV
DCT-20-4-18	4	-18	543.93	483.14	12%
			480.74		
			424.74		
DCT-20-4-28	4	-28	371.93	363.66	10%
			323.64		
			395.41		
DCT-21-4-18	4	-18	612.15	575.22	18%
			656.97		
			456.53		
DCT-21-4-28	4	-28	431.69	379.23	13%
			370.88		
			335.11		
DCT-22-4-24	4	-24	582.65	594.85	10%
			656.49		
			545.42		
DCT-22-4-34	4	-34	382.09	346.20	10%
			315.35		
			341.16		
DCT-33-4-24	4	-24	624.01	544.37	13%
			490.42		
			518.69		
DCT-33-4-34	4	-34	516.45	474.26	13%
			NA		
			432.07		
DCT-34-4-24	4	-24	760.42	747.07	10%
			811.81		
			668.98		
DCT-34-4-34	4	-34	396.59	440.35	13%
			417.56		
			506.89		
DCT-35-4-24	4	-24	636.47	645.41	9%
			706.73		

			593.02		
DCT-35-4-34	4	-34	443.15 725.83 429.30	436.22	2%
DCT-77-4-24	4	-24	446.09 592.37 603.51	547.32	16%
DCT-77-4-34	4	-34	468.27 533.07 395.12	465.48	15%
DCT-W-4-24	4	-24	252.52 245.93 255.91	251.46	2%
DCT-W-4-34	4	-34	344.46 351.82 383.25	359.84	6%

Table 5. DCT test results for specimens with 7% air void content

Mixture Identification	Void [%]	Temp [˚C]	G_f [J/m^2]	Mean G_f [J/m^2]	COV
DCT-20-7-18	7	-18	550.53 412.48 551.16	504.72	16%
DCT-20-7-28	7	-28	345.04 338.93 341.99	341.99	1%
DCT-21-7-18	7	-18	633.40 530.33 513.30	559.01	12%
DCT-21-7-28	7	-28	396.34 347.99 388.76	377.70	7%
DCT-22-7-24	7	24	415.71 460.63 445.94	440.76	5%
DCT-22-7-34	7	34	352.68	322.47	10%

			285.88		
			328.85		
DCT-33-7-24	7	-24	626.75	594.38	12%
			512.20		
			644.21		
DCT-33-7-34	7	-34	365.93	340.81	8%
			344.63		
			311.87		
DCT-34-7-24	7	-24	618.27	670.92	16%
			795.78		
			598.71		
DCT-34-7-34	7	-34	406.62	476.18	13%
			527.71		
			494.20		
DCT-35-7-24	7	-24	718.58	647.36	13%
			556.99		
			666.50		
DCT-35-7-34	7	-34	489.96	473.02	3%
			464.24		
			464.86		
DCT-77-7-24	7	-24	517.18	526.62	5%
			505.12		
			557.54		
DCT-77-7-34	7	-34	500.86	428.05	24%
			355.23		
			NA		
DCT-NY-7-12	7	-12	523.06	435.99	17%
			402.47		
			382.45		
DCT-NY-7-22	7	-22	NA	302.70	2%
			299.16		
			306.24		
DCT-W-7-24	7	-24	192.97	233.83	15%
			250.77		
			257.75		
DCT-W-7-34	7	-34	376.63	349.32	7%
			334.33		

			336.99		

Table 6. DCT test results for conditioned specimens

Mixture Identification	Void [%]	Temp [˚C]	G_f [J/m^2]	Mean G_f [J/m^2]	COV
DCT-20-7-28	7	-28	247.42	269.83	12%
			NA		
			292.25		
DCT-21-7-28	7	-28	NA	307.35	7%
			322.04		
			292.66		
DCT-22-7-34	7	-34	348.17	365.99	16%
			317.16		
			432.64		
DCT-33-7-34	7	-34	272.17	355.06	21%
			380.93		
			412.07		
DCT-34-7-34	7	-34	286.07	350.13	18%
			408.68		
			355.63		
DCT-35-7-34	7	-34	499.38	451.73	11%
			459.36		
			396.46		
DCT-77-7-34	7	-34	403.20	399.83	8%
			366.60		
			429.68		
DCT-NY-7-22	7	-22	299.31	275.44	8%
			268.97		
			258.04		
DCT-W-7-34	7	-34	234.53	265.58	19%
			323.27		
			238.95		

The DCT test results for field cores are reported in Table 7.

Table 7. DCT test results for field specimens

Mixture Identification	Void [%]	Temp [˚C]	G_f [J/m^2]	Mean G_f [J/m^2]	COV
DCT-20-7-28	7	-28	283.00	278	12%
			283.00		
			267.00		
DCT-21-7-28	7	-28	282.00	327	6%
			331.00		
			367.00		
DCT-22-7-34	7	-34	282.00	247	15%
			235.00		
			223.00		
DCT-33-7-34	7	-34	317.00	334	12%
			339.00		
			346.00		
DCT-34-7-34	7	-34	278.00	372	16%
			313.00		
			525.00		
DCT-35-7-34	7	-34	344.00	312	19%
			297.00		
			295.00		
DCT-77-7-34	7	-34	373.00	395	13%
			290.00		
			522.00		

DCT results for tests performed at UMN

Three randomly selected mixtures were also DCT tested at the UMN. The fracture energy was computed from the Load-CMOD curve as described above. The results are shown in Table 8.

Table 8. DCT test results for mixtures tested at the UMN

Mixture Identification	Void [%]	Temp [˚C]	G_f [J/m^2]	Mean G_f [J/m^2]	COV
DCT-21-4-18	4	-18	606.54	629.63	5%
			619.62		
			662.73		

DCT-21-4-28	4	-28	525.02 420.12 815.74	472.57	16%
DCT-20-7-18	7	-18	586.55 661.11 424.04	557.24	22%
DCT-20-7-28	7	-28	500.23 622.52 519.12	547.29	12%
DCT-22-7-24	7	-24	608.75 653.07 666.48	642.77	5%
DCT-22-7-34	7	-34	671.52 481.41 671.52	608.15	18%

SCB for laboratory compacted and field samples

The semi circular bending (SCB) test method takes advantage of the simple specimen preparation from Superpave Gyratory compacted cylinders and the simple loading setup. A schematic of the test set-up is shown in Figure 7 .

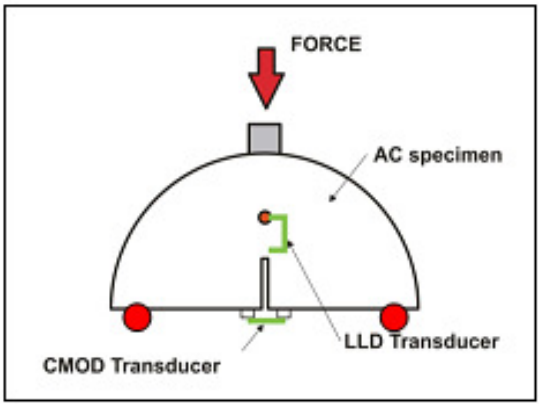

Figure 7. SCB test scheme

An MTS servo-hydraulic testing system equipped with an environmental chamber was used to perform the SCB test. The load line displacement (LLD) was measured using a vertically mounted Epsilon extensometer with 38 mm gage length and ±1 mm range; one end was mounted on a button that was permanently fixed on a specially made frame, and the other end was attached to a metal button glued to the sample. The crack mouth opening displacement (CMOD) was recorded by an Epsilon clip gage with 10 mm gage length and a +2.5 and -1 mm range. The clip gage was attached at the bottom of the specimen. A constant CMOD rate of 0.0005mm/s

was used and the load and load line displacement (P-u), as well as the load versus LLD curves were plotted. A contact load with maximum load of 0.3 kN was applied before the actual loading to ensure uniform contact between the loading plate and the specimen. The testing was stopped when the load dropped to 0.5 kN in the post peak region. All tests were performed inside an environmental chamber. Liquid nitrogen was used to obtain the required low temperature. The temperature was controlled by the environmental chamber temperature controller and verified using an independent platinum RTD thermometer.

A total of 129 samples were SCB tested. Out of these specimens, eight broke during test before data acquisition process was completed. Typical Load versus LLD plots obtained from SCB tests are shown in Figure 8.

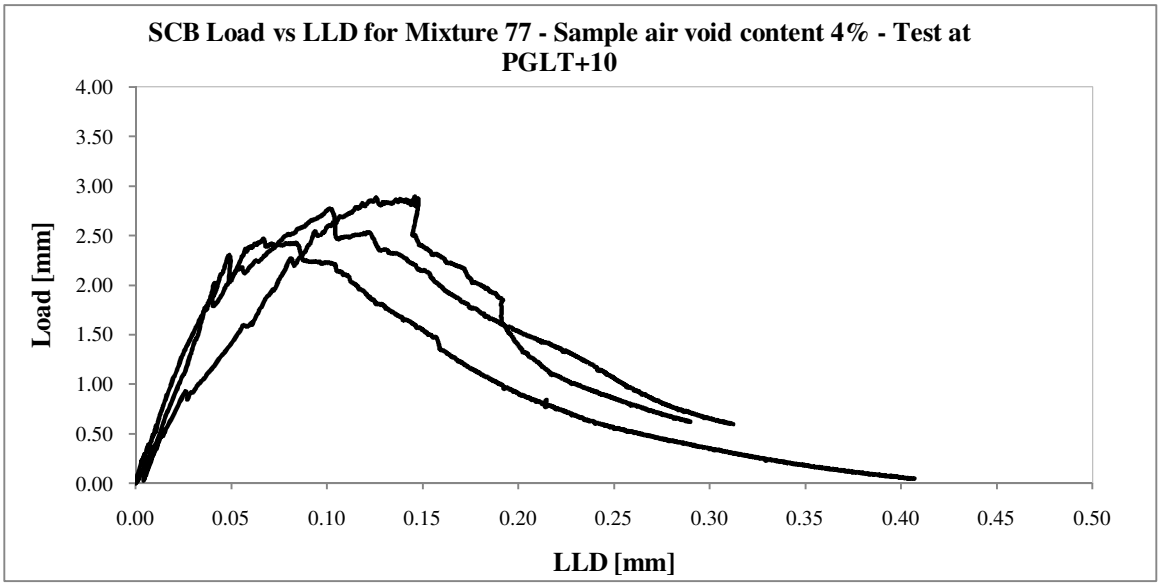

Figure 8. Typical Load-LLD plots from SCB tests of three replicates

The tail part of the Load-LLD curve can be reasonably obtained by fitting the data curve in post peak region following a method described elsewhere (5).The load and load line displacement data were used to calculate the fracture toughness and fracture energy as described in the National Pooled Fund Study 776 (6).

SCB results for laboratory compacted and field samples

The fracture energy and fracture parameters were computed from the SCB test results. Table 9 through Table 11, report the results obtained at UMN.

Table 9. SCB test results for specimens with 4% air void content

Mixture Identification	Void [%]	Temp. [˚C]	K_{IC} MPa/$m^{0.5}$	Mean K_{IC} MPa/$m^{0.5}$	COV	G_f [J/m^2]	Mean G_f [J/m^2]	COV
SCB-20-4-18	4	-18	0.96	0.98	4%	1252.57	926.90	50%
			1.01			601.23		
			NA			NA		
SCB-20-4-28	4	-28	0.86	0.99	19%	799.09	767.82	6%
			1.13			736.54		
			NA			NA		
SCB-21-4-18	4	-18	0.85	0.82	8%	716.56	770.21	13%
			0.74			704.60		
			0.86			889.47		
SCB-21-4-28	4	-28	0.95	0.96	7%	566.11	645.17	22%
			1.03			808.04		
			0.90			561.34		
SCB-22-4-24	4	-24	0.80	0.88	7%	838.20	657.68	27%
			0.93			651.99		
			0.90			482.85		
SCB-22-4-34	4	-34	1.00	0.98	14%	518.37	501.28	5%
			0.83			484.19		
			1.10			1126.61		
SCB-33-4-24	4	-24	0.91	0.86	10%	1020.53	776.13	29%
			0.76			577.20		
			0.91			730.66		
SCB-33-4-34	4	-34	0.94	0.90	5%	725.55	661.22	18%
			0.85			527.45		
			0.91			730.66		
SCB-34-4-24	4	-24	0.91	0.91	11%	728.68	1066.42	29%
			1.01			1146.17		
			0.81			1324.42		
SCB-34-4-34	4	-34	1.09	1.06	4%	955.18	852.49	14%
			1.08			727.54		
			1.00			874.76		
SCB-35-4-24	4	-24	0.90	0.95	7%	983.94	1185.69	24%
			1.00			1387.45		
			NA			NA		

SCB-35-4-34	4	-34	0.96	1.00	4%	491.93	642.99	27%
			1.03			827.74		
			1.01			609.29		
SCB-77-4-24	4	-24	0.80	0.85	6%	1100.23	1099.41	1%
			0.90			1112.27		
			0.84			1085.72		
SCB-77-4-34	4	-34	0.85	0.91	9%	539.58	643.73	23%
			0.97			747.87		
			NA			NA		
SCB-W-4-24	4	-24	0.86	0.85	3%	483.11	541.40	16%
			0.85			638.05		
			0.82			503.04		
SCB-W-4-34	4	-34	0.96	0.91	6%	398.10	450.00	29%
			0.86			351.14		
			0.92			600.77		

Table 10. SCB test results for specimens with 7% air void content

Mixture Identification	Void [%]	Temp. [˚C]	K_{IC} MPa/$m^{0.5}$	Mean K_{IC} MPa/$m^{0.5}$	COV	G_f [J/m^2]	Mean G_f [J/m^2]	COV
SCB-20-7-18	7	-18	0.70	0.73	6%	656.86	726.90	17%
			0.78			865.73		
			0.72			658.11		
SCB-20-7-28	7	-28	0.77	0.81	4%	704.02	615.32	13%
			0.84			578.30		
			0.81			563.64		
SCB-21-7-18	7	-18	0.68	0.71	10%	567.65	772.11	26%
			0.66			785.92		
			0.80			962.76		
SCB-21-7-28	7	-28	0.44	0.66	29%	NA	659.92	14%
			0.79			725.20		
			0.74			594.63		
SCB-22-7-24	7	24	0.86	0.81	6%	1207.52	715.52	3%
			0.78			701.10		
			0.77			729.94		
SCB-22-7-34	7	34	0.81	0.75	13%	488.67	408.20	23%
			0.64			302.22		

			0.80			433.72		
SCB-33-7-24	7	-24	0.69 0.77 0.68	0.71	7%	721.36 685.56 719.16	708.70	3%
SCB-33-7-34	7	-34	0.75 0.81 0.67	0.74	10%	460.32 477.30 413.92	450.51	7%
SCB-34-7-24	7	-24	0.85 0.76 0.87	0.82	7%	964.55 798.82 719.06	827.48	15%
SCB-34-7-34	7	-34	0.80 0.79 0.73	0.77	5%	506.15 514.47 599.30	539.97	10%
SCB-35-7-24	7	-24	0.85 1.16 0.53	1.00	22%	1135.29 1323.54 443.20	1229.42	11%
SCB-35-7-34	7	-34	0.74 1.03 0.88	0.88	17%	448.29 604.78 528.10	527.06	15%
SCB-77-7-24	7	-24	0.74 0.83 0.66	0.74	12%	1138.51 781.17 633.19	707.18	15%
SCB-77-7-34	7	-34	0.67 0.71 0.89	0.76	16%	500.38 528.52 693.71	574.20	18%
SCB-NY-7-12	7	-12	0.89 0.75 0.78	0.81	9%	794.94 564.53 599.85	653.11	19%
SCB-NY-7-22	7	-22	0.91 0.89 0.78	0.86	8%	512.70 572.67 545.62	543.66	6%
SCB-W-7-24	7	-24	0.89 0.76 0.69	0.78	13%	513.49 415.40 369.26	432.72	17%
SCB-W-7-34	7	-34	0.79 0.74 NA	0.76	5%	424.38 333.04 NA	378.71	17%

Table 11. SCB test results for conditioned specimens

Mixture Identification	Void [%]	Temp. [˚C]	K_{IC} MPa/$m^{0.5}$	Mean K_{IC} MPa/$m^{0.5}$	COV	G_f [J/m^2]	Mean G_f [J/m^2]	COV
SCB-20-7-28	7	-28	0.88	0.84	5%	703.02	700.66	21%
			0.80			846.63		
			0.85			552.35		
SCB-21-7-28	7	-28	0.77	0.88	12%	374.55	523.10	25%
			0.88			572.69		
			0.99			622.06		
SCB-22-7-34	7	-34	0.94	1.01	6%	525.28	653.86	17%
			1.03			728.69		
			1.06			707.61		
SCB-33-7-34	7	-34	0.69	0.73	6%	438.34	526.92	17%
			0.78			612.47		
			0.71			529.95		
SCB-34-7-34	7	-34	0.84	0.85	6%	NA	567.91	22%
			0.80			479.96		
			0.91			655.86		
SCB-35-7-34	7	-34	0.80	0.85	5%	703.05	652.65	17%
			0.88			727.97		
			0.87			526.94		
SCB-77-7-34	7	-34	0.85	0.82	11%	674.39	607.51	24%
			0.88			704.70		
			0.72			443.46		
SCB-NY-7-22	7	-22	0.83	0.87	8%	439.52	499.98	14%
			0.83			579.48		
			0.94			480.93		
SCB-W-7-34	7	-34	0.84	0.81	4%	362.44	384.98	8%
			0.78			NA		
			0.82			407.53		

The SCB specimens, obtained from field cored samples, were also subjected to the SCB test in order to evaluate their fracture parameters. Table 12 reports the results.

Table 12. SCB test results for field cored samples

Mixture Identification	Void [%]	Temp. [˚C]	K_{IC} MPa/$m^{0.5}$	Mean K_{IC} MPa/$m^{0.5}$	COV	G_f [J/m^2]	Mean G_f [J/m^2]	COV
SCB-20-7-28	7	-28	0.67	0.68	5%	235.82	207.16	12%
			0.66			187.45		
			0.72			198.23		
SCB-21-7-28	7	-28	0.72	0.79	15%	169.79	162.41	6%
			0.72			155.03		
			0.93			292.94		
SCB-22-7-34	7	-34	0.73	0.77	4%	276.44	306.49	15%
			0.80			282.45		
			0.78			360.58		
SCB-33-7-34	7	-34	0.85	0.80	8%	278.16	246.34	12%
			0.74			220.88		
			0.82			239.99		
SCB-34-7-34	7	-34	0.73	0.81	10%	245.97	288.36	16%
			0.79			280.30		
			0.89			338.82		
SCB-35-7-34	7	-34	0.86	0.85	7%	454.87	421.29	19%
			0.90			329.39		
			0.78			479.62		
SCB-77-7-34	7	-34	0.96	0.87	12%	316.51	301.46	13%
			0.89			330.83		
			0.76			257.04		

SCB results for tests performed at UIUC

Three randomly selected mixture were also SCB tested at the UIUC, and the results are reported in Table 13.

Table 13. SCB test results for mixtures tested at the UIUC

Mixture Identification	Void [%]	Temp. [˚C]	K_{IC} MPa/$m^{0.5}$	Mean K_{IC} MPa/$m^{0.5}$	COV	G_f [J/m^2]	Mean G_f [J/m^2]	COV
SCB-35-4-24	4	-24	0.857	0.967	12%	412	436	7%
			1.087			425		
			0.957			470		
SCB-35-7-24	7	-24	0.857	0.855	2%	515	512	2%
			0.837			501		
			0.871			520		
SCB-NY-7-12	7	-12	0.786	0.798	1%	341	349	15%
			0.806			405		
			0.803			300		

It must be noted however, that the above reported fracture energy were not computed using LLD measurements. Instead, the displacement of the loading piston, recorded through its LVDT, was used.

Indirect Tensile Test IDT Creep Stiffness and Strength

Two parameters, creep compliance and strength were determined using the current AASHTO specification T 322-03, (7). Each mixture was tested at two different temperatures determined based on the PG grade of the binder. At each temperature, three replicates were tested. First, all IDT specimens were tested for the creep stiffness and later for the strength. Both procedures are specified in AASHTO T 322-03 and the resultant parameters are calculated as follows:

- Creep stiffness:

$$D(t) = \frac{\Delta X \cdot D_{avg} \cdot b_{avg}}{P_{avg} \cdot GL} \cdot C_{cmpl},$$

$D(t)$ – creep compliance,

ΔX – trimmed mean of the horizontal deformations,

D_{avg} – average specimen diameter,

b_{avg} - average specimen thickness,

P_{avg} – average force during the test,

GL – gage length (38mm)

C_{cmpl} – creep compliance parameter at any given time, computed as

$$C_{cmpl} = 0.6354 \cdot \left(\frac{X}{Y}\right)^{-1} - 0.332, \text{ where}$$

X – horizontal deformation,

Y – vertical deformation.

Creep stiffness *S(t)* at the time *t* was calculated as the inverse of the creep compliance *D(t)*, i.e. *S(t)=1/D(t)*.

- Tensile strength:

$$S = \frac{2 \cdot P_{fail}}{\pi \cdot b \cdot D},$$

where

P_{fail} – failure (peak) load,

b, D – specimen thickness and diameter, respectively.

IDT test results for laboratory compacted and field samples

Table 14 through Table 19 report the IDT test results obtained at UMN.

Table 14. IDT creep stiffness test results for specimens with 4% air void content

Mixture Identification	Void [%]	Temp [˚C]	Creep Stiffnes @ 60			Creep Stiffnes @ 500		
			S [GPa]	Mean	COV	S [GPa]	Mean	COV
IDT-20-4-18	4	-18	12.05	11.81	3%	8.41	8.41	0%
			11.58			8.41		
			NA			NA		
IDT-20-4-28	4	-28	24.75	21.18	17%	18.54	17.19	7%
			21.34			16.78		
			17.44			16.26		
IDT-21-4-18	4	-18	18.60	11.89	22%	18.60	7.63	32%
			10.04			5.92		
			13.73			9.34		
IDT-21-4-28	4	-28	17.98	19.79	9%	14.94	17.02	11%
			21.48			18.38		
			19.92			17.73		
IDT-22-4-24	4	-24	NA	11.00	11%	NA	7.83	14%
			11.84			8.59		
			10.16			7.06		
IDT-22-4-34	4	-34	27.51	29.91	12%	22.66	23.64	8%
			34.08			25.89		
			28.15			22.36		
IDT-33-4-24	4	-24	13.83	15.28	8%	9.43	10.75	11%
			15.70			11.45		

			16.32			11.38		
IDT-33-4-34	4	-34	23.41	19.85	16%	18.25	15.81	16%
			18.87			15.88		
			17.26			13.30		
IDT-34-4-24	4	-24	18.28	15.31	17%	12.67	11.12	12%
			13.87			10.26		
			13.80			10.44		
IDT-34-4-34	4	-34	16.40	21.40	26%	15.69	18.75	17%
			27.30			22.04		
			20.50			18.52		
IDT-35-4-24	4	-24	17.12	16.42	8%	11.46	11.11	3%
			17.22			11.13		
			14.91			10.73		
IDT-35-4-34	4	-34	25.33	25.17	9%	21.21	20.61	6%
			27.45			21.44		
			22.73			19.17		
IDT-77-4-24	4	-24	13.56	12.79	5%	9.21	8.86	4%
			12.46			8.48		
			12.34			8.89		
IDT-77-4-34	4	-34	21.60	21.82	24%	20.20	21.65	11%
			27.26			20.32		
			16.58			24.44		
IDT-W-4-24	4	-24	13.54	15.07	10%	13.48	15.13	13%
			16.62			14.56		
			15.04			17.34		
IDT-W-4-34	4	-34	26.70	26.10	4%	22.74	21.46	5%
			24.79			20.74		
			26.79			20.91		

Table 15. IDT creep stiffness test results for specimens with 7% air void content

Mixture Identification	Void [%]	Temp [˚C]	Creep Stiffnes @ 60			Creep Stiffnes @ 500		
			S [GPa]	Mean	COV	Mean	COV	S [GPa]

IDT-20-7-18	7	-18	13.01 10.42 10.77	11.40	12%	8.67 6.88 6.40	7.32	16%
IDT-20-7-28	7	-28	17.47 17.35 18.50	17.77	4%	15.09 15.45 14.73	15.09	2%
IDT-21-7-18	7	-18	13.50 7.44 13.60	13.55	1%	8.65 5.03 8.85	8.75	2%
IDT-21-7-28	7	-28	16.15 17.13 18.68	17.32	7%	10.30 11.73 14.54	12.19	18%
IDT-22-7-24	7	24	17.61 14.37 26.31	15.99	14%	14.47 11.08 15.03	13.52	16%
SCB-22-7-34	7	34	14.86 12.82 27.69	13.84	10%	21.94 21.93 24.90	22.93	7%
IDT-33-7-24	7	-24	7.97 9.14 13.08	10.06	27%	5.03 5.44 8.74	5.24	6%
IDT-33-7-34	7	-34	17.52 18.15 25.00	20.22	20%	13.73 13.88 18.48	15.37	18%
IDT-34-7-24	7	-24	14.94 10.78 11.04	12.25	19%	9.31 6.74 6.82	7.62	19%
IDT-34-7-34	7	-34	13.79 37.03 17.71	15.75	18%	13.11 30.32 13.99	13.55	5%
IDT-35-7-24	7	-24	11.66 13.44 11.70	12.26	8%	7.59 9.15 6.85	7.86	15%
IDT-35-7-34	7	-34	25.38 14.57 15.47	15.02	4%	21.07 13.89 13.76	16.24	26%

IDT-77-7-24	7	-24	12.65	12.85	9%	9.47	8.91	11%
			14.04			9.46		
			11.85			7.80		
IDT-77-7-34	7	-34	22.52	18.94	23%	16.81	17.41	5%
			14.01			16.94		
			20.30			18.47		
IDT-NY-7-12	7	-12	21.21	9.76	3%	14.17	6.66	5%
			9.52			6.31		
			10.00			7.01		
IDT-NY-7-22	7	-22	9.56	8.80	8%	7.73	7.03	9%
			8.59			6.73		
			8.24			6.62		
IDT-W-7-24	7	-24	24.57	19.27	28%	19.61	15.67	23%
			13.77			12.47		
			19.47			14.94		
IDT-W-7-34	7	-34	23.18	23.68	2%	22.82	21.66	5%
			24.26			20.79		
			23.59			21.36		

Table 16. IDT creep stiffness test results for conditioned specimens

Mixture Identification	Void [%]	Temp [˚C]	Creep Stiffnes @ 60			Creep Stiffnes @ 500		
			S [GPa]	Mean	COV	Mean	COV	S [GPa]
IDT-20-7-28	7	-28	13.32	17.50	24%	10.50	13.34	20%
			21.87			15.76		
			17.31			13.76		
IDT-21-7-28	7	-28	14.99	17.26	11%	10.58	12.47	13%
			18.56			13.22		
			18.23			13.61		
IDT-22-7-34	7	-34	25.94	26.39	3%	19.40	20.87	7%
			27.34			21.09		
			25.88			22.12		
IDT-20-7-34	7	-34	24.29	23.21	10%	21.14	17.69	18%
			20.43			15.09		
			24.90			16.82		
IDT-20-7-34	7	-34	24.73	24.10	4%	19.74	19.91	1%
			24.42			20.14		

			23.13			19.85		
IDT-20-7-34	7	-34	20.84	20.83	6%	14.38	14.62	3%
			22.02			15.06		
			19.61			14.43		
IDT-20-7-28	7	-28	26.05	25.17	3%	21.07	20.81	3%
			24.45			20.14		
			24.99			21.21		
IDT-NY-7-22	7	-22	8.15	8.01	7%	6.69	6.78	7%
			7.43			6.39		
			8.46			7.27		
IDT-W-7-34	7	-34	30.12	29.80	3%	25.31	25.44	5%
			30.35			26.74		
			28.92			24.26		

Table 17. IDT tensile strength test results for specimens with 4% air void content

Mixture Identification	Void [%]	Temp [˚C]	IDT strength [MPa]	Mean	COV
IDT-20-4-18	4	-18	5.65	5.54	3%
			5.42		
			NA		
IDT-20-4-28	4	-28	5.08	4.90	3%
			4.85		
			4.77		
IDT-21-4-18	4	-18	5.41	5.24	5%
			5.06		
			NA		
IDT-21-4-28	4	-28	4.86	4.89	2%
			4.80		
			5.01		
IDT-22-4-24	4	-24	NA	5.20	7%
			4.96		
			5.44		
IDT-22-4-34	4	-34	5.23	5.26	2%
			5.38		
			5.18		
IDT-33-4-24	4	-24	4.96	4.65	10%
			4.91		

			4.10		
IDT-33-4-34	4	-34	4.83 4.16 4.37	4.45	8%
IDT-34-4-24	4	-24	5.64 4.86 5.30	5.26	7%
IDT-34-4-34	4	-34	5.14 4.91 4.59	4.88	6%
IDT-35-4-24	4	-24	5.58 5.70 5.71	5.67	1%
IDT-35-4-34	4	-34	5.13 5.87 5.28	5.43	7%
IDT-77-4-24	4	-24	4.45 4.88 4.85	4.73	5%
IDT-77-4-34	4	-34	4.74 3.72 4.50	4.32	12%
IDT-W-4-24	4	-24	5.87 5.71 4.64	5.41	12%
IDT-W-4-34	4	-34	4.64 4.27 4.48	4.47	4%

Table 18. IDT tensile strength test results for specimens with 7% air void content

Mixture Identification	Void [%]	Temp [˚C]	IDT strength [MPa]	Mean	COV
IDT-20-7-18	7	-18	4.36	4.27	4%
			4.36		
			4.08		
IDT-20-7-28	7	-28	NA	4.31	3%
			4.39		
			4.22		
IDT-21-7-18	7	-18	4.45	4.72	5%
			4.90		
			4.82		
IDT-21-7-28	7	-28	4.30	4.27	4%
			4.44		
			4.07		
IDT-22-7-24	7	24	4.78	5.00	6%
			4.88		
			5.34		
SCB-22-7-34	7	34	4.30	4.36	8%
			4.72		
			4.07		
IDT-33-7-24	7	-24	3.56	3.80	7%
			4.06		
			3.78		
IDT-33-7-34	7	-34	3.74	3.14	24%
			3.37		
			2.30		
IDT-34-7-24	7	-24	4.25	4.51	5%
			4.70		
			4.58		
IDT-34-7-34	7	-34	3.32	3.61	7%
			3.82		
			3.70		
IDT-35-7-24	7	-24	4.60	4.50	4%
			4.63		
			4.28		
IDT-35-7-34	7	-34	4.65	4.54	3%
			4.39		
			4.59		
IDT-77-7-24	7	-24	3.97	3.72	10%

			3.46		
			NA		
IDT-77-7-34	7	-34	3.71	3.75	1%
			3.77		
			3.78		
IDT-NY-7-12	7	-12	7.06	6.74	5%
			6.40		
			6.77		
IDT-NY-7-22	7	-22	6.35	6.67	8%
			7.26		
			6.39		
IDT-W-7-24	7	-24	4.35	4.00	15%
			4.33		
			3.33		
IDT-W-7-34	7	-34	3.68	3.92	6%
			3.88		
			4.19		

Table 19. IDT tensile strength test results for conditioned specimens

Mixture Identification	Void [%]	Temp [˚C]	IDT strength [MPa]	Mean	COV
IDT-20-7-28	7	-28	3.96	3.88	4%
			3.97		
			3.70		
IDT-21-7-28	7	-28	4.30	4.12	5%
			4.17		
			3.91		
IDT-22-7-34	7	-34	4.60	4.53	4%
			4.66		
			4.34		
IDT-20-7-34	7	-34	3.19	3.57	10%
			3.63		
			3.88		
IDT-20-7-34	7	-34	NA	3.93	3%
			3.85		
			4.02		
IDT-20-7-34	7	-34	4.59	4.72	5%
			4.56		
			5.02		
IDT-20-7-28	7	-28	3.48	3.31	6%

			3.11		
			3.34		
IDT-NY-7-22	7	-22	6.77	6.88	1%
			6.94		
			6.94		
IDT-W-7-34	7	-34	3.91	3.97	3%
			4.13		
			3.89		

IDT Creep stiffness and strength were also obtained for the specimens cored from the MnROAD test sections. The results are presented in Table 20 and Table 21.

Table 20. IDT creep stiffness test results for field specimens

Mixture Identification	Void [%]	Temp [˚C]	Creep Stiffnes @ 60			Creep Stiffnes @ 500		
			S [GPa]	Mean	COV	S [GPa]	Mean	COV
IDT-20-7-28	7	-18	23.657	22.279	5%	18.315	17.561	4%
			21.821			17.528		
			21.359			16.840		
IDT-21-7-28	7	-18	23.017	21.125	9%	18.649	17.776	7%
			21.097			18.217		
			19.260			16.462		
IDT-22-7-34	7	-34	23.180	25.476	13%	20.735	21.088	2%
			26.411			19.537		
			27.772			21.441		
IDT-33-7-34	7	-34	26.548	24.546	11%	19.707	18.429	8%
			21.448			16.842		
			25.640			18.737		
IDT-34-7-34	7	-34	22.702	20.220	17%	18.243	18.450	15%
			17.737			15.883		
			25.291			21.223		
IDT-35-7-34	7	-34	22.938	21.727	8%	19.755	17.134	14%
			20.516			16.518		
			19.260			15.129		
IDT-77-7-34	7	-34	26.647	26.050	21%	19.475	17.769	14%
			20.381			16.063		
			31.123			20.121		

Table 21. IDT tensile strength test results for field specimens

Mixture Identification	Void [%]	Temp [˚C]	IDT strength [MPa]	Mean	COV
IDT-20-7-28	7	-18	3.761	3.746	1%
			3.790		
			3.686		
IDT-21-7-28	7	-18	3.396	3.777	9%
			3.836		
			4.100		
IDT-22-7-34	7	-34	3.430	3.507	5%
			3.719		
			3.373		
IDT-33-7-34	7	-34	3.473	3.605	4%
			3.578		
			3.764		
IDT-34-7-34	7	-34	3.830	3.718	4%
			3.531		
			3.794		
IDT-35-7-34	7	-34	4.129	3.839	8%
			3.895		
			3.494		
IDT-77-7-34	7	-34	3.914	4.124	4%
			4.226		
			4.230		

3. ANALYSIS OF THE EXPERIMENTAL DATA

In this chapter the laboratory test results are analyzed to evaluate the effect of the various variables on the fracture parameters. MacAnova statistical software package was utilized to perform statistical analysis and the analysis of variance (ANOVA) was used to examine the differences among the mean response values of the different treatment group. The significance of the differences was tested at 0.05% level of error.

In running the statistical tests, particular attention was paid to some aspect of the ANOVA models. The methods of analysis of experimental results by comparing the average responses of different treatment groups using ANOVA or contrasts and pairwise comparison, are based on the assumption that the errors in the data are independent normals with constant variance. If these model assumptions do not hold, the inference may be misleading. Therefore, for each of the ANOVA model used in this study, the nature and degree to which the model-assumption were violated was checked, and corrective measures were taken, if needed. Graphical and numerical tools (provided in MacAnova) such as the normal probability plots and residual plots were used to assess the violation of the assumption. The primary tool used to dealing with the violation of assumptions, was the transformation of the response to a different scale (square root, logarithm etc.). In addition, the occurrence of unbalanced data, that is, that all factor-level combinations do not have the same amount of replication, necessitated ANOVA models adjusted to type III sum of squares.

The ANOVA models were constructed in subsequent steps. In each step, non-significant higher order terms were excluded from the model and the ANOVA was performed on the resulting new model. The last models, containing only significant terms, are presented in the report. Note that, in some models the symbol '^' (power) is used followed by 2 or 3. These models need to be read as models that allow 2 or 3 way factor interaction.

The '*NY*' mixture was not included in the statistical analysis, since information was not available for all factor level combinations.

Effects of Mixture Type, Air Void Content and Temperature on the Fracture parameters

Data analysis of DCT, SCB, and IDT strength for laboratory compacted specimens.

Figure 9, summarizes fracture energy results obtained from DCT tests performed on the unconditioned laboratory compacted specimens, at the above indicated test temperatures: PGLT+10˚C and PGLT. The specimens tested, were compacted at two different air void content levels: 4% and 7%, respectively. The computed DCT fracture energy responses range from approximately 190 J/m^2 to 800 J/m^2. The plot in the figure indicates that, for fixed air void content level, fracture energy mean values obtained from specimens tested at the highest test temperature, PGLT+10˚C, are always considerably larger than those obtained from specimen tested at the lowest level of the test temperature, PG, except for mixture '*Wisconsin*'. The fracture energy response from mixture '*Wisconsin*', suggests that the mixture has higher resistance to cracking at a lower temperature than at a higher one. Overall, the effect of the air void content on the DCT fracture energy, for the tested mixtures, seems to be minimal.

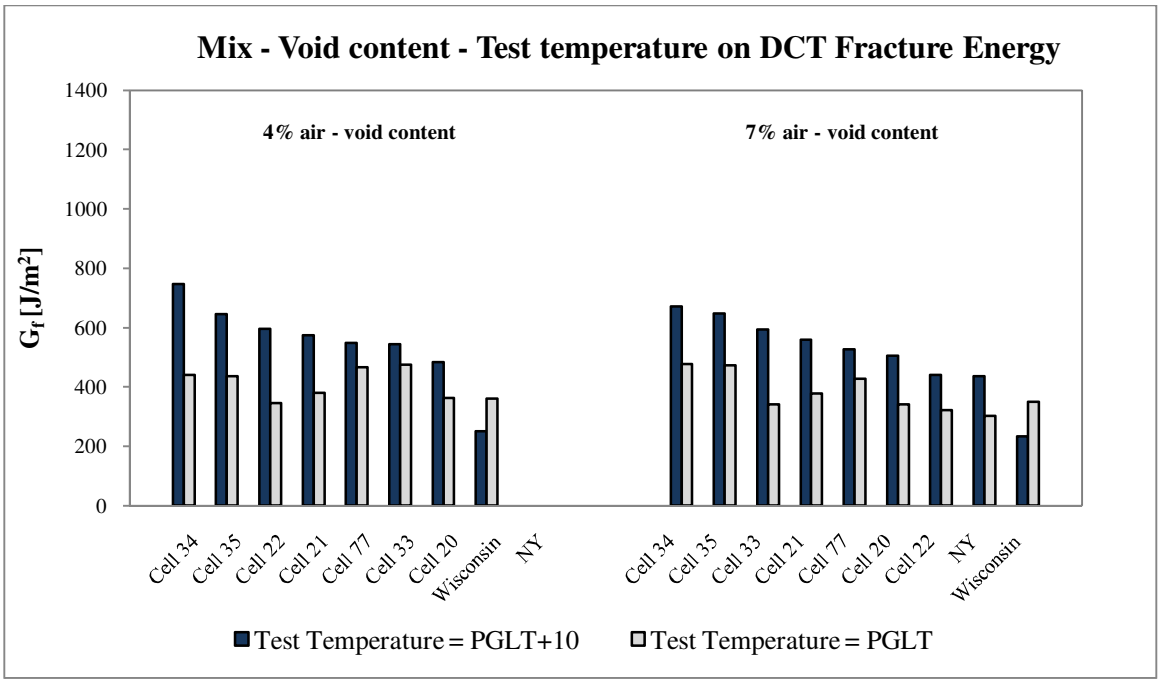

Figure 9. DCT fracture energy test results

Figure 10 and Figure 11, summarize the results of SCB fracture energy and fracture toughness, respectively. The results refer to laboratory compacted unconditioned specimens.

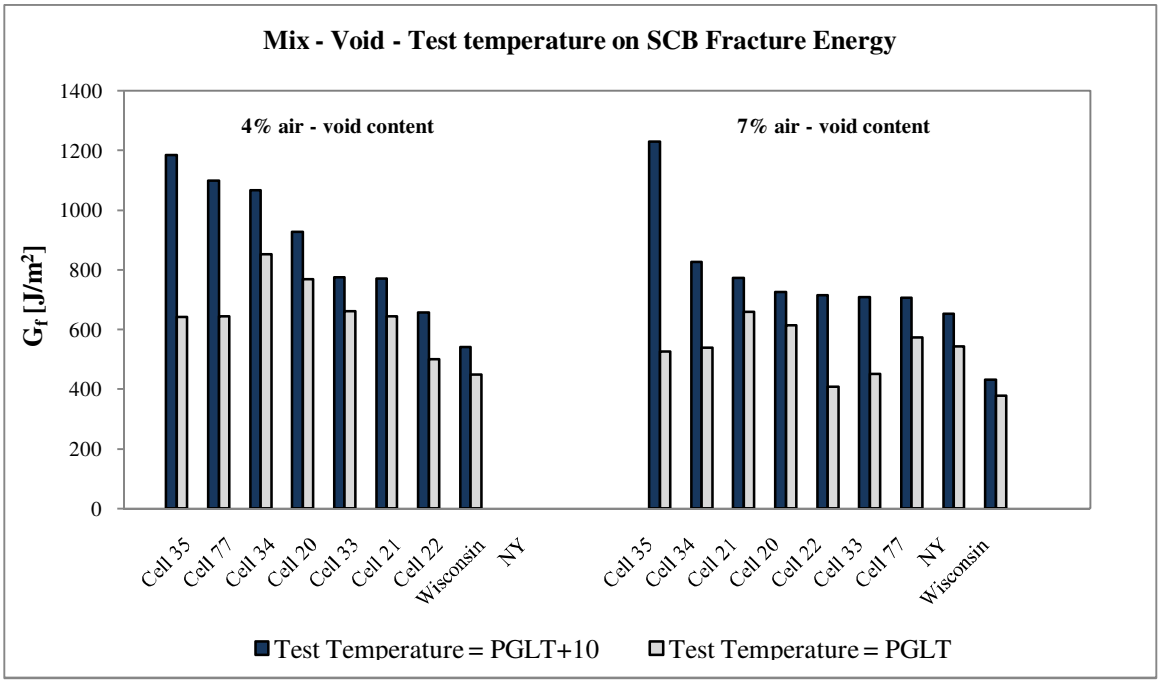

Figure 10. SCB fracture energy test results

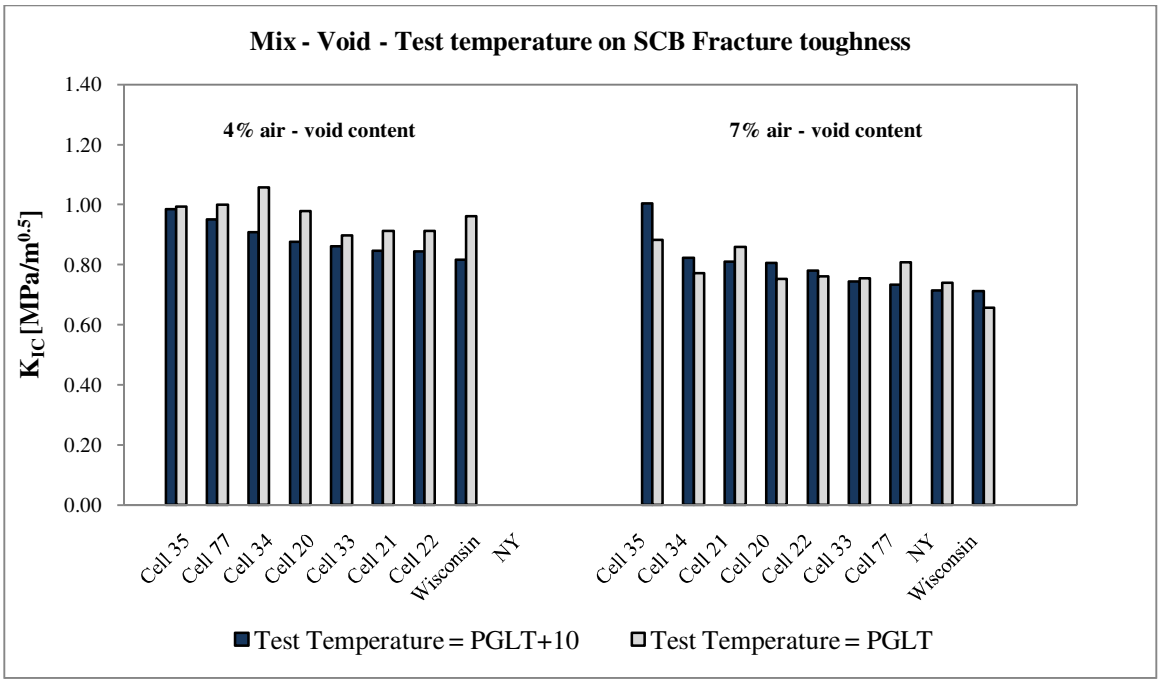

Figure 11. SCB fracture toughness test results

The SCB fracture energy values vary between 300 and 1380 J/m^2, a larger range than that observed for DCT fracture energy. The SCB fracture energy values obtained at PGLT+10˚C are always higher than those obtained at PGLT, regardless of the air void content. It can also be observed that SCB fracture energy decreases when air void content increases.

The computed SCB fracture toughness values vary from 0.45 to 1.20 MPa/m$^{0.5}$. For specimens with 4% air void content, the SCB fracture toughness value increases when the temperature decreases. Contrarily to what observed for fracture energy, the K_{IC} results suggest that testing temperature has a minimal effect on the response. In addition, a mixed behavior is observed: mixtures 21, 33, 77, and NY have slightly higher toughness values at the lowest testing temperature, while the others have higher fracture toughness at the highest testing temperature.

A summary of the strength results obtained from IDT tensile test is shown in Figure 12. The measured tensile strength ranged from 2.30 to 7 MPa, approximately. It can be noticed that the strength of the tested material was higher for mixtures with lower air void content. In addition, for most of the mixtures, except for 4% for mixture 22, and 7% for mixtures 35 and 77, the strength values obtained at PGLT+10˚C were higher than the values obtained at PGLT. It can be also observed that the NY mixture has a significantly higher IDT strength than all the other mixtures with 7% air voids.

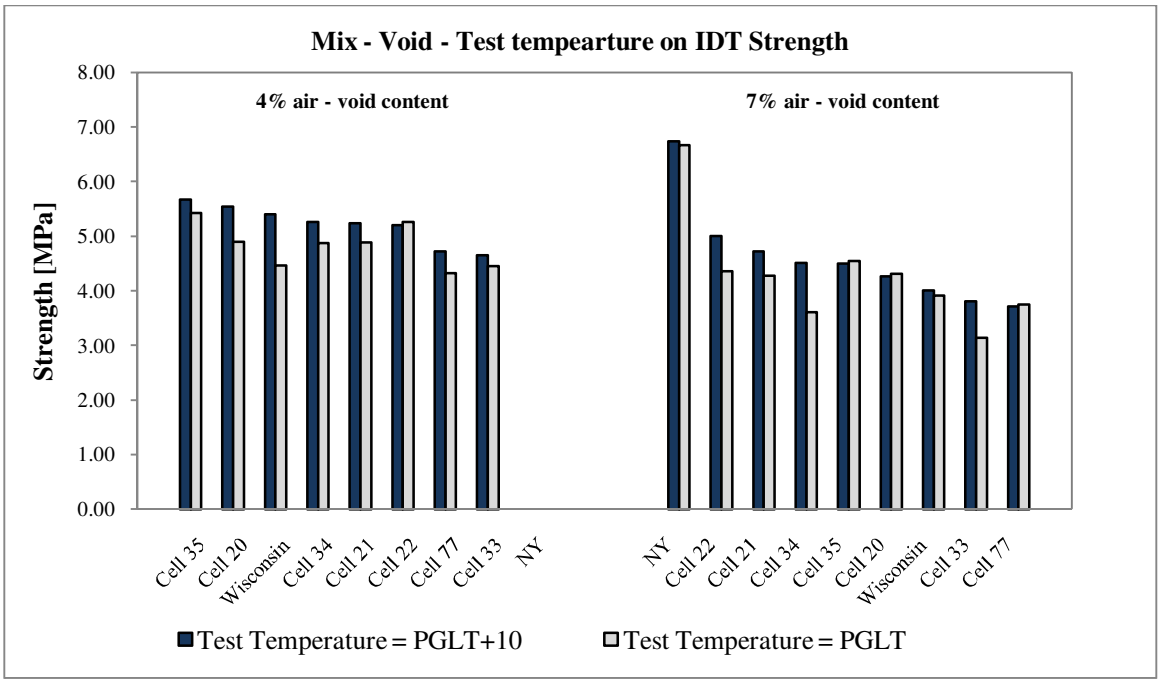

Figure 12. IDT tensile strength test results

Statistical analysis of DCT, SCB, and IDT strength for laboratory compacted specimens.

The factorial structure of the experiments allowed for a complete factorial analysis by means of ANOVA. The analyzed datasets, for each fracture parameter, consisted of a factorial structure composed of 32 treatments combinations as follows:

a. Eight type of mixtures
b. Two level of testing temperature: PGLT and PGLT +10˚C
c. Two level of air void contents: 4% and 7%

The null hypothesis can be formulated as follow: all the main effects and higher order interaction factor's effects, caused by the investigated variables, are null. This means that the test data can be described by a single overall mean value, which is not affected by mix, temperature and void content. The variables do not significantly alter the overall single mean. The null hypothesis is tested against the alternative hypothesis, that at least one effect is significantly different from zero, thus there is at least one group mean which significantly differ from the single overall mean. The significance is tested at 0.05 error level.

The same statistical analysis is performed, separately, for DCT fracture energy, SCB fracture energy and fracture toughness, and IDT tensile strength.

ANOVA tables for the different fracture parameters are presented below. Only the significant factors are reported. The model considered for each test methods are also highlighted.

Table 22. ANOVA table for DCT, SCB and IDT strength of laboratory specimens

Model used is for DCT fracture energy GF=mix+temp+mix.temp

SS are Type III sums of squares

	DF	SS	MS	F	P-value
CONSTANT	1	2.014e+07	2.014e+07	5419.09047	< 1e-08
mix	7	6.361e+05	90872	24.45070	< 1e-08
temp	1	4.3874e+05	4.3874e+05	118.05176	< 1e-08
mix.temp	7	2.5731e+05	36758	9.89045	< 1e-08
ERROR1	77	2.8617e+05	3716.5		

Model used for SCB fracture energy is log(GF)= mix+void+temp+mix.temp

SS are Type III sums of squares

	DF	**SS**	**MS**	**F**	**P-value**
CONSTANT	1	3580.5	3580.5	92398.70117	< 1e-08
mix	7	3.337	0.47672	12.30227	< 1e-08
void	1	0.65472	0.65472	16.89597	0.00010717
temp	1	2.3065	2.3065	59.52226	< 1e-08
mix.temp	7	0.63107	0.090153	2.32652	0.034296
ERROR1	69	2.6738	0.03875		

Model used for SCB fracture toughness is KIC=mix+void

SS are Type III sums of squares

	DF	**SS**	**MS**	**F**	**P-value**
CONSTANT	1	64.574	64.574	7887.49082	< 1e-08
mix	7	0.23146	0.033066	4.03894	0.00076684
void	1	0.49785	0.49785	60.80993	< 1e-08
ERROR1	81	0.66314	0.0081869		

Model used for IDT tensile strength is Strength=(mix+void+temp)

SS are Type III sums of squares

	DF	**SS**	**MS**	**F**	**P-value**
CONSTANT	1	1811.2	1811.2	14756.78378	< 1e-08
mix	7	11.023	1.5747	12.82991	< 1e-08
void	1	16.199	16.199	131.97942	< 1e-08
temp	1	3.1487	3.1487	25.65447	2.7229e-06
ERROR1	77	9.4507	0.12274		

According to the ANOVA table for DCT fracture energy, the main effects for mix type and test temperature are highly significant. The air void content and all higher order factor interactions, except for the mix to test temperature interaction effect, are estimated to be not significant.

The ANOVA table for the SCB fracture energy indicates that the main effects of mixture type, air void content, and test temperature are highly significant. In addition, the mix to test

temperature interaction factor is also moderately significant. All other higher order interactions are not significant.

The ANOVA table for the SCB fracture toughness analysis confirms the findings inferred from Figure 11: only the main effects for mixture type and void content are highly significant. The effects of test temperature and of higher order interactions factors are not significant.

The ANOVA for the IDT strength indicates that all main effects are significant and that higher order interaction factors are not significant.

Multiple comparisons, at 5% level of significance, were performed to compare and rank the tested mixtures, according the different test methods. The outcomes are reported in Table 23, in which statistically similar mixtures are grouped together. The letter A is used to indicate best performing group of mixtures. The letter B refers to the second best performing group of mixtures, and so on.

Table 23. Statistical grouping and ranking for laboratory compacted mixtures

Mixture Type	DCT G_f [J/m^2]		SCB G_f [J/m^2]		SCB K_{IC} [$MPa/m^{0.5}$]		IDT strength [MPa]	
	Group Mean	Rank	Group Mean	Rank	Group Mean	Rank	Group Mean	Rank
20	423.38	C	741.61	A	0.858	A/B	4.7195	A/B/C
21	472.79	B /C	716.57	A	0.787	B	4.7397	A/B/C
22	426.07	C	563.13	B/C	0.853	A/B	4.9232	A/B
33	489.75	B/C	649.14	A/B	0.804	B	4.012	E
34	583.63	A	821.59	A	0.890	A	4.5663	B/C/D
35	560.89	A/B	834.04	A	0.955	A	5.1029	A
77	497.67	B/C	772.26	A	0.806	B	4.1864	D/E
Wisconsin	298.61	D	457.25	C	0.831	B	4.4487	C/D/E

According to DCT fracture energy, the mixtures are divided in 4 groups. Mixtures 34 and 35, with the two highest fracture energy values, are ranked in group A. The mixture '*Wisconsin'*, with the lowest fracture energy, was the only one ranked in group D.

The SCB fracture energy, groups the mixtures into 3 different categories. Mixture's 20, 21, 34, 35, and 77 are considered to have statistically significant higher fracture energy. Again, mixture '*Wisconsin*' is ranked alone in the last group.

The SCB fracture toughness, divides the mixtures into two categories. Mixture 34 and 35 are again listed among the best performing mixtures.

Finally, according to the IDT test data, the mixtures are categorized into five statistically different levels of strength. Mixture 35 is again ranked in group A.

Data analysis of DCT, SCB, and IDT strength for field specimens.

Test specimens obtained from field cores, were tested and analyzed through an identical process used for the laboratory compacted specimens. The results for the field specimens are presented in Figure 13to Figure 16. In the plots, the field cores are ranked from best to worst for each fracture parameter. For comparison purposes, the laboratory compacted mixture results are also included in the figures.

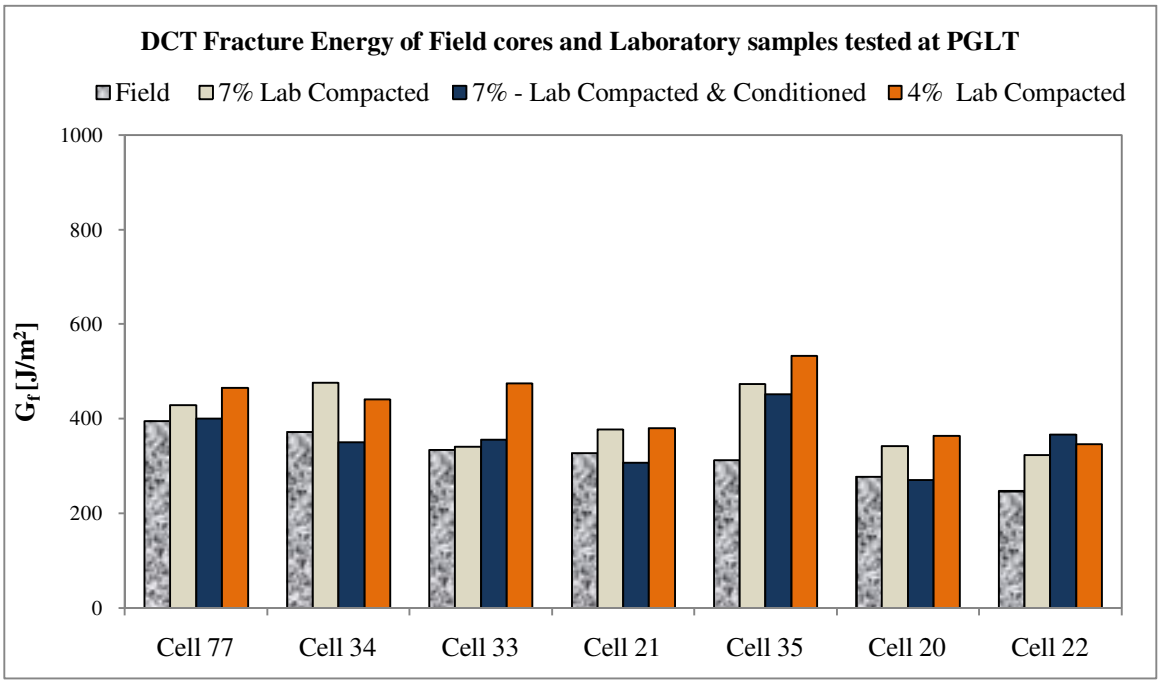

Figure 13. DCT fracture energy test results for field cores

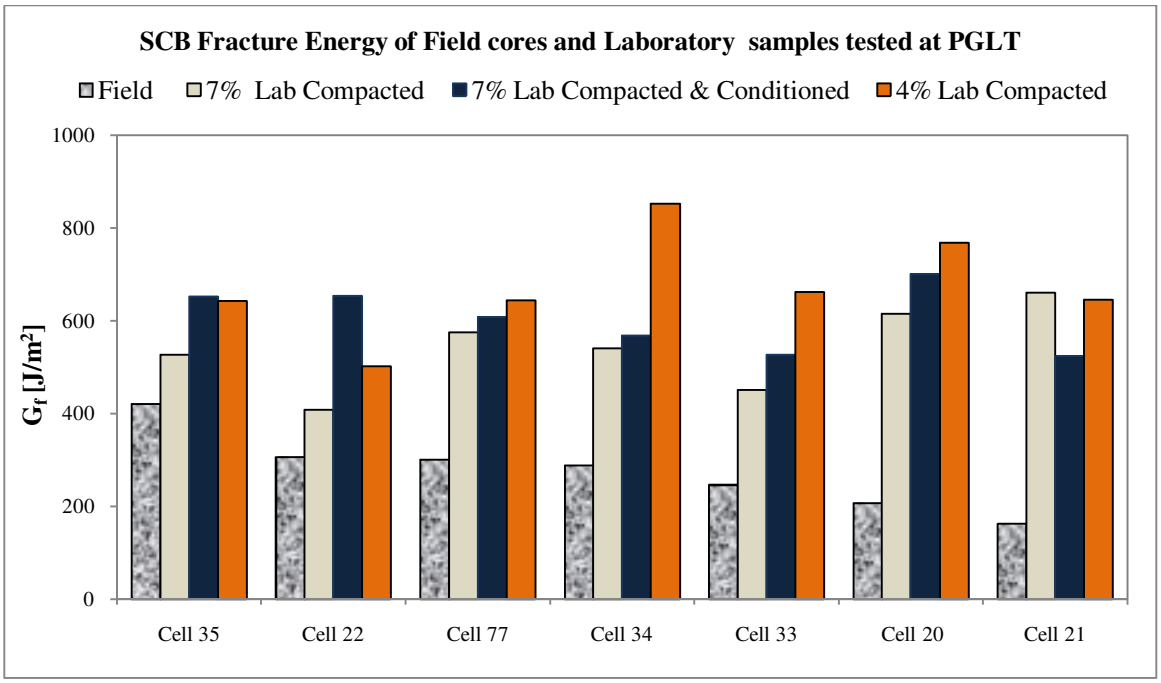

Figure 14. SCB fracture energy test results for field cores

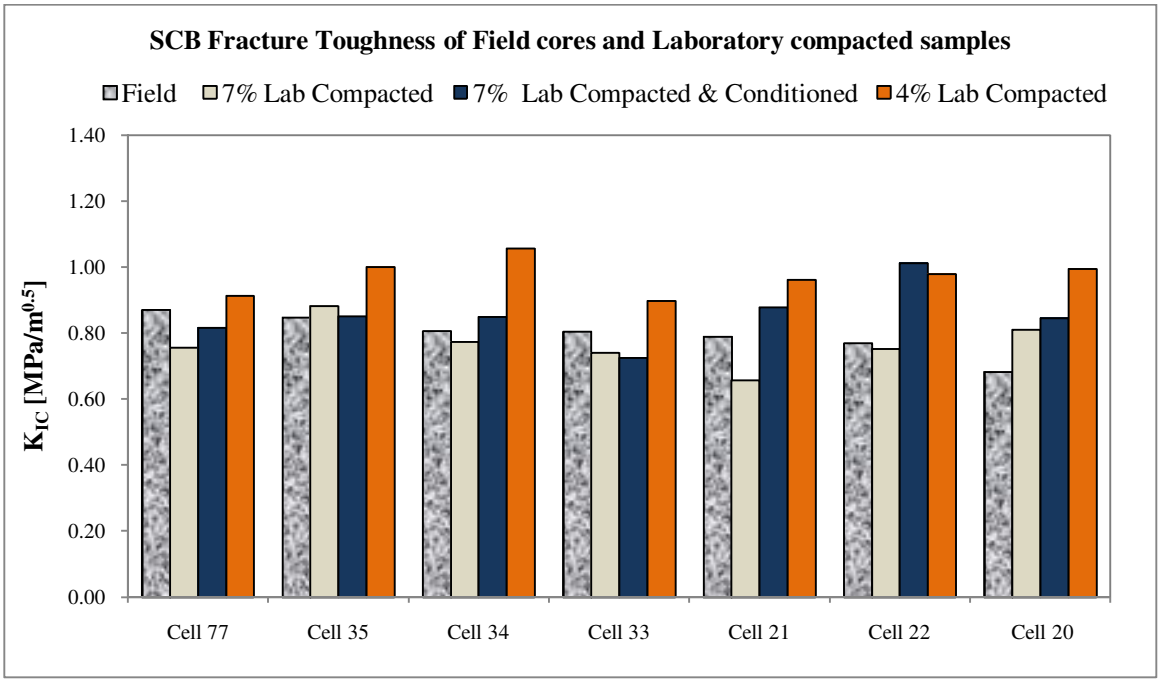

Figure 15. SCB fracture toughness test results for field cores

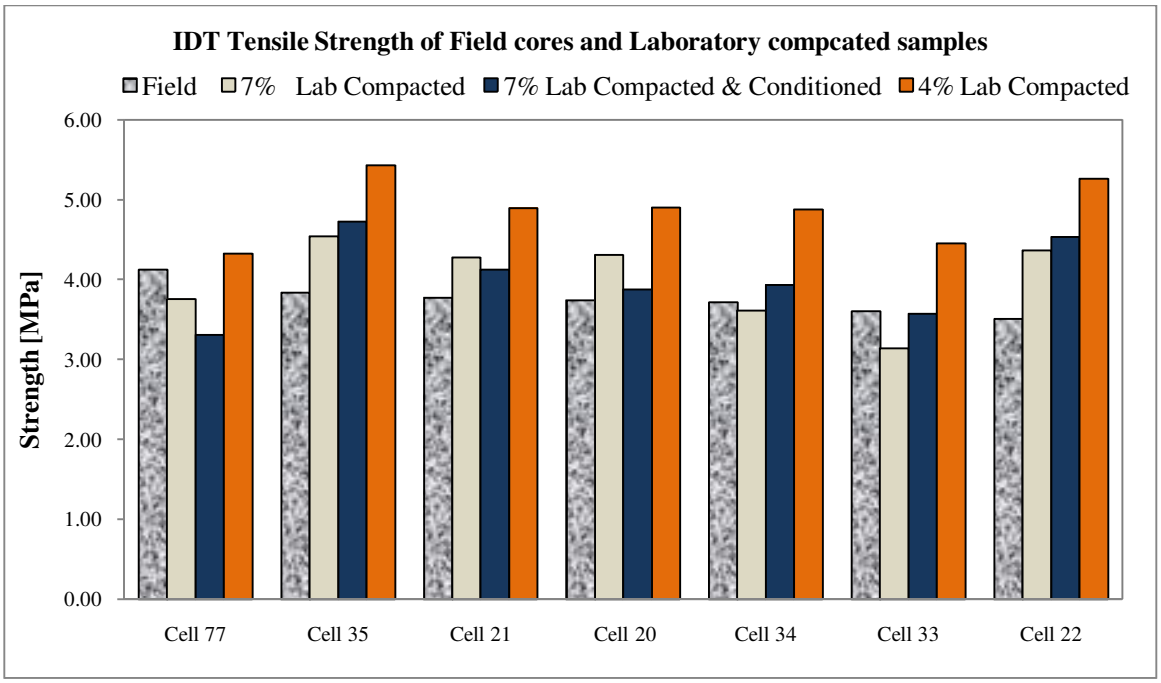

Figure 16. IDT tensile strength test results for field cores

In Figure 13, the DCT fracture energy values for the field cores are comparable to the fracture energy values for the laboratory compacted specimens. This is not true for the SCB results in Figure 14: the SCB fracture energy for the field specimens is considerably lower compared to the laboratory compacted specimens.

In Figure 15, the fracture toughness of the field cores is compared to the fracture toughness of the laboratory compacted specimens. Contrarily to SCB fracture energy, the fracture toughness for field cores appears to be comparable to the fracture toughness of laboratory compacted samples.

In Figure 16, the seven tested mixtures are ranked from the largest to the smallest, with regard to their IDT strength response. The plot also compares the field samples results to laboratory compacted specimens results. The strength of the field cores do not appear to vary significantly for the different mixture.

With regard to field cores, it is worth mentioning that mixture 77 is ranked first according to DCT fracture energy, SCB fracture toughness and IDT strength.

Statistical analysis of DCT, SCB, and IDT strength for field cored specimens.

The ANOVA tables for the different fracture test parameters are reproduced in Table 24. Accordingly, the mixture type variance is significant only for the SCB fracture energy. For the other parameters, the field cored specimens are statistically similar.

Table 24. ANOVA table for DCT, SCB and IDT strength of field specimens

Model used is for DCT fracture energy log(GF)=(mix)					
	DF	**SS**	**MS**	**F**	**P-value**
CONSTANT	1	695.75	695.75	19892.36164	< 1e-08
mix	6	0.4127	0.068783	1.96658	0.13936
ERROR1	14	0.48966	0.034976		

Model used for SCB fracture energy is log(GF)=mix summaries are sequential					
	DF	**SS**	**MS**	**F**	**P-value**
CONSTANT	1	627.07	627.07	29690.95230	< 1e-08
mix	6	1.4091	0.23484	11.11943	0.0001786
ERROR1	13	0.27456	0.02112		

Model used for SCB fracture toughness is KIC=mix					
	DF	**SS**	**MS**	**F**	**P-value**
CONSTANT	1	13.294	13.294	2283.57501	< 1e-08
mix	6	0.065606	0.010934	1.87829	0.15526
ERROR1	14	0.0815	0.0058214		

Model used for IDT strength is Strength=mix					
	DF	**SS**	**MS**	**F**	**P-value**
CONSTANT	1	296.82	296.82	5974.84282	< 1e-08
mix	6	0.68544	0.11424	2.29962	0.093478
ERROR1	14	0.69549	0.049678		

Following, a multiple comparison was carried out using the SCB fracture energy test data. The mixtures were ranked from the best performing (A) to poor performing ones. Similarly to the laboratory compacted analyses, mixture that are statically not different are included in one group. The outcome is shown in Table 25. It can be noticed that mixture 35, is again ranked at the top of the ranking. While mixture 21, contrarily to what was observed in laboratory specimens analysis, has a poor SCB fracture energy result.

Table 25. Mixture ranking SCB fracture energy – field specimens

SCB fracture energy [J/m^2]		
Mix Type	Group Mean	Rank
21	162.41	C
20	207.16	B/C
33	246.34	B/C
34	288.36	A/B
77	301.46	A/B
22	306.49	A/B
35	421.29	A

Comparison of field cores and laboratory compacted test results

In Figure 17 to Figure 20 the results for the field specimens are plotted against the similar results for the laboratory specimens tested at PGLT.

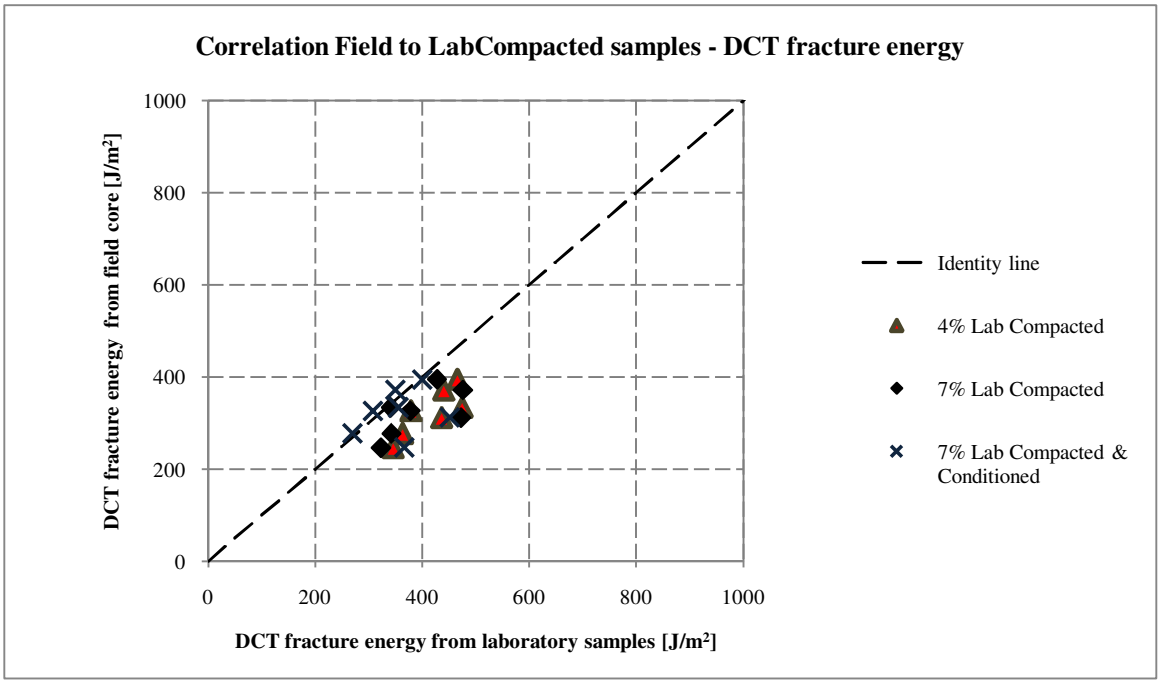

Figure 17. Results comparison field to laboratory compacted, DCT fracture energy

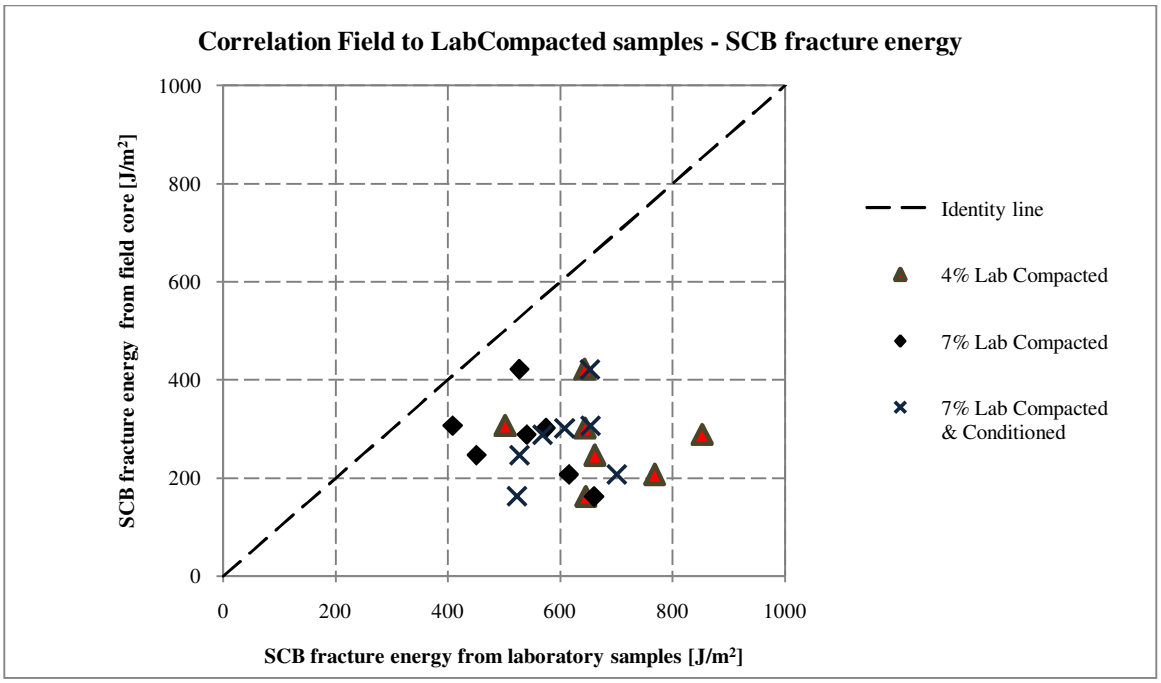

Figure 18. Results comparison field to laboratory compacted, SCB fracture energy

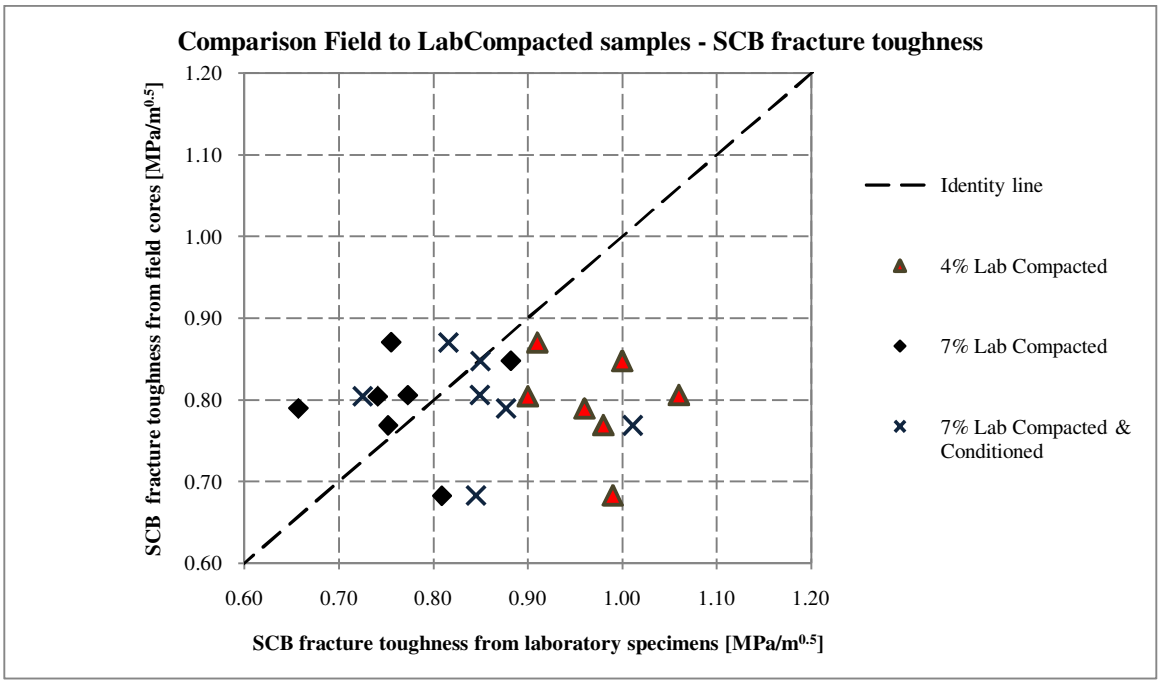

Figure 19. Results comparison field to laboratory compacted, SCB fracture toughness

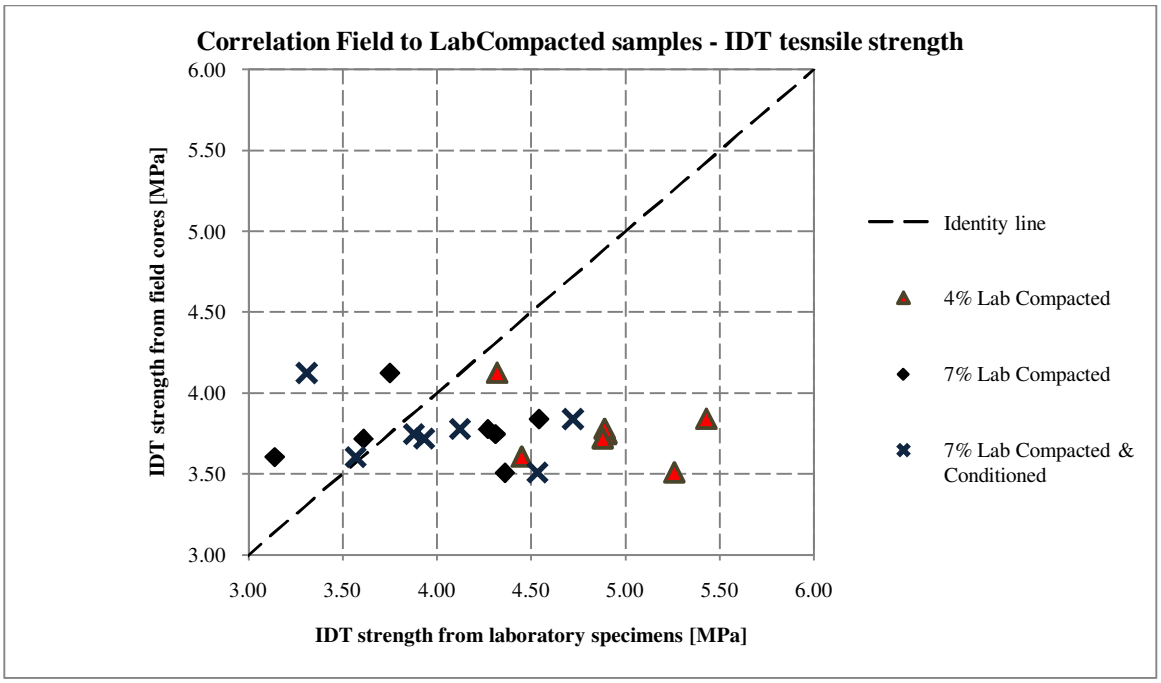

Figure 20. Results comparison field to laboratory compacted, IDT tensile strength

For DCT fracture energy, all the correlation points are located along the identity line. By looking closer at the points, it can be observed that the 7% conditioned laboratory specimens correlate best with the field DCT fracture response.

The correlation points for the SCB fracture energy are noticeably skewed to the right. The reason for this is that the laboratory SCB fracture energy responses are considerably higher than those obtained from field specimens. The "best" correlation is obtained for the non-conditioned 7% laboratory.

For the SCB fracture toughness and the IDT strength results, relatively poor correlations are observed between field and laboratory specimens. The point are more dispersed and far from the identity line.

Finally, the linear correlation coefficient, r, that measures the strength and direction of a linear relationship between two variables, was computed for each test method. The correlation coefficient ranges from -1 to +1. The closer r is to +1 or -1, the more closely the two data sets are related. The outcomes are reported in Table 26. Accordingly, high correlations coefficients are observed for DCT and SCB fracture energy results.

Table 26. Correlation coefficients field vs. laboratory samples data I

Correlation coefficients of Field data to Lab				
Test conditions for laboratory samples	SCB Fracture energy	SCB Fracture toughness	DCT Fracture energy	IDT Strength
7%- PGLT	-0.48	0.05	0.64	0.02
7%- PGLT-Conditioning	0.38	-0.25	0.26	-0.44
4%- PGLT	-0.20	-0.25	0.81	-0.41

Comparison of experimental results obtained at UIUC and UMN

As mentioned in the introduction, DCT test were performed at UMN for three randomly selected mixtures. Likewise, SCB tests were performed at UIUC for three randomly selected mixtures. The results are discussed next.

DCT tests performed at UMN

Three mixtures were randomly selected and DCT tested at UMN using the same procedures and specification used by the UIUC research team. The mixtures tested at UMN were 20, 21, and 22. Comparison of the results is shown in Figure 21.

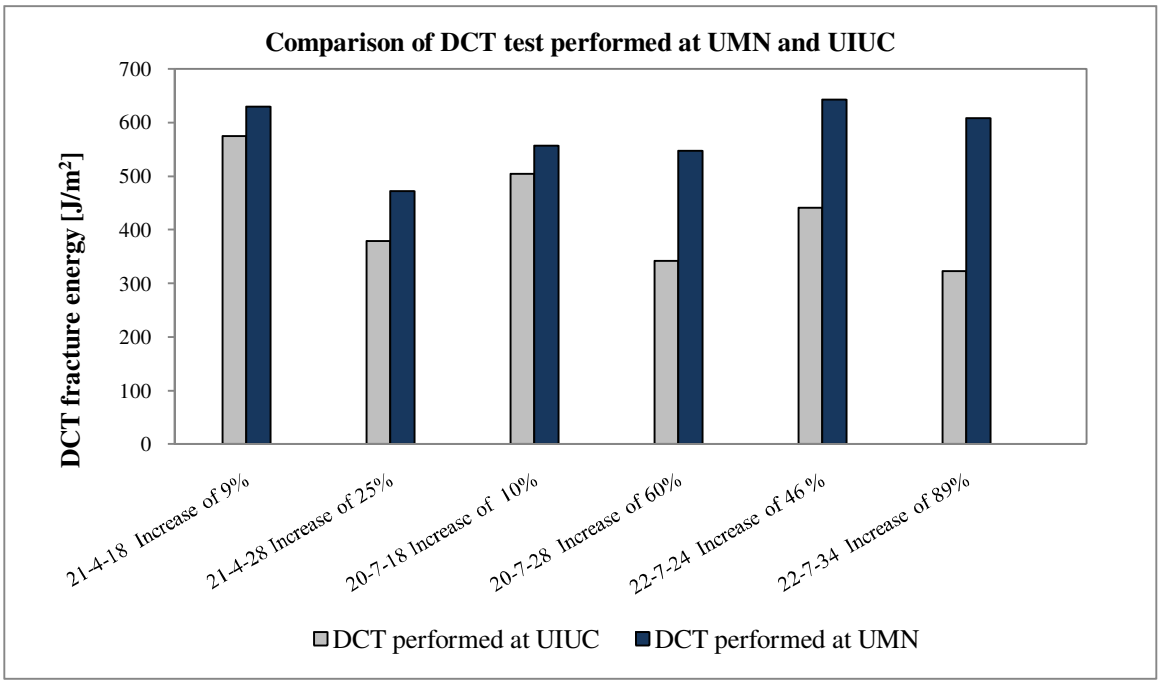

Figure 21. Comparison DCT test result performed at different laboratories

Overall, it is observed that DCT fracture energy values from UMN are higher than those from UIUC. The differences ranged from 9% to 89%. To understand the reason for the considerable discrepancies, the test results were investigated further. The Load vs. CMOD and

the CMOD vs. Time plots for the three replicates of mixture 22, that has the highest difference, are shown in Figure 22.

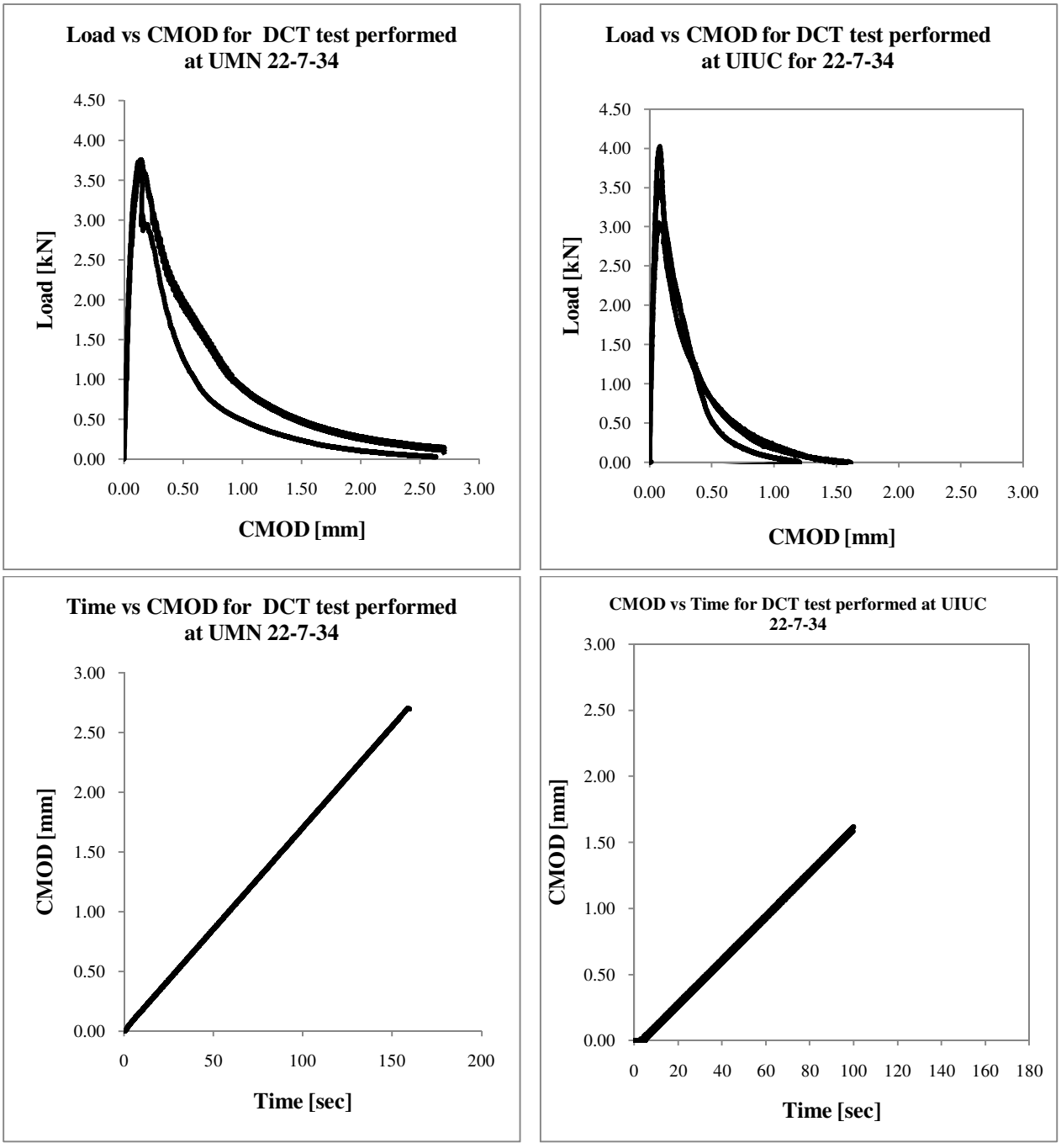

Figure 22. Load vs. CMOD and Time vs. CMOD plots

The Load-CMOD curves presented in the Figure 22 show that post-peak curve from UMN test data decreases slower than the post-peak curves from UIUC. The registered peak loads

are also slightly higher for UIUC performed tests. The CMOD vs. Time plots were also produced to check for a possible cause of the discrepancy. For the tests performed at UMN, time was recorded for each test. In the test data obtained from UIUC, time was not provided. Thus, a time column were calculated based on sampling rate of 50Hz, as indicated by UIUC researches.

SCB tests performed at UIUC

Three randomly selected mixtures were SCB tested at UIUC. The mixtures tested were mixture 35 at two different void contents, and mixture 'NY'. The results shown in Figure 23a indicate considerable differences between UIUC and UMN results. As mentioned previously, the SCB test performed at UIUC did not use LLD measurements. Instead, the displacement of the loading piston, recorded through its LVDT, was used. Although this is not the recommended approach, for the sake of comparison, the SCB fracture energy using the piston head movement were also computed for the SCB tests performed at UMN.

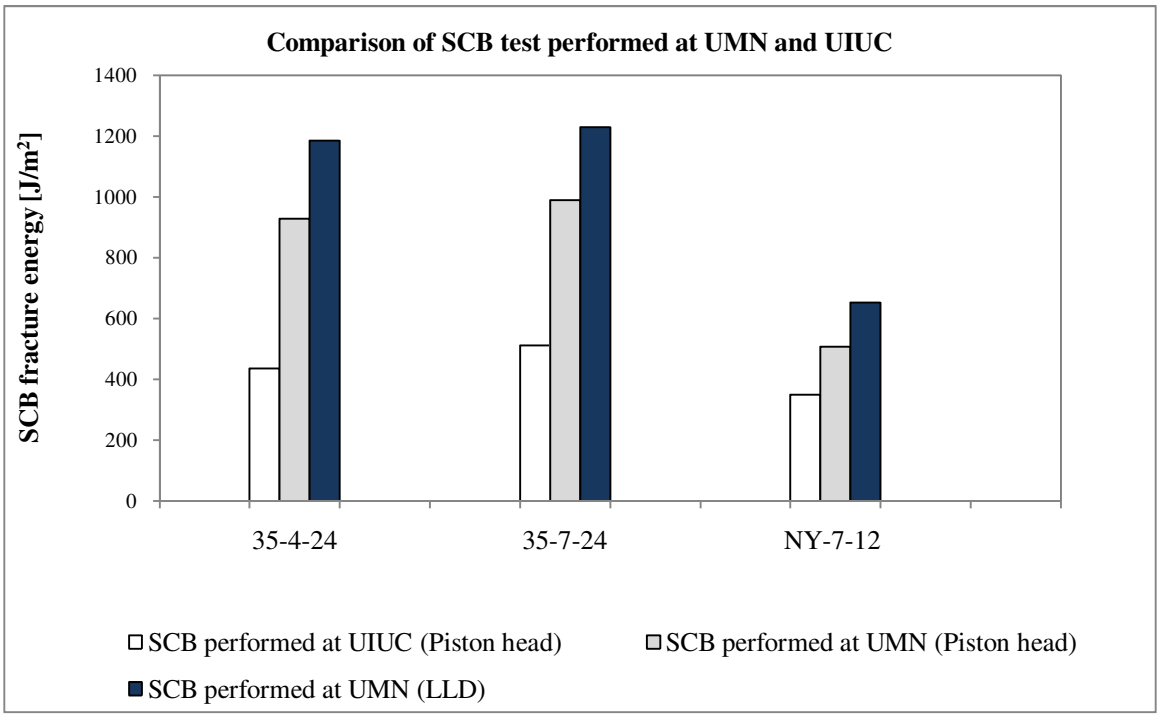

Figure 23a. SCB fracture energy from test performed at different laboratories

The fracture toughness values of the mixtures were also computed from the test data obtained from UIUC and compared to the test performed at UMN. The results are reported in Figure 23b. For fracture toughness the results are in good agreement.

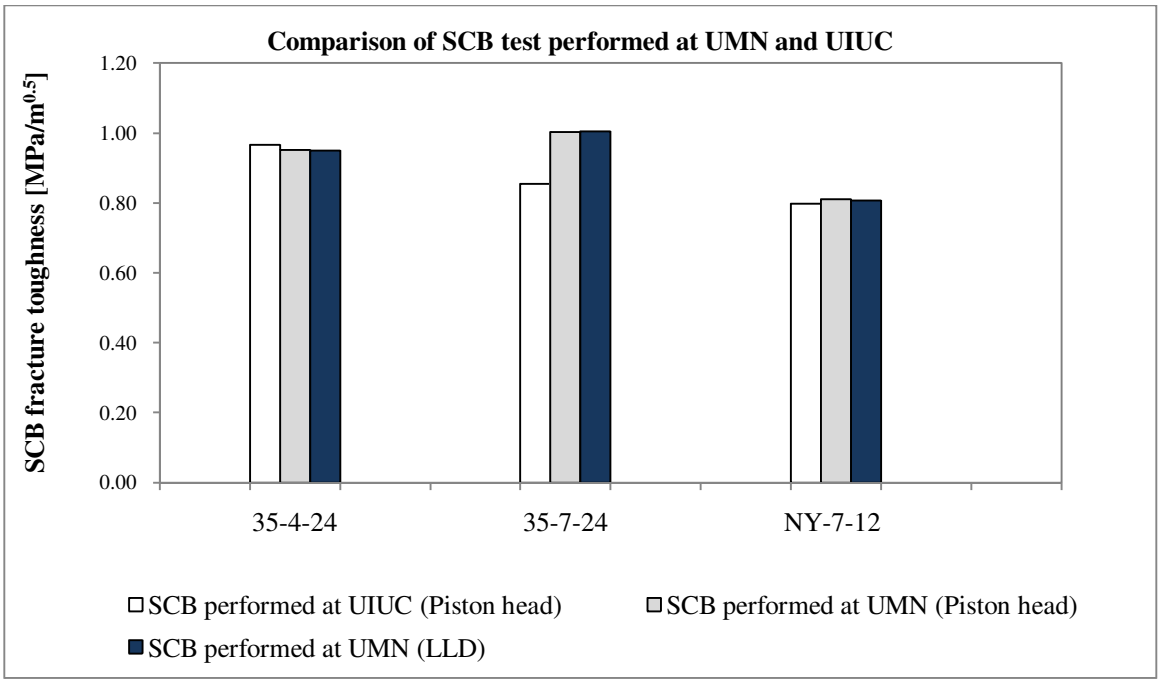

Figure 23b. SCB fracture toughness from test performed at different laboratories

The test results were investigated further. The Load vs. LVDT and the CMOD vs. Time plots for the replicates of mixture 35 are shown in Figure 22. Similar to the DCT data, the Load vs. LVDT curves show that post-peak curve from UMN test data decreases slower than the post-peak curves from UIUC.

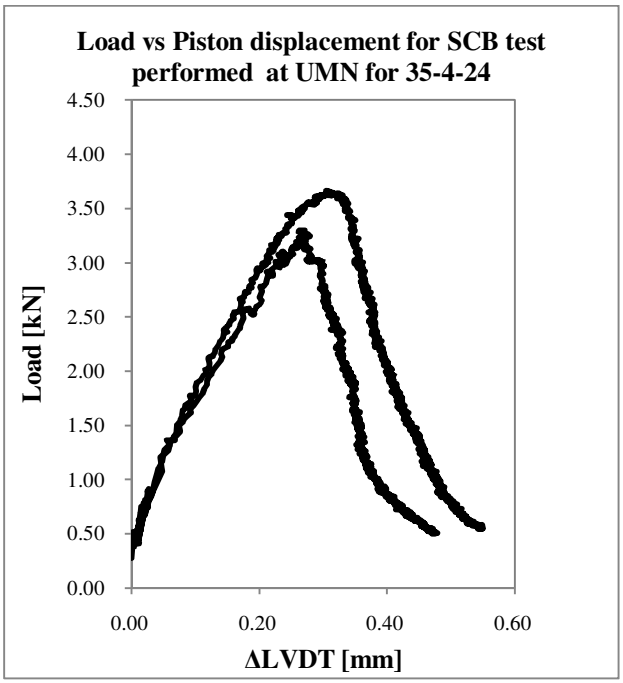

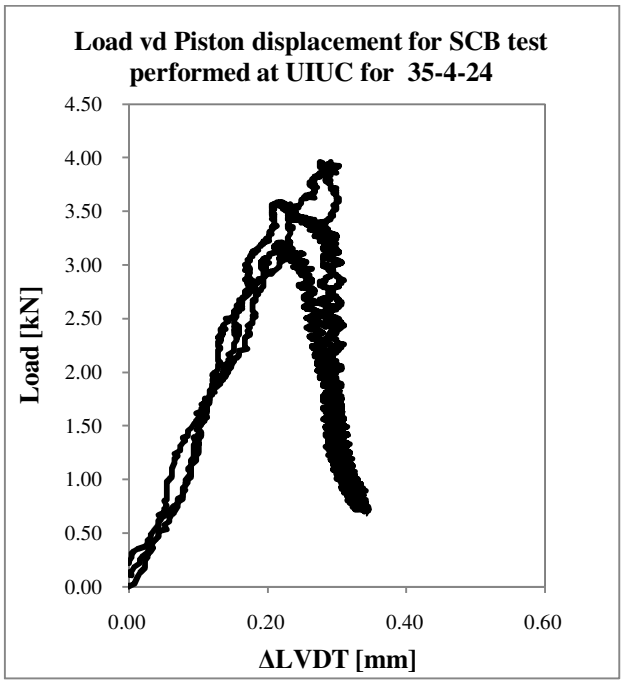

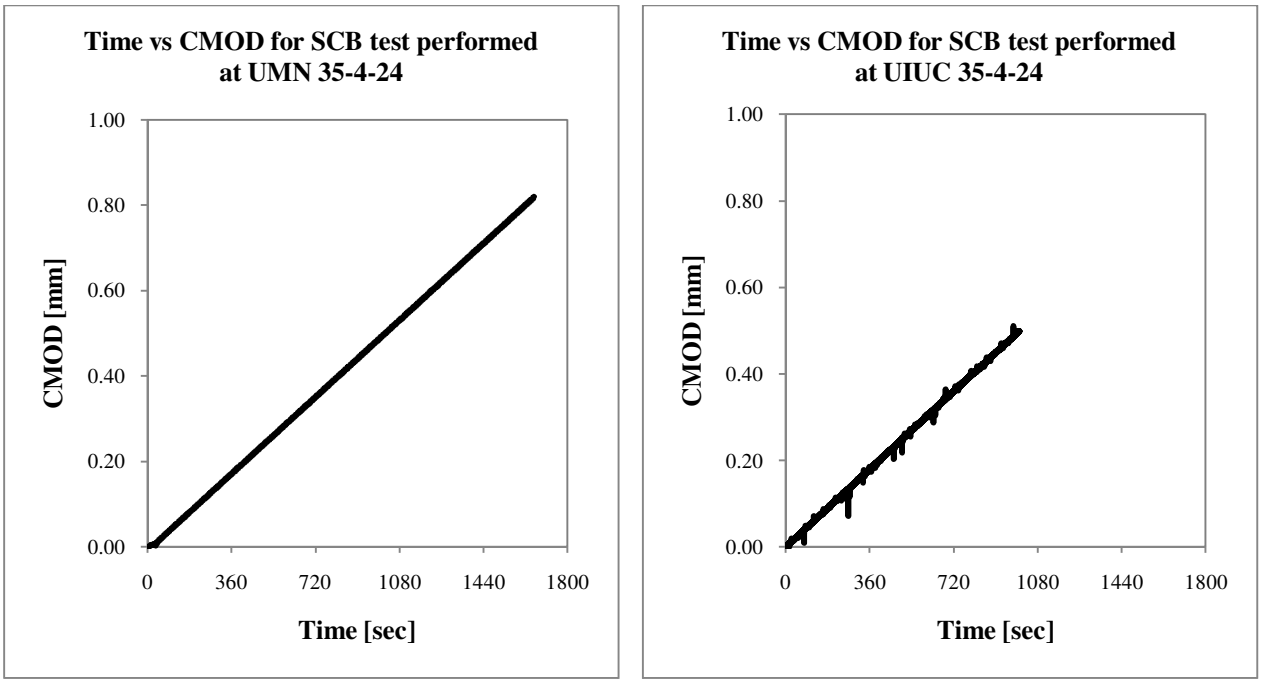

Figure 24. SCB fracture toughness from test performed at different laboratories

Data analysis of IDT creep stiffness for laboratory compacted specimens.

The results for the creep stiffness, computed from the IDT creep test data, are reported next. Figure 24 and Figure 25 summarize the result for creep stiffness at 60 and 500 sec, respectively. It can be noticed that, the tested mixtures are always stiffer at the lowest test temperature. In addition, the effect of test temperature on the material stiffness appears to be more pronounced at the 4% air void content. The mixtures are ranked from the largest to the smallest stiffness measured at PGLT+10. Therefore, it can be observed that the ranking changes considerably with test temperature.

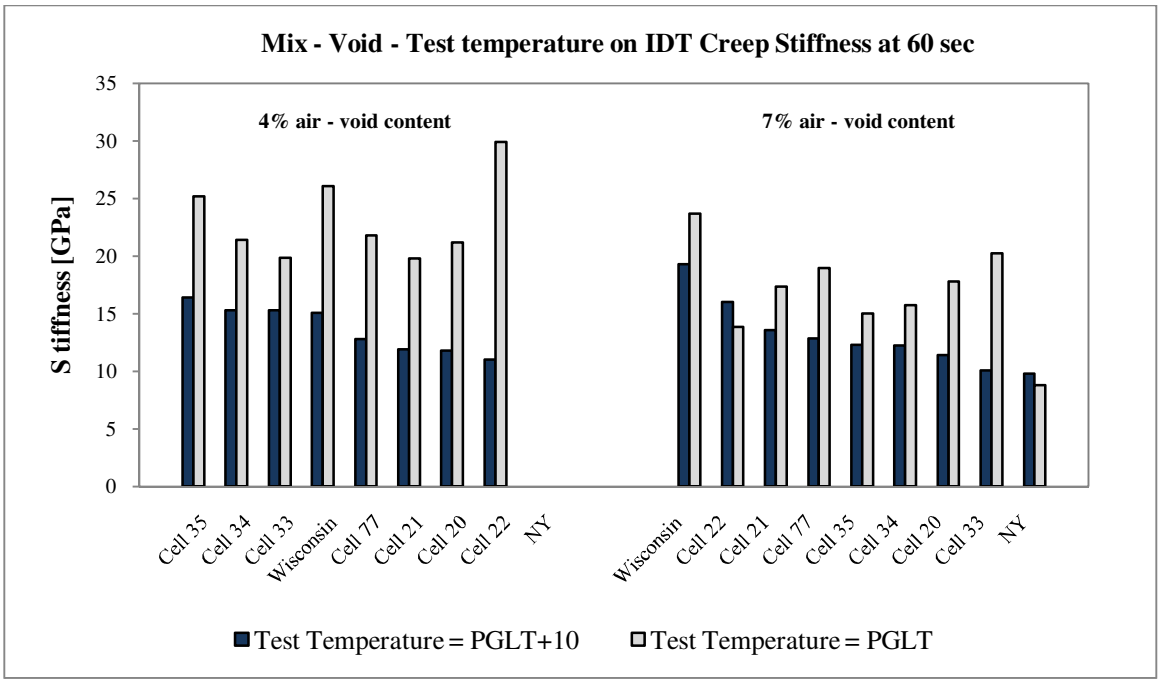

Figure 24. IDT creep stiffness at 60 sec test results

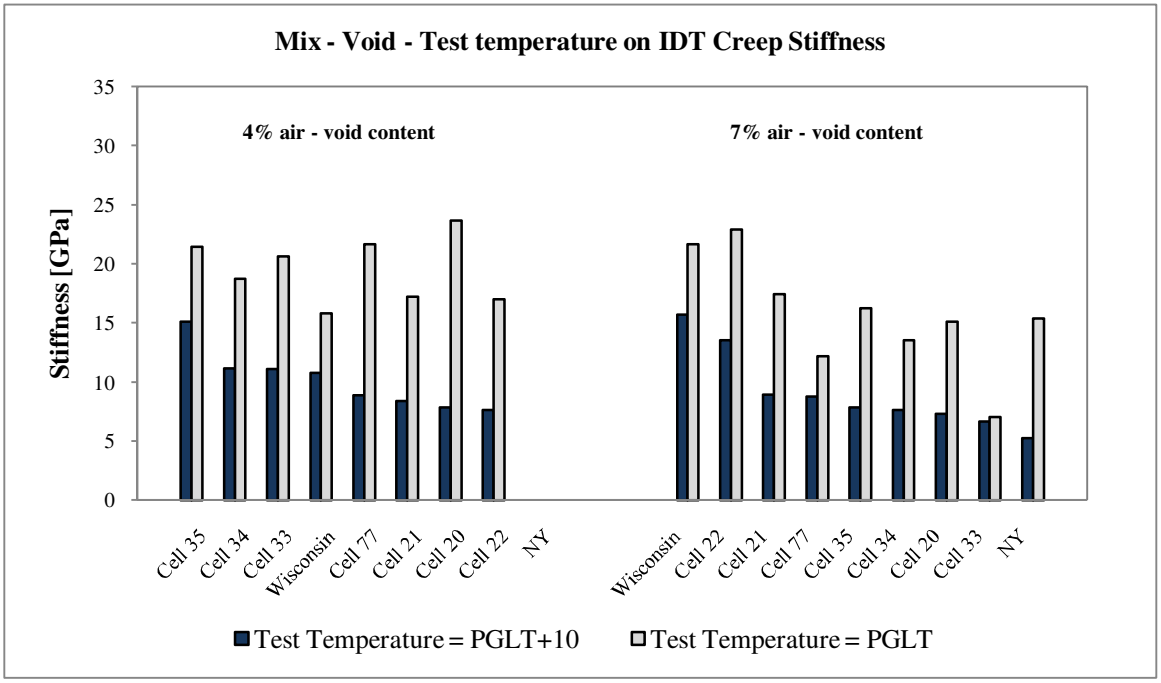

Figure 25. IDT creep stiffness at 500 sec test results

Statistical analysis of IDT creep stiffness for laboratory compacted specimens.

Table 27 reports the ANOVA outcomes for stiffness at 60 and 500 sec, respectively. Accordingly, the main effects for mix, void content, and test temperatures are highly significant for both parameters. In addition, the higher order factor interactions were also found to be highly significant. A multiple comparison performed on the stiffness data (see Table 28) indicates that, mixture '*Wisconsin'* stiffness mean value is statistically higher than the stiffness of the other mixtures.

Table 27. ANOVA tables for IDT creep stiffness for laboratory specimens

Model used for IDT c. stiffness at 60sec is log(S60)=(mix+void+temp)^3

SS are Type III sums of squares

	DF	SS	MS	F	P-value
CONSTANT	1	664.08	664.08	28570.06912	< 1e-08
mix	7	0.77976	0.11139	4.79245	0.00028232
void	1	0.46086	0.46086	19.82708	4.0952e-05
temp	1	3.504	3.504	150.74818	< 1e-08
mix.void	7	0.43698	0.062425	2.68569	0.018006
mix.temp	7	0.11248	0.016068	0.69130	0.67894
void.temp	1	0.2825	0.2825	12.15388	0.00096001
mix.void.temp	7	0.83352	0.11907	5.12288	0.00015179
ERROR1	56	1.3016	0.023244		

Model used is IDT creep stiffness at S500=(mix+void+temp)^3

SS are Type III sums of squares

	DF	SS	MS	F	P-value
CONSTANT	1	17072	17072	4826.90692	< 1e-08
mix	7	511.75	73.108	20.66977	< 1e-08
void	1	65.554	65.554	18.53419	6.5098e-05
temp	1	1558.3	1558.3	440.56793	< 1e-08
mix.void	7	96.71	13.816	3.90611	0.0014966
mix.temp	7	96.365	13.766	3.89219	0.0015386
void.temp	1	21.32	21.32	6.02785	0.017101
mix.void.temp	7	62.878	8.9825	2.53964	0.023763
ERROR1	58	205.14	3.5369		

Table 28. Statistical grouping and ranking of mixtures with regard to stiffness

IDT creep stiffness [MPa]				
Mix Type	S60 Mean	Rank	S500 Mean	Rank
20	12.33	B/C	15.878	B
21	12.039	C	16.222	B
22	17.81	A	19.043	A/B
33	12.388	B/C	16.354	B
34	12.69	B/C	16.219	B
35	13.954	B/C	17.418	A/B
77	14.207	B	16.599	B
Wisconsin	18.481	A	21.028	A

Data analysis of IDT creep stiffness for field cored specimens.

Figure 26 and Figure 27 MnROAD mixtures are ranked from largest to smallest creep stiffness for tests performed at PGLT. The stiffness results for field cores indicate that mixture 35 is the least stiff mixture and mixture 22 is the stiffest mixture. In addition, the plot shows that the conditioned 7% laboratory compacted specimen are comparable to field cores, with regard to S(60s). When S(500s) is considered, the responses from unconditioned 4% laboratory compacted specimens appear to be closer to the field results.

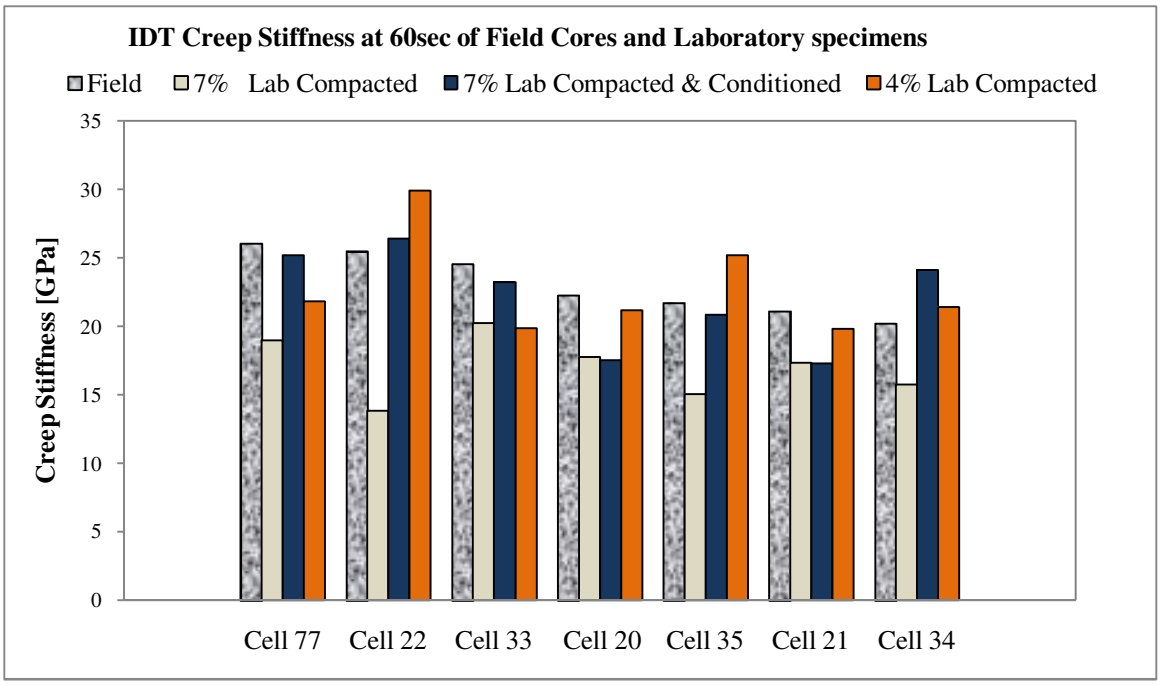

Figure 26. IDT creep stiffness at 60 sec test results for field cores

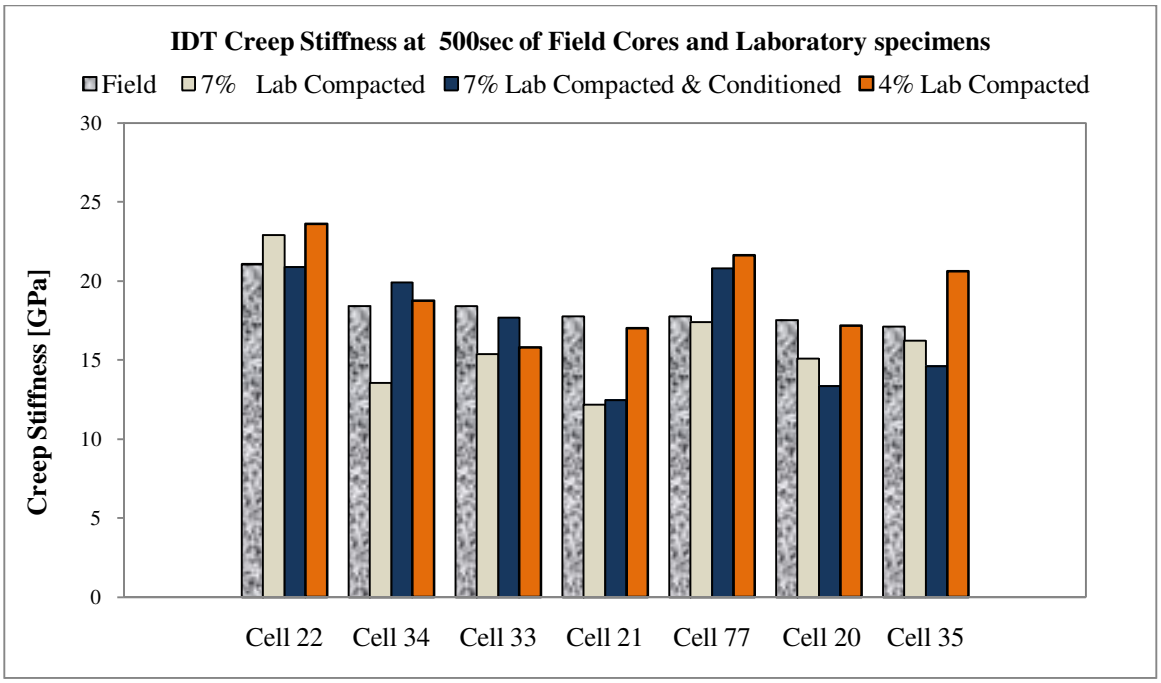

Figure 27. IDT creep stiffness at 500sec test results for field cores

Statistical analysis of IDT creep stiffness for field cored specimens.

Table 29 summarizes the ANOVA tables performed for IDT creep stiffness of field mixtures. From the table it appears that the variance of response due to mixture type is not significant.

Table 29. ANOVA tables for IDT creep stiffness for field specimens

Model used for IDT c.stiffness at 60 sec is S60=mix					
	DF	**SS**	**MS**	**F**	**P-value**
CONSTANT	1	11331	11331	1214.28832	< 1e-08
mix	6	86.136	14.356	1.53844	0.23681
ERROR1	14	130.64	9.3316		

Model for IDT c.stiffness at 500 sec used is S500=mix					
	DF	**SS**	**MS**	**F**	**P-value**
CONSTANT	1	7073.7	7073.7	2201.89166	< 1e-08
mix	6	22.259	3.7098	1.15479	0.38278
ERROR1	14	44.976	3.2126		

IDT creep stiffness correlation field cores to laboratory compacted

Similarly to the fracture and strength test parameters, the creep stiffness values obtained from laboratory compacted specimens were compared to stiffness values of same mixture obtained from field cored specimens, as shown in Figure 28 and Figure 29. The plots appear to suggest that for creep stiffness measured at 60 sec, best field to lab-compacted correlation are observed for the 7% conditioned specimens.

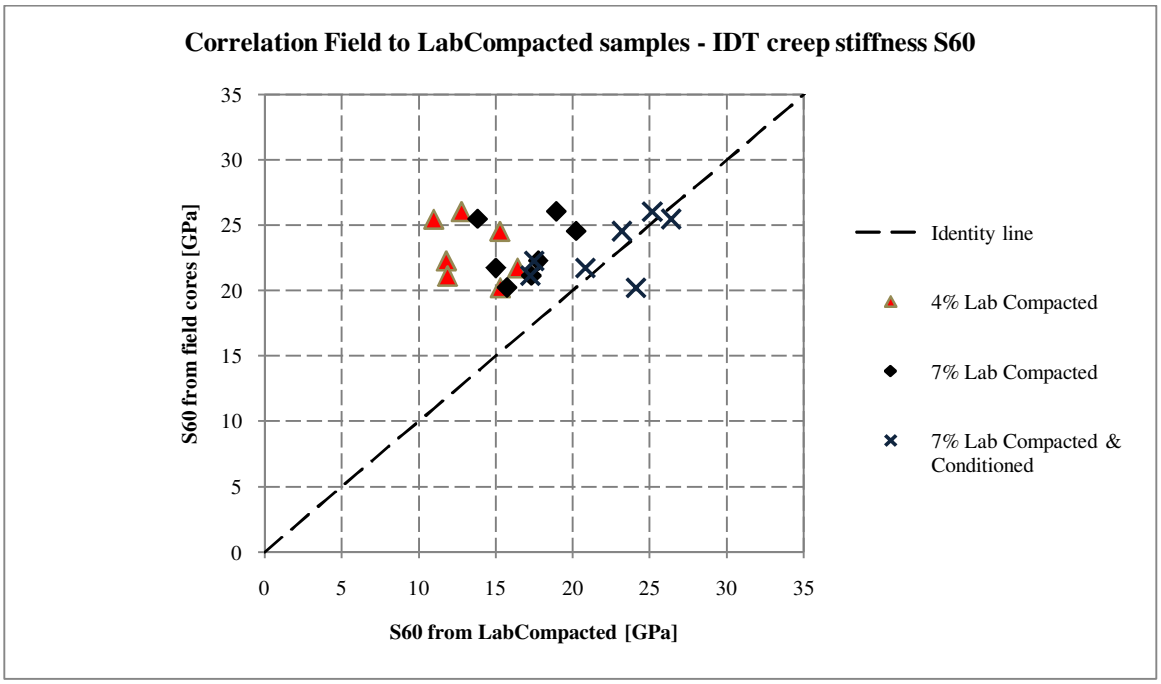

Figure 28. Results comparison field to laboratory compacted, IDT creep stiffness @ 60sec

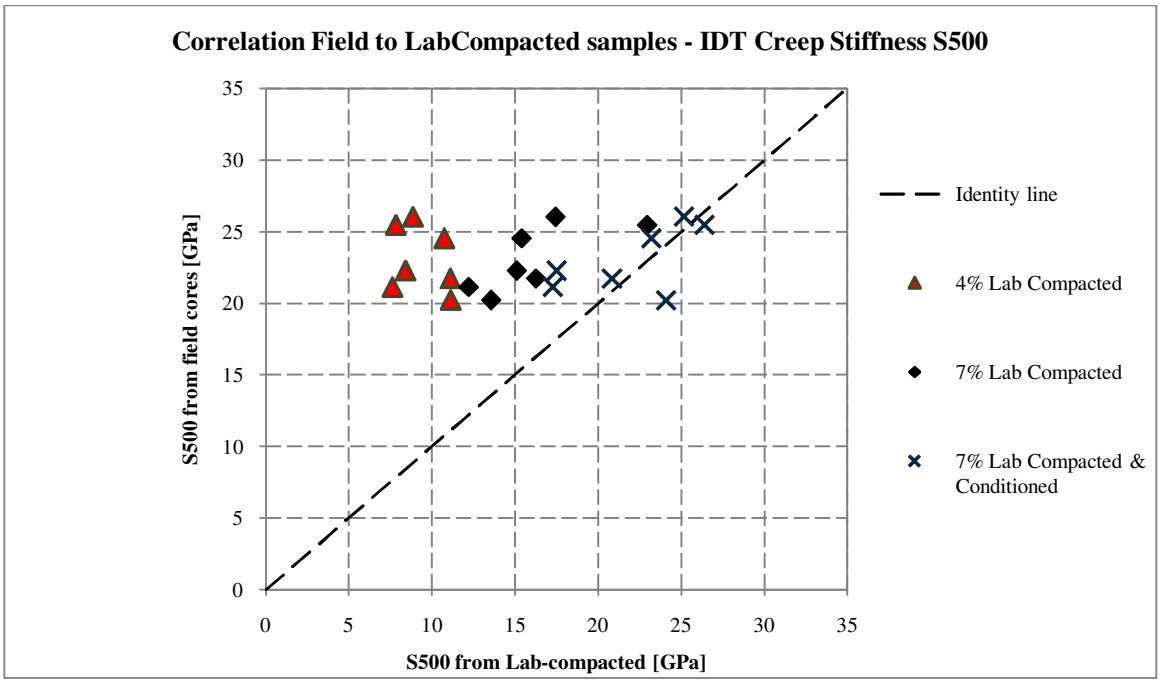

Figure 29. Results comparison field to laboratory compacted, IDT creep stiffness @ 500sec

An analysis of the correlation coefficients of the test data, shown below, indicate that for S60, laboratory specimens of 7% air void content, conditioned and tested at PGLT have the highest correlation coefficient. For stiffness measured at 500sec, the 7% specimens tested at PGLT offers best correlation.

Table 30. Correlation coefficients field vs laboratory samples data II

Correlation coefficients of Field data to Lab		
Test conditions for laboratory samples	IDT Creep stiffness S60	IDT Creep stiffness S500
7%- PGLT	0.26	0.73
7%- PGLT-Conditioned	0.61	0.61
4%- PGLT	0.36	0.47

Effects of long term mix conditioning

In this section, the effect of long term mix conditioning on the mixtures fracture properties, is investigated. The objective is to assess the sensibility to mix conditioning of the various test protocols. Test responses, obtained from specimens conditioned for 5 days at 85˚C prior to testing, were compared to test responses obtained from the unconditioned specimens. The specimens considered for this investigation, were all compacted to 7% void content, and were tested at the lowest test temperature, PGLT.

Effect of mix conditioning on DCT, SCB and IDT strength

Figure 30 comprises the conditioned vs. non-conditioned plots for the DCT and SCB parameters, as well IDT tensile strength. The mixtures are ranked from the largest to the smallest increase in response due to conditioning. The mixtures, for which the response differed significantly from the responses of the majority of the mixtures, are highlighted (dotted circles). For DCT fracture energy, it appears that the mix conditioning decreases the fracture energy in all mixtures, except for cells 22 and 33. On the contrary, for SCB fracture energy there is an increase in fracture energy due to conditioning for all mixtures, except mixture 21 and NY. In agreement to the SCB fracture energy, the SCB fracture toughness values increase with mix conditioning for all mixtures, except for mixtures 33 and 35. Finally, the plot corresponding to IDT tensile strength appears to suggest that conditioning increase the strength of the mixtures except for mixtures 21, 20, and 77.

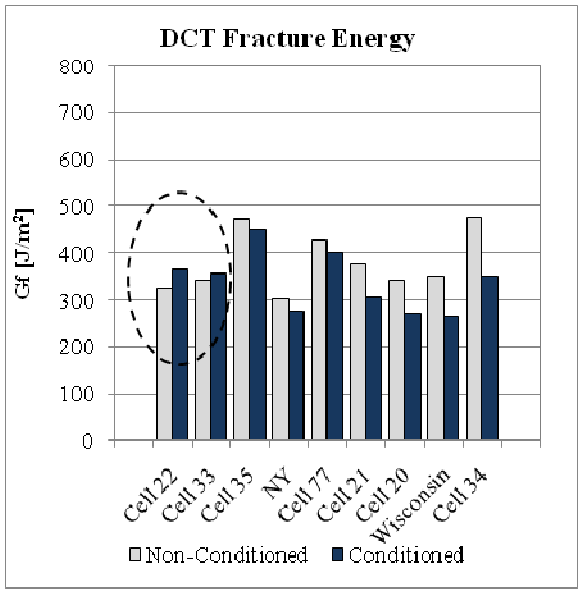

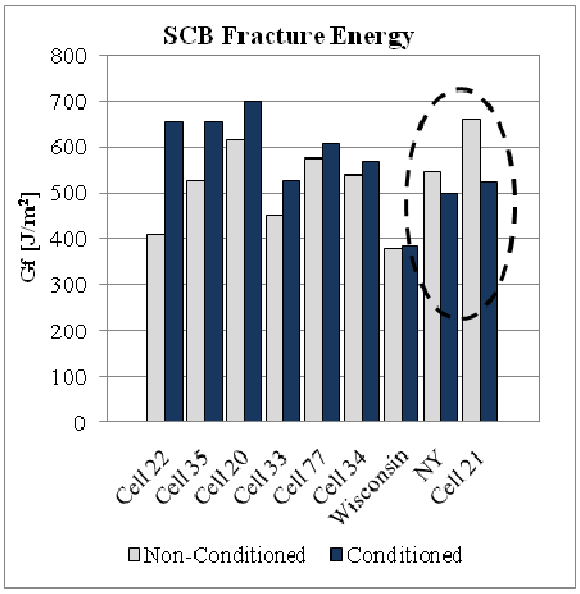

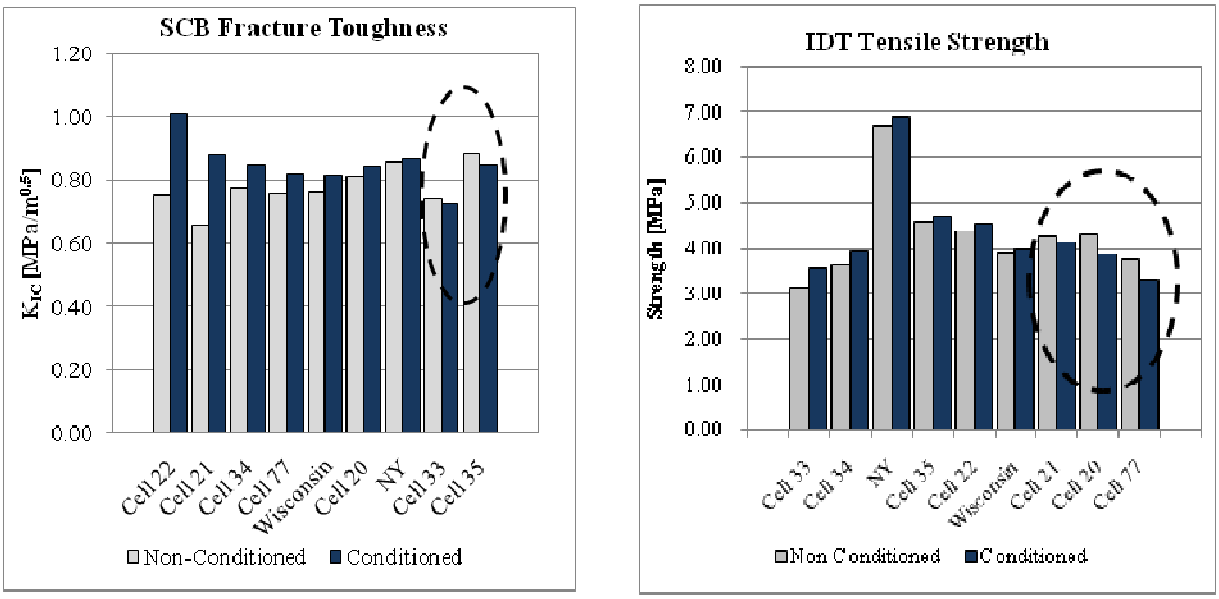

Figure 30. Effect of mix conditioning on DCT, SCB, and IDT tensile strength

Additional Statistical analysis for mix conditioning, DCT, SCB, and IDT strength

The effects of mix conditioning on the different parameters were also investigated through ANOVA, and the above mentioned findings were confirmed. Table 31, presents the outcome of the analysis. Accordingly, mix conditioning resulted to be significant only for DCT fracture energy and SCB fracture toughness. Therefore, based on DCT data, there is a statistically significant decrease in fracture energy due to mix conditioning. On contrary, SCB fracture toughness increases due to mix conditioning. The ANOVA tables also show that the two-way interaction factors, mix to mix-conditioning, are considered statistically irrelevant for all the studied cases.

Table 31. ANOVA mix-conditioning effect on DCT,SCB, and IDT strength, lab-compacted

Model used is for DCT fracture energy GF=(mix+cond)^2
SS are Type III sums of squares

	DF	SS	MS	F	P-value
CONSTANT	1	6.2465e+06	6.2465e+06	3057.039	< 1e-08
mix	8	1.5238e+05	19047	9.32183	1.5641e-06
cond	1	20677	20677	10.11950	0.0032534
mix.cond	8	32083	4010.4	1.96268	0.084287
ERROR1	32	65386	2043.3		

Model used is for SCB fracture energy GF=(mix+cond)^2
SS are Type III sums of squares

	DF	SS	MS	F	P-value
CONSTANT	1	1.4451e+07	1.4451e+07	1563.291	< 1e-08
mix	8	2.4041e+05	30051	3.25101	0.0080211
cond	1	26463	26463	2.86282	0.10037
mix.cond	8	1.2675e+05	15843	1.71395	0.13325
ERROR1	32	2.958e+05	9243.7		

Model used isfor SCB fracture toughness K_{IC}=(mix+cond)^2
SS are Type III sums of squares

	DF	SS	MS	F	P-value
CONSTANT	1	34.766	34.766	4616.927	< 1e-08
mix	8	0.11953	0.014941	1.98419	0.077883
cond	1	0.071656	0.071656	9.51611	0.0039631
mix.cond	8	0.12194	0.015242	2.02422	0.072171
ERROR1	35	0.26355	0.00753		

Model used is for IDT strength =(mix+cond)^2
SS are Type III sums of squares

	DF	SS	MS	F	P-value
CONSTANT	1	948.19	948.19	10897.96566	< 1e-08
mix	8	48.809	6.1011	70.12230	< 1e-08
cond	1	0.018151	0.018151	0.20861	0.65076
mix.cond	8	1.09	0.13625	1.56594	0.17192
ERROR1	34	2.9582	0.087006		

Effect of mix conditioning on IDT creep stiffness.

Figure 31, presents the conditioned and unconditioned mixtures, plotted against their corresponding IDT creep stiffness. The stiffness values measured at 60 seconds are generally higher for the conditioned mixtures. For stiffness measured at 500 seconds it can be observed that stiffness increases due to conditioning for mixtures 34, Wisconsin, 77, 33, and 21. A considerable decrease in stiffness is observed for the rest of the mixtures, which are highlighted by dotted circles in the figure.

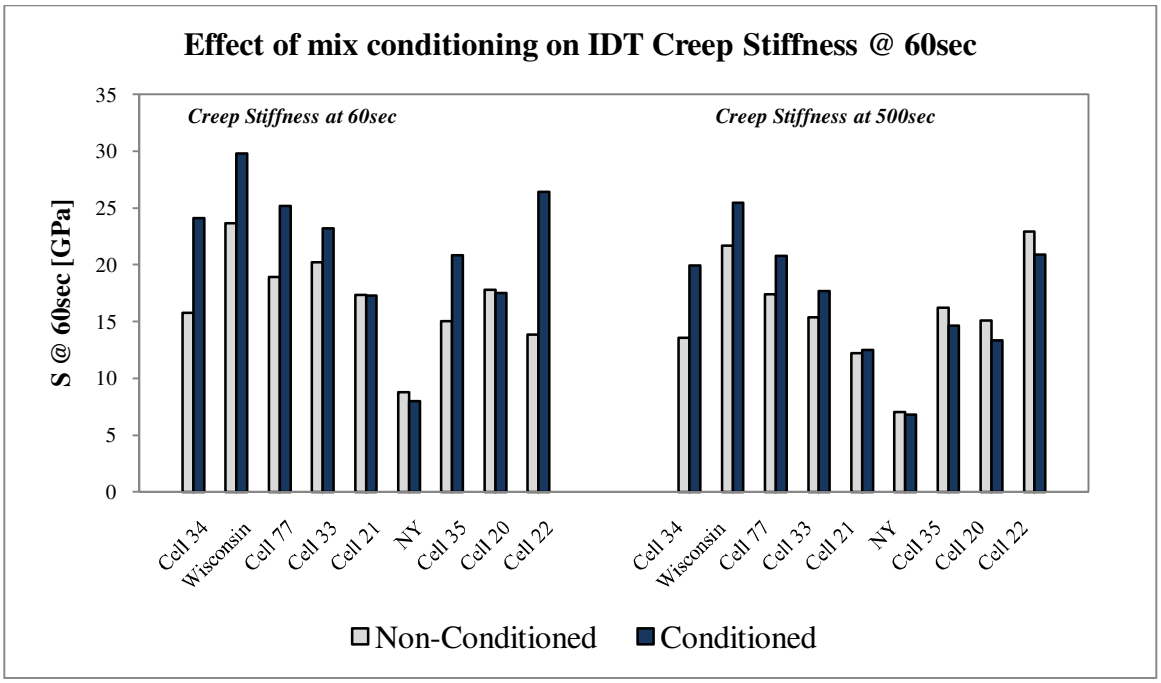

Figure 31. Effect of mix conditioning on IDT creep stiffness

Additional Statistical analysis for mix conditioning, IDT creep stiffness

The ANOVA analyses for evaluating the effect of mix conditioning on the mixture's stiffness are reported in Table 32. The main effect for conditioning if significant only for stiffness measured at 60 sec. Therefore, conditioning increases significantly the stiffness of the mixture obtained after 60s of loading.

Table 32. ANOVA mix-conditioning effect on IDT creep stiffness

Model used for IDT stiffness at 60 sec is S60= mix+cond					
	DF	SS	MS	F	P-value
CONSTANT	1	21452	21452	1212.85729	< 1e-08
mix	8	1307.3	163.42	9.23941	2.3372e-07
cond	1	110.45	110.45	6.24449	0.016264
ERROR1	44	778.22	17.687		

Model used for IDT stiffness at 500 sec is S500= mix+cond					
	DF	SS	MS	F	P-value
CONSTANT	1	14896	14896	1802.28526	< 1e-08
mix	8	1262.5	157.82	19.09393	< 1e-08
cond	1	3.9643	3.9643	0.47963	0.49223
ERROR1	44	363.67	8.2653		

Effects of asphalt modification on mixture properties

The effects of polymer and acid modification, as well as of RAP fractionation and binder's PG low limit on the fracture properties of the mixtures were also investigated. The mixtures considered for the analysis of polymer and acid modified asphalts are listed in Table 33. Two polymers, SBS and Elvaloy, and one acid modifier PPA were used in preparing the mixtures, as shown in the table below.

Table 33. Mixtures for polymer and acid modified asphalt analysis

Mixture	Modifiers
33	PPA
34	SBS+PPA
35	SBS
77	Elvaloy + PPA

Effects of modified asphalts on DCT, SCB, and IDT strength of laboratory compacted specimens

Visual inspection of Figure 32 reveals that SBS, alone or in combination to PPA, enhances the material's mechanical responses, regardless of the test conditions and test method. It is also shown that the fracture properties of mixtures containing Elvaloy+PPA are not significantly different from the mixtures containing only PPA.

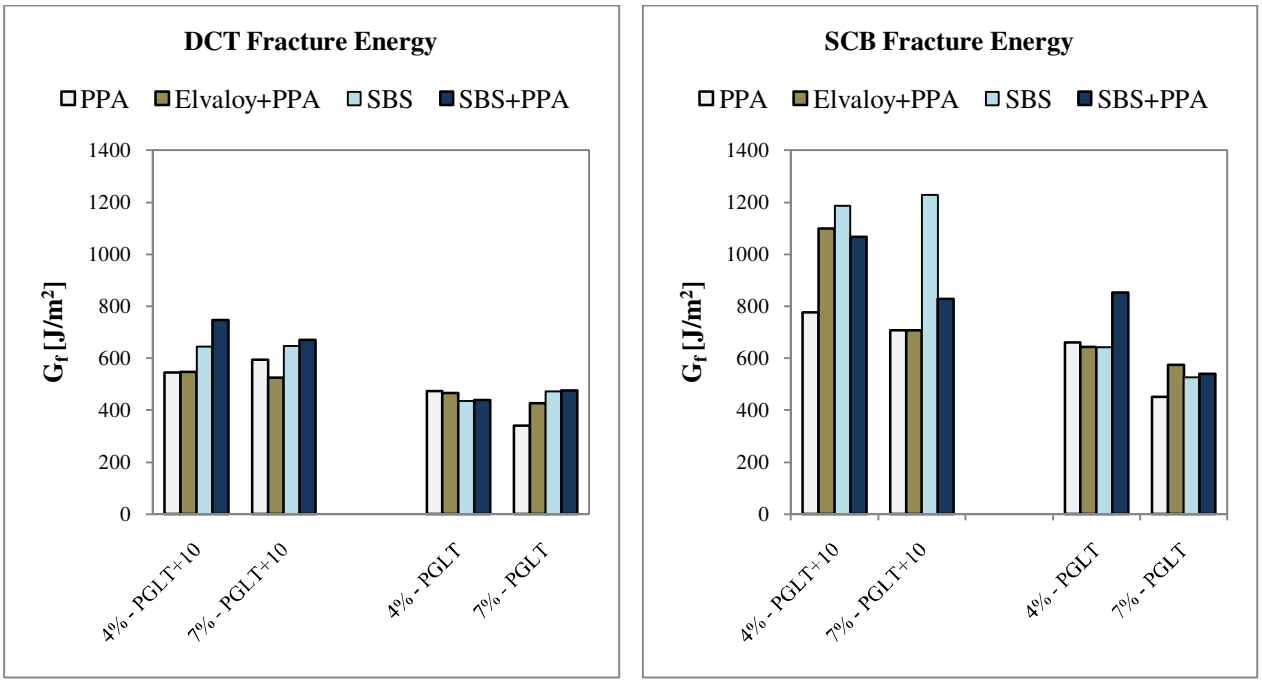

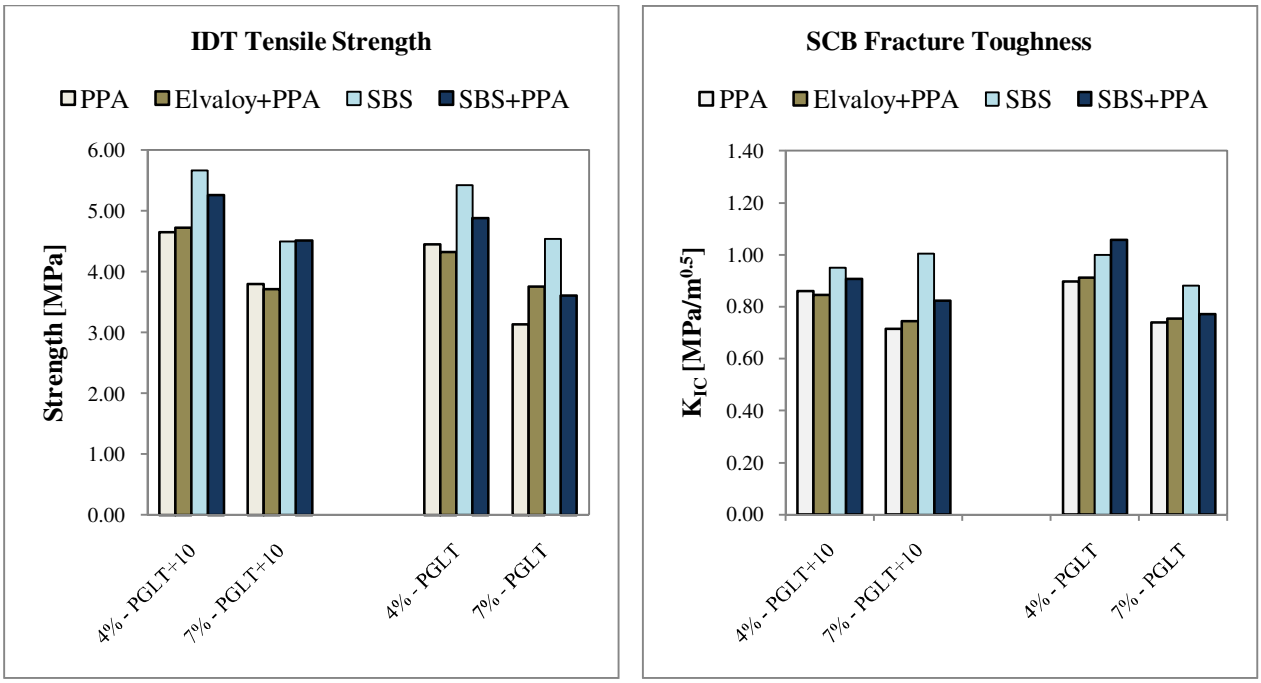

Figure 32. Effect of polymer and acid modifiers on DCT, SCB, and IDT tensile strength

The ANOVA, shown in Table 34, indicates that using asphalt modifiers is considered to be significant for all the test parameters: DCT and SCB fracture energy, SCB fracture toughness, and IDT strength.

Table 34. ANOVA evaluating effects of modifiers

Model used for DCT fracture energy is GF=temp+modifiers

SS are Type III sums of squares

	DF	SS	MS	F	P-value
CONSTANT	1	1.2209e+07	1.2209e+07	2308.13342	< 1e-08
temp	1	3.539e+05	3.539e+05	66.90404	< 1e-08
modifiers	3	77711	25904	4.89698	0.0055308
ERROR1	39	2.063e+05			

Model used is SCB fracture energy log(GF)=void+temp+modifiers

SS are Type III sums of squares

	DF	SS	MS	F	P-value
CONSTANT	1	1897.4	1897.4	46453.65344	< 1e-08
void	1	0.60762	0.60762	14.87653	0.00043057
temp	1	1.9125	1.9125	46.82436	4.016e-08
modifiers	3	0.42338	0.14113	3.45521	0.02576
ERROR1	38	1.5521	0.040845		

Model used is K_{IC}=void+modifiers

SS are Type III sums of squares

	DF	SS	MS	F	P-value
CONSTANT	1	33.467	33.467	4182.18515	< 1e-08
void	1	0.19104	0.19104	23.87329	1.7013e-05
modifiers	3	0.16512	0.05504	6.87796	0.00076321
ERROR1	40	0.32009	0.0080023		

Model used for IDT strength is Strength=void+temp+modifiers

SS are Type III sums of squares

	DF	SS	MS	F	P-value
CONSTANT	1	897.22	897.22	7126.90887	< 1e-08
void	1	10.803	10.803	85.81134	< 1e-08
temp	1	1.439	1.439	11.43021	0.0016535
modifiers	3	7.8154	2.6051	20.69340	3.4762e-08
ERROR1	39	4.9098	0.12589		

A multiple comparison procedure with error level of 5% was performed on the group means. The outcomes are presented in Table 35.

For DCT fracture energy, SBS and SBS+PPA modified asphalts, increase significantly the material's response, compared to PPA and Elvaloy+PPA modified asphalts. The difference in DCT fracture energy between mixture with SBS and mixtures with SBS+PPA modified asphalt is deemed to be not significant. For SCB fracture energy, SBS, SBS+PPA and Elvaloy+PPA modified asphalts, are statistically equivalent. In addition, all three type asphalt modifiers provide statistically higher SCB fracture energy than PPA alone.

For SCB fracture toughness, SBS and SBS+PPA containing mixtures have higher toughness values than the mixtures containing PPA or Elvaloy+PPA. Finally, the IDT strength confirms that SBS modified mixtures have higher strength values that the mixtures with PPA or with combination of PPA and Elvaloy. In addition, the difference between SBS+PPA and SBS is considered to be significant; SBS alone provides higher material strength.

Table 35. Statistical grouping and ranking of modifiers - labcompcated

Modifier	DCT G_f [J/m^2]		SCB G_f [J/m^2]		SCB K_{IC} [$MPa/m^{0.5}$]		IDT strength [MPa]	
	Group Mean	Rank	Group Mean	Rank	Group Mean	Rank	Group Mean	Rank
SBS	560.89	A/B	834.04	A	0.96	A	5.10	A
SBS+PPA	583.63	A	821.59	A/B	0.89	A/B	4.57	B
Elavaloy+PPA	495.72	B	772.26	A/B	0.81	B	4.19	C
PPA	489.75	B	649.14	B	0.80	B	4.01	C

Effect of asphalt modification on DCT, SCB, and IDT strength of field specimens

In Figure 33, the field mixtures containing acid and polymer modifiers are plotted along with their corresponding laboratory compacted mixtures.

It can be observed that generally SBS or SBS+PPA containing mixtures perform better. This finding is similar to what was observed for the laboratory compacted mixtures.

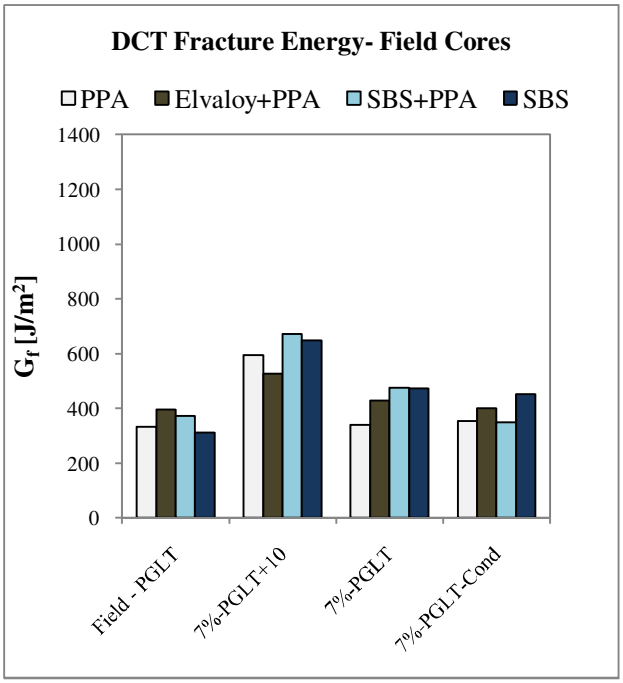

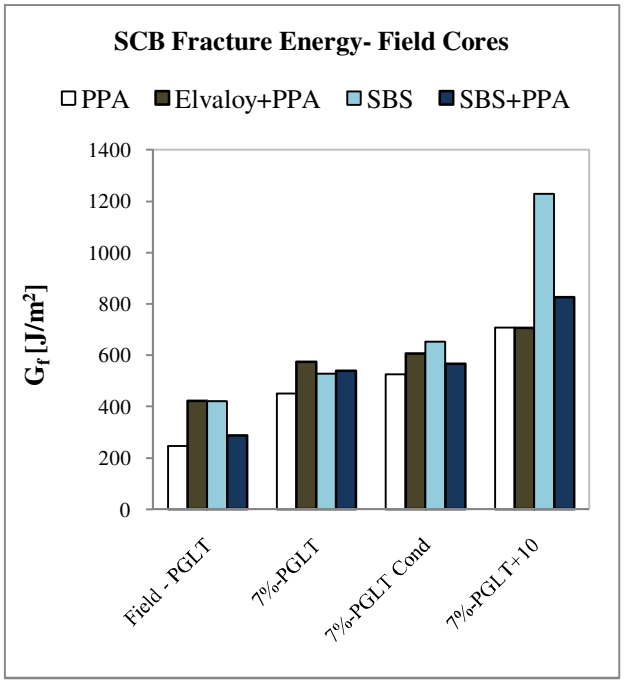

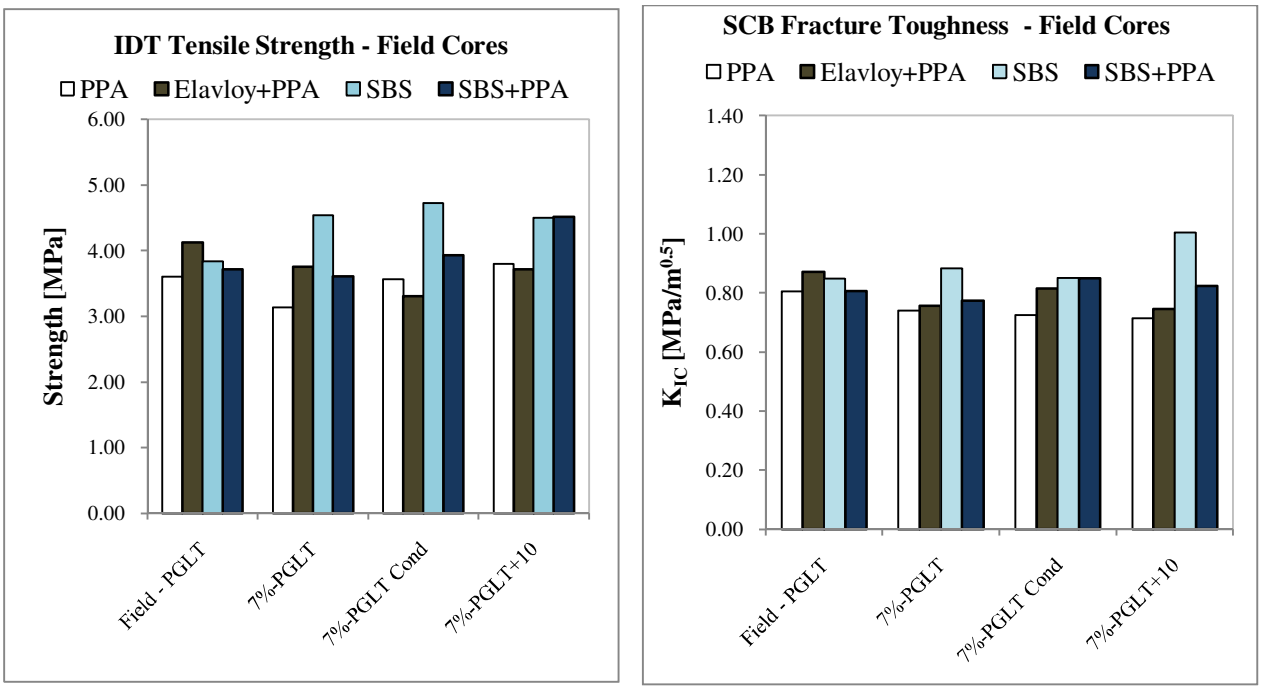

Figure 33. Effect of polymer and acid modifiers on DCT, SCB, and IDT strength – field

However, the effect of asphalt modification on field cored samples, resulted to be significant only for SCB fracture energy. The corresponding ANOVA tables are reported in Table 36.

Table 36. ANOVA evaluating effects of modifiers on SCB fracture energy – field

Model used fro DCT fracture energy is GF=modifiers					
	DF	SS	MS	F	P-value
CONSTANT	1	1.4974e+06	1.4974e+06	183.28357	8.5095e-07
modifiers	3	12500	4166.8	0.51001	0.68643
ERROR1	8	65360	8170		

Model used for SCB fracture energy is GF=modifiers					
	DF	SS	MS	F	P-value
CONSTANT	1	1.1859e+06	1.1859e+06	428.36754	3.1118e-08
modifiers	3	50710	16903	6.10589	0.01827
ERROR1	8	22147	2768.4		

Model used for SCB fracture toughness is KIC=modifiers					
	DF	SS	MS	F	P-value
CONSTANT	1	8.3063	8.3063	1387.68951	< 1e-08
modifiers	3	0.0094789	0.0031596	0.52786	0.6755
ERROR1	8	0.047886	0.0059857		

Model used for IDT strength is Strength=modifiers					
	DF	SS	MS	F	P-value
CONSTANT	1	175.25	175.25	3805.55936	< 1e-08
modifiers	3	0.44722	0.14907	3.23716	0.08173
ERROR1	8	0.36841	0.046051		

For the SCB fracture energy the modifiers are ranked as in Table 37.

Table 37. Statistical grouping and ranking of modified field mixtures

SCB fracture energy [J/m^2]		
Modifier	Group Mean	Rank
SBS	421.29	A
Elvaloy+PPA	301.46	A/B
SBS+PPA	288.36	A/B
PPA	246.34	B

Effects of modified asphalts on IDT creep stiffness of laboratory compacted specimens

The effects of polymer and acid modified asphalt on the stiffness of the mixtures were also investigated through the IDT creep stiffness parameter. Figure 34 compares the results for the different test temperature and void content.

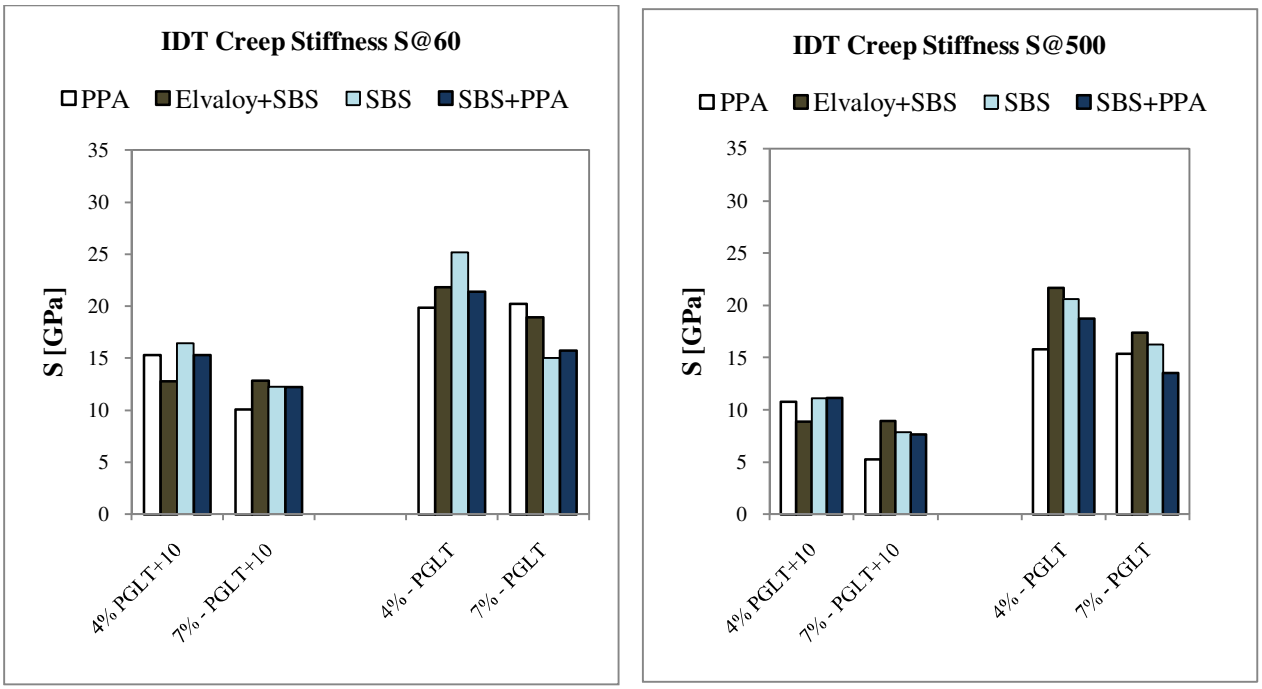

Figure 34. Effect of polymer and acid modifiers on IDT creep stiffness

The plots in the figure appear to suggest that modifiers composed of SBS alone or a combination of SBS and PPA, generally produce materials with higher stiffness values compared to modifiers with only PPA. The effect of Elvaloy is also observed in increased stiffness. However, the differences in stiffness due to varying modifiers are considered not statistically significant, see Table 38.

Table 38. ANOVA evaluating effects of modifiers on IDT creep stiffness

Model used for IDT c.stiffness at 60 sec is log(S60)=void+temp+modifiers

SS are Type III sums of squares

	DF	SS	MS	F	P-value
CONSTANT	1	352.07	352.07	10967.34407	< 1e-08
void	1	0.56943	0.56943	17.73833	0.00013979
temp	1	1.7778	1.7778	55.38072	< 1e-08
modifiers	3	0.040319	0.01344	0.41866	0.74058
ERROR1	40	1.2841	0.032101		

Model used for IDT c.stiffness at 500 sec is lgS500=(void+temp+modifiers)

SS are Type III sums of squares

	DF	SS	MS	F	P-value
CONSTANT	1	288.05	288.05	10833.07310	< 1e-08
void	1	0.82663	0.82663	31.08760	1.865e-06
temp	1	5.19	5.19	195.18503	< 1e-08
modifiers	3	0.2213	0.073768	2.77423	0.053757
ERROR1	40	1.0636	0.02659		

Effects of modified asphalts on IDT creep stiffness of field specimens

The effects of polymer and acid modified asphalt, on specimens cored from the MnROAD cells, were also investigated. The plots in Figure 35, indicate that mixtures containing PPA or Elvaloy+PPA have higher stiffness at 60 sec than mixtures containing SBS or SBS+PPA. However, when stiffness is measured at 500 sec, the difference diminishes.

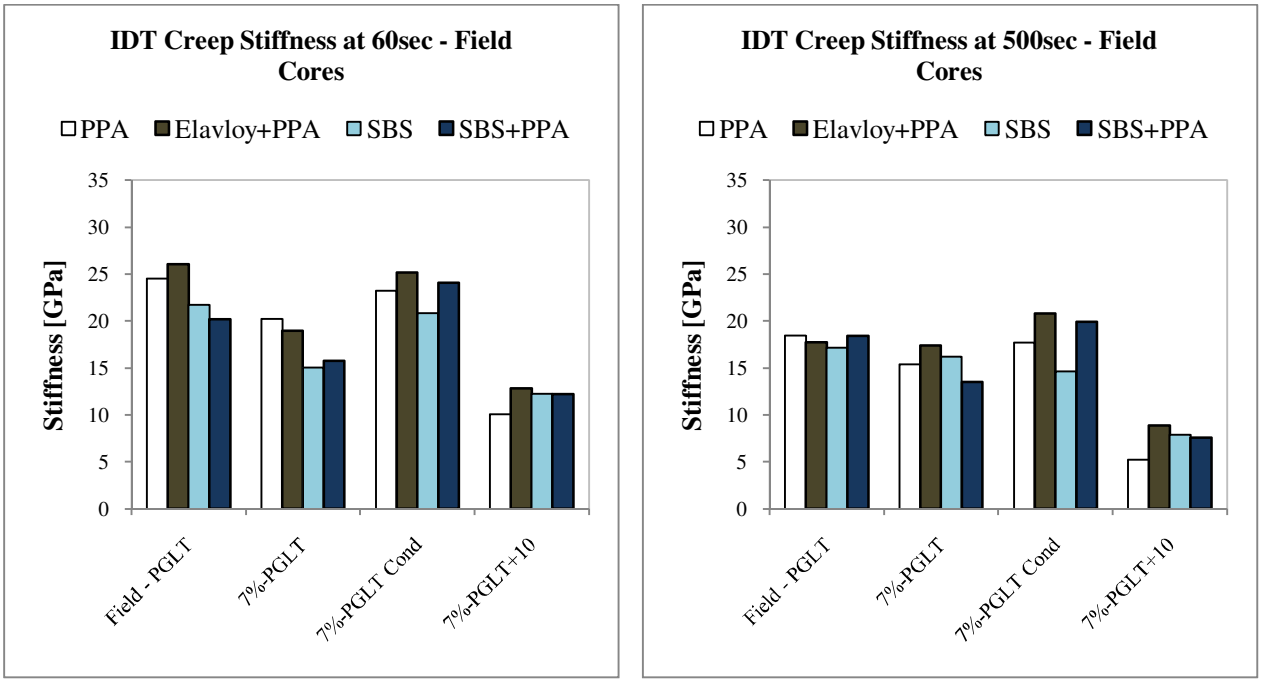

Figure 35. Effect of polymer and acid modifiers on IDT creep stiffness – field cores

The polymer –acid modification treatment, investigated by means of ANOVA (as shown in Table 39), was found to be not significant for both stiffness parameters.

Table 39. ANOVA evaluating effects of modifiers on IDT creep stiffness – field

Model used for IDT c.stiffness at 60 sec is S60=modifiers					
	DF	SS	MS	F	P-value
CONSTANT	1	6544.2	6544.2	478.10268	2.0192e-08
modifiers	3	50.322	16.774	1.22548	0.36195
ERROR1	8	109.5	13.688		

Model used for IDT c.stiffness at 500 sec is S500=modifiers					
	DF	SS	MS	F	P-value
CONSTANT	1	3949.3	3949.3	802.90495	< 1e-08
modifiers	3	4.0864	1.3621	0.27692	0.8406
ERROR1	8	39.35	4.9188		

Effect of RAP fractioning

Next, mixtures containing 30% of non-fractioned RAP were compared to mixtures containing 30% of fractioned RAP. The mixtures selected for this investigation were similar in all aspects, except for the fractioning of RAP. Therefore, results obtained from mixtures 20 and 21were used.

Table 40. Mixtures for RAP fractioning analysis

Mixture	Modifiers
20	Non-fractioned
21	Fractioned

Effects of RAP fractioning on DCT, SCB and IDT for laboratory compacted specimens

Figure 36 summarize the results for RAP fractioning effects. For DCT, the plot appears to suggest an increase in fracture energy due to RAP fractioning. The plot for SCB fracture energy shows mixed behavior. Increase in fracture energy due to fractioning is observed for mixtures tested at PGLT+10˚C. The opposite is observed for mixtures tested at the lowest test temperature. Similar behavior is observed for the IDT strength. The SCB fracture toughness decreases as a result of RAP fractioning.

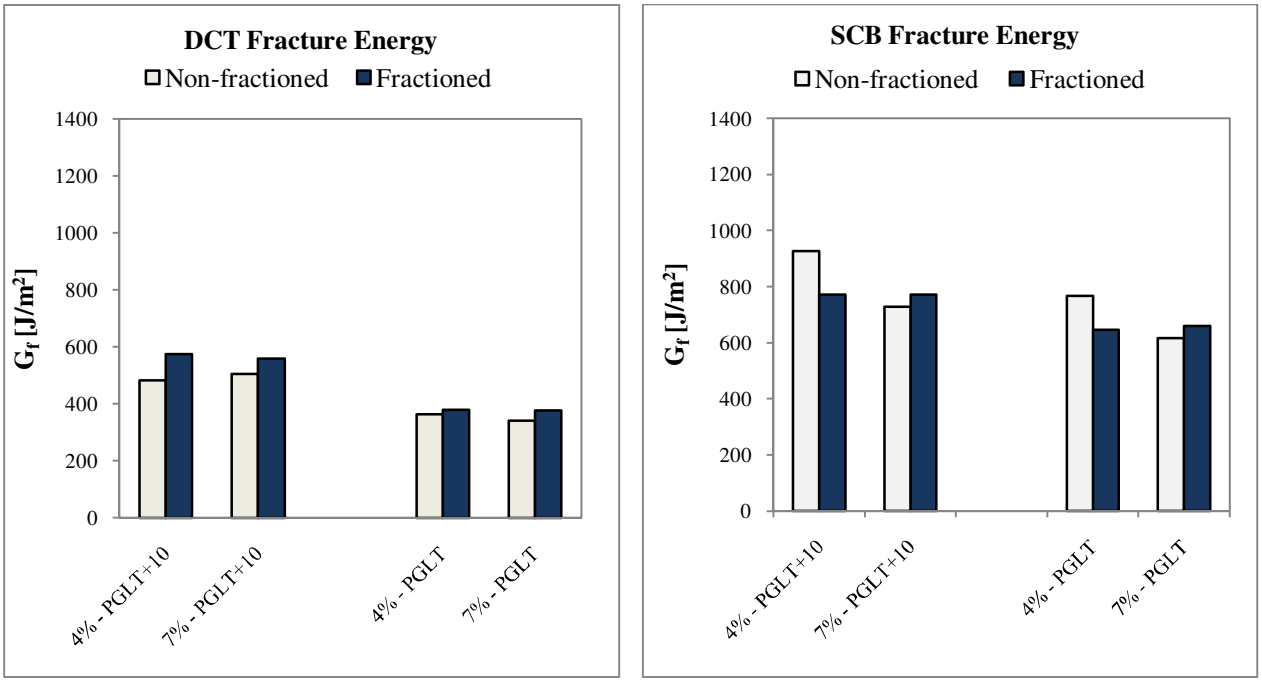

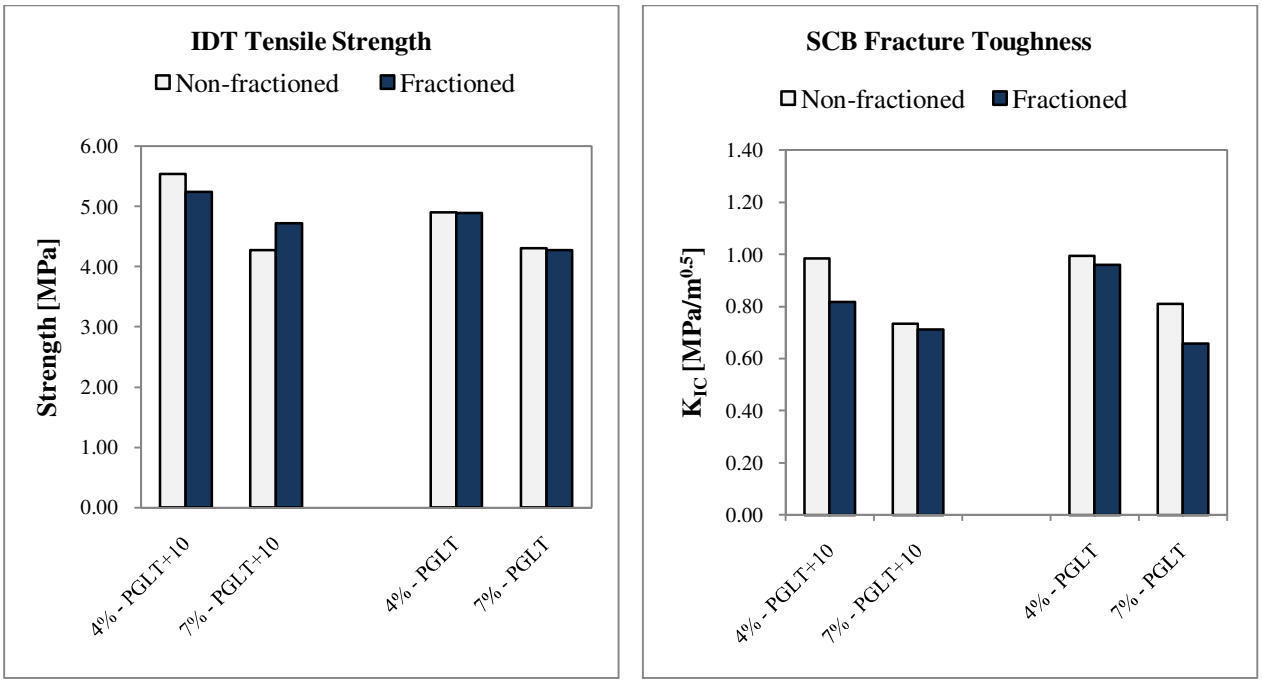

Figure 36. Effect of RAP fractioning on DCT, SCB, and IDT tensile strength

The statistical analysis, shown in Table 41, indicates that only the decrease in fracture toughness observed from the SCB test, is statistically significant.

Table 41. ANOVA evaluating effects of RAP fractioning

Model used DCT fracture energy is log(GF)=void+temp+ fractioning

SS are Type III sums of squares

	DF	SS	MS	F	P-value
CONSTANT	1	1025.8	1025.8	62049.350	< 1e-08
void	1	0.030761	0.030761	1.86068	0.18424
temp	1	0.94786	0.94786	57.33552	4.8815e-08
fractioning	1	0.015162	0.015162	0.91716	0.34704
ERROR1	26	0.42983	0.016532		

Model used is for SCB fracture energy log(GF)= void+temp+ fractioning

SS are Type III sums of squares

	DF	SS	MS	F	P-value
CONSTANT	1	899.58	899.58	21994.44736	< 1e-08
void	1	0.044021	0.044021	1.07629	0.31406
temp	1	0.13636	0.13636	3.33390	0.085483
fractioning	1	0.0097489	0.0097489	0.23836	0.63163
ERROR1	17	0.69531	0.0409		

Model used for SCB fracture toughness is K_{IC}= void+temp+ fractioning

SS are Type III sums of squares

	DF	SS	MS	F	P-value
CONSTANT	1	14.989	14.989	1514.99552	< 1e-08
void	1	0.23921	0.23921	24.17808	0.00011112
temp	1	0.011785	0.011785	1.19114	0.28949
fraction	1	0.046	0.046	4.64943	0.044839
ERROR1	18	0.17809	0.0098938		

Model used IDT strength is Strength= void+temp+ fractioning

SS are Type III sums of squares

	DF	SS	MS	F	P-value
CONSTANT	1	471.32	471.32	8991.37044	< 1e-08
void	1	2.8298	2.8298	53.98366	1.1397e-06
temp	1	0.61284	0.61284	11.69119	0.0032688
fractioning	1	0.025298	0.025298	0.48261	0.49663
ERROR1	17	0.89112	0.052419		

Effects of RAP fractioning on DCT, SCB and IDT for field mixtures

Figure 37, presents the effects of RAP fractioning for the field mixtures. DCT fracture energy increases due to fractioning, regardless of the test condition. SCB fracture energy appears to increase due to RAP fractioning, for mixtures tested at PGLT+10˚C, and to decrease for mixtures tested at the lowest test temperature. The opposite is observed for SCB fracture toughness. For IDT strength, the effect of fractioning is apparent only for mixtures compacted with 7% air void content. These findings are in agreement with what was observed above for the laboratory compacted samples.

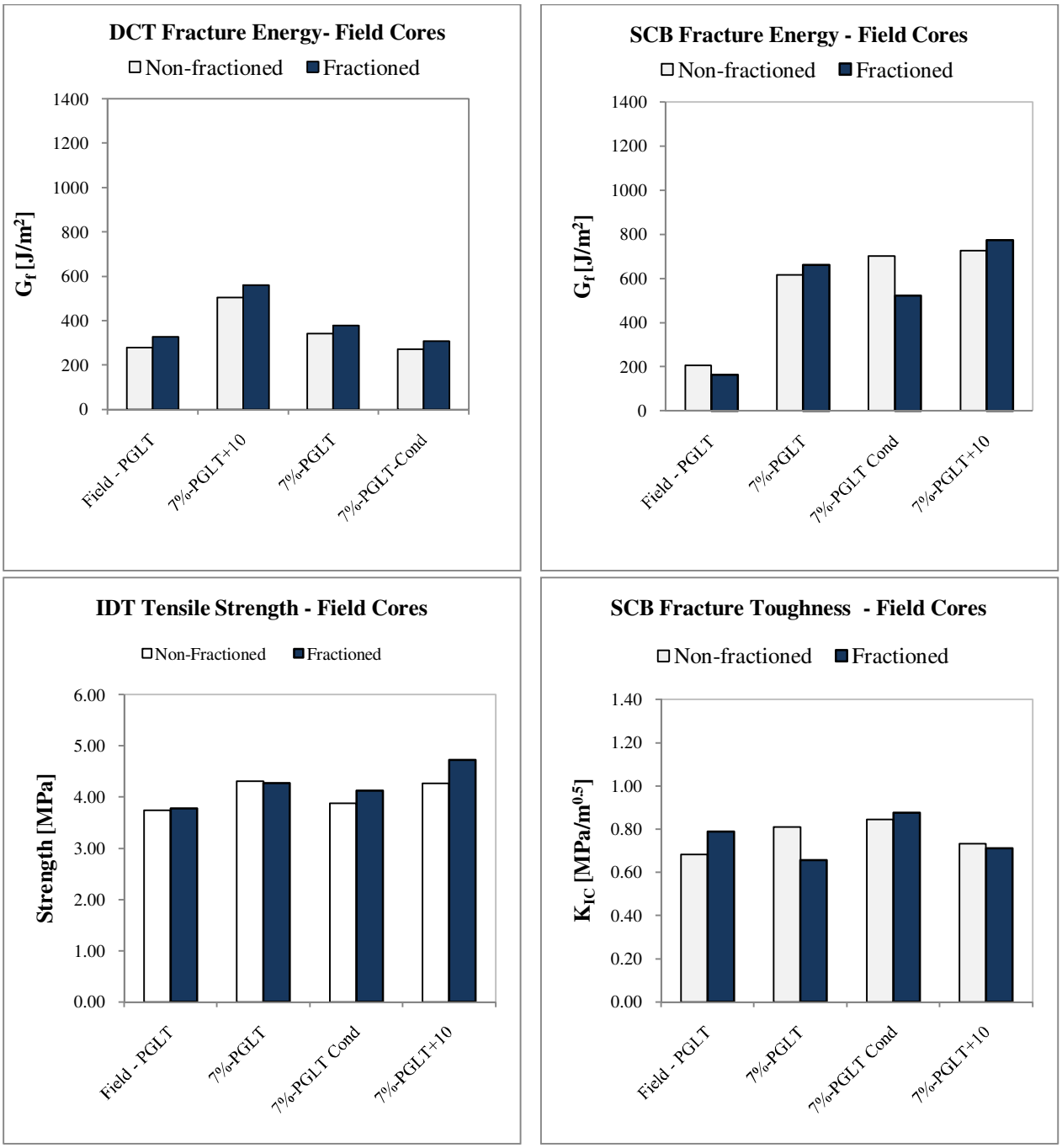

Figure 37. Effect of RAP fractioning on DCT, SCB, and IDT tensile strength –field

The corresponding ANOVA tables are shown in **Error! Not a valid bookmark self-reference.**. The main effect for RAP fractioning is not significant for DCT and SCB fracture parameters and for IDT strength.

Table 42. ANOVA evaluating effects of RAP fractioning– field

Model used for DCT fracture energy is GF=fractioning					
	DF	SS	MS	F	P-value
CONSTANT	1	5.4783e+05	5.4783e+05	574.94648	1.7942e-05
fractioning	1	3601.5	3601.5	3.77978	0.12378
ERROR1	4	3811.3	952.83		

Model used for SCB fracture energy is log(GF)= fractioning					
SS are Type III sums of squares					
	DF	**SS**	**MS**	**F**	**P-value**
CONSTANT	1	130.24	130.24	11914.92119	1.6951e-06
fractioniong	1	0.068872	0.068872	6.30092	0.086925
ERROR1	3	0.032791	0.01093		

Model used for SCB fracture toughness is log(K_{IC})=fractioning					
	DF	**SS**	**MS**	**F**	**P-value**
CONSTANT	1	0.58702	0.58702	49.10883	0.002183
fractioning	1	0.028609	0.028609	2.39341	0.19675
ERROR1	4	0.047813	0.011953		

Model used for IDT strength is Strength = fractioning					
	DF	**SS**	**MS**	**F**	**P-value**
CONSTANT	1	84.897	84.897	1313.95062	3.4577e-06
fractioning	1	0.001501	0.001501	0.02323	0.88624
ERROR1	4	0.25845	0.064612		

Effects of RAP fractioning on IDT creep stiffness for laboratory compacted mixtures

Figure 38 shows the effect of RAP fractioning on the mixtures' stiffness. The effect of RAP fractioning on the material response is not significant.

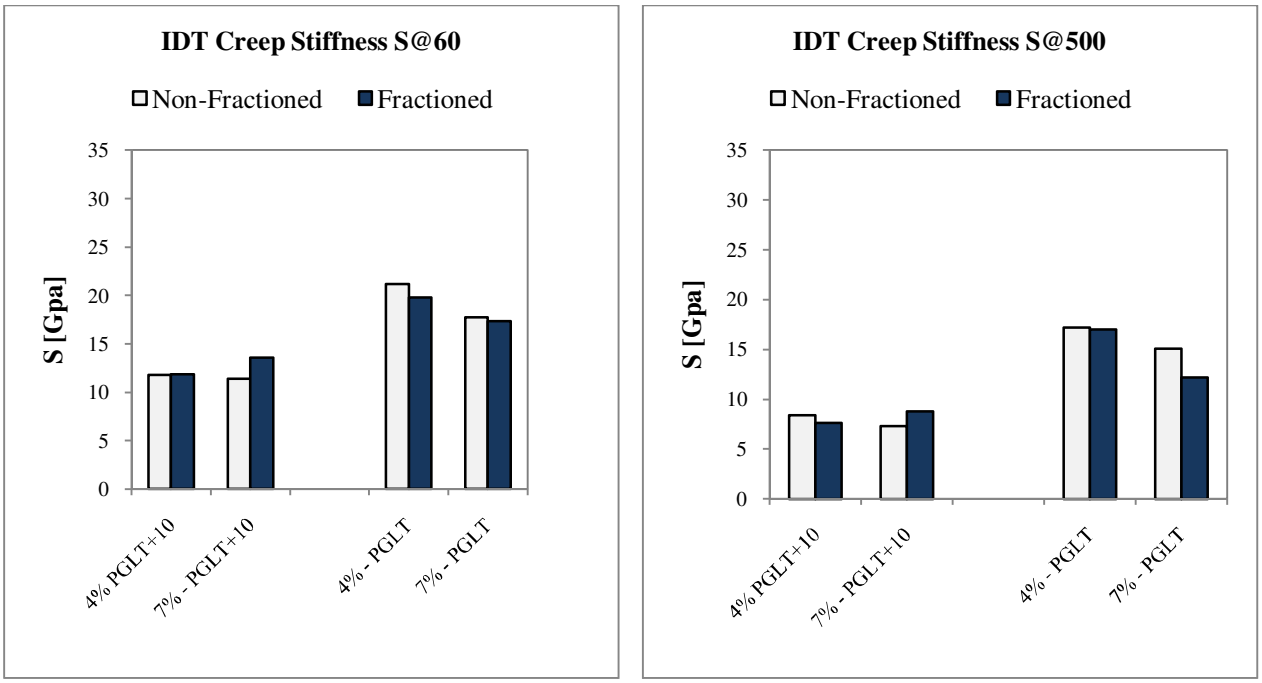

Figure 38. Effect of RAP fractioning on IDT creep stiffness

The corresponding ANOVA tables are presented next. The tables confirms the above stated finding.

Table 43. ANOVA evaluating effects of RAP fractioning on IDT creep stiffness

Model used IDT c.stiffness at 60 sec is S60= void+ temp+ fractioning

SS are Type III sums of squares

	DF	SS	MS	F	P-value
CONSTANT	1	4968.1	4968.1	1193.84147	< 1e-08
void	1	12.024	12.024	2.88930	0.10739
temp	1	240.62	240.62	57.82219	7.2336e-07
fractioning	1	0.052164	0.052164	0.01254	0.91217
ERROR1	17	70.744	4.1614		

Model used for IDT c.stiffness at 500 sec is S500= void+ temp+ fractioning

SS are Type III sums of squares

	DF	SS	MS	F	P-value
CONSTANT	1	2798.2	2798.2	871.46100	< 1e-08
void	1	22.535	22.535	7.01824	0.016869
temp	1	276.49	276.49	86.10978	4.5794e-08
fractioniong	1	3.2303	3.2303	1.00605	0.32992
ERROR1	17	54.585	3.2109		

Effects of RAP fractioning on IDT creep stiffness for field mixtures

The results for RAP fractioning, with regard to creep stiffness computed from test results of field cored specimens are presented in Figure 39. The plots indicate that the effect of RAP fractioning on the IDT creep stiffness is minimal.

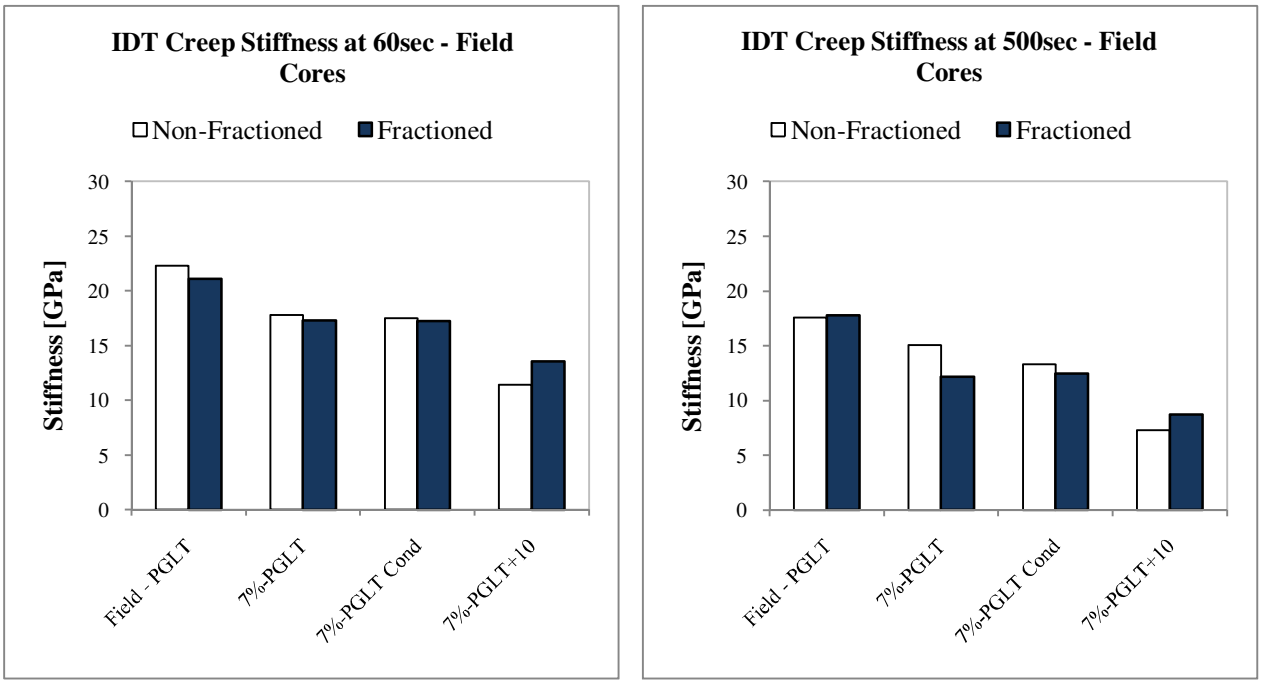

Figure 39. Effect of RAP fractioning on IDT creep stiffness -field

Effects of binder PG low limit

To conclude the investigation, the effects of binder's PG low limit were analyzed. The mixtures considered for this part of analysis are reported in Table 44. These are plain mixtures, both containing 30% of fractioned RAP.

Table 44. Mixtures for PG low limit analysis

Mixture	Binder Grade
21	PG 58-28
22	PG 58-34

Effects of binder PG low limit on DCT, SCB and IDT for laboratory specimens

Figure 40 summarize the results for mixtures with different PG low limit. According to the plots, PG 58-28 appears to have a slight edge on PG 58-34 with regard to DCT and SCB

fracture energy. For SCB fracture toughness and IDT tensile strength, the opposite is true: PG 58-34 appear to increase the responses in both test methods. Only SCB fracture energy differences are statistically significant, as reported in Table 45.

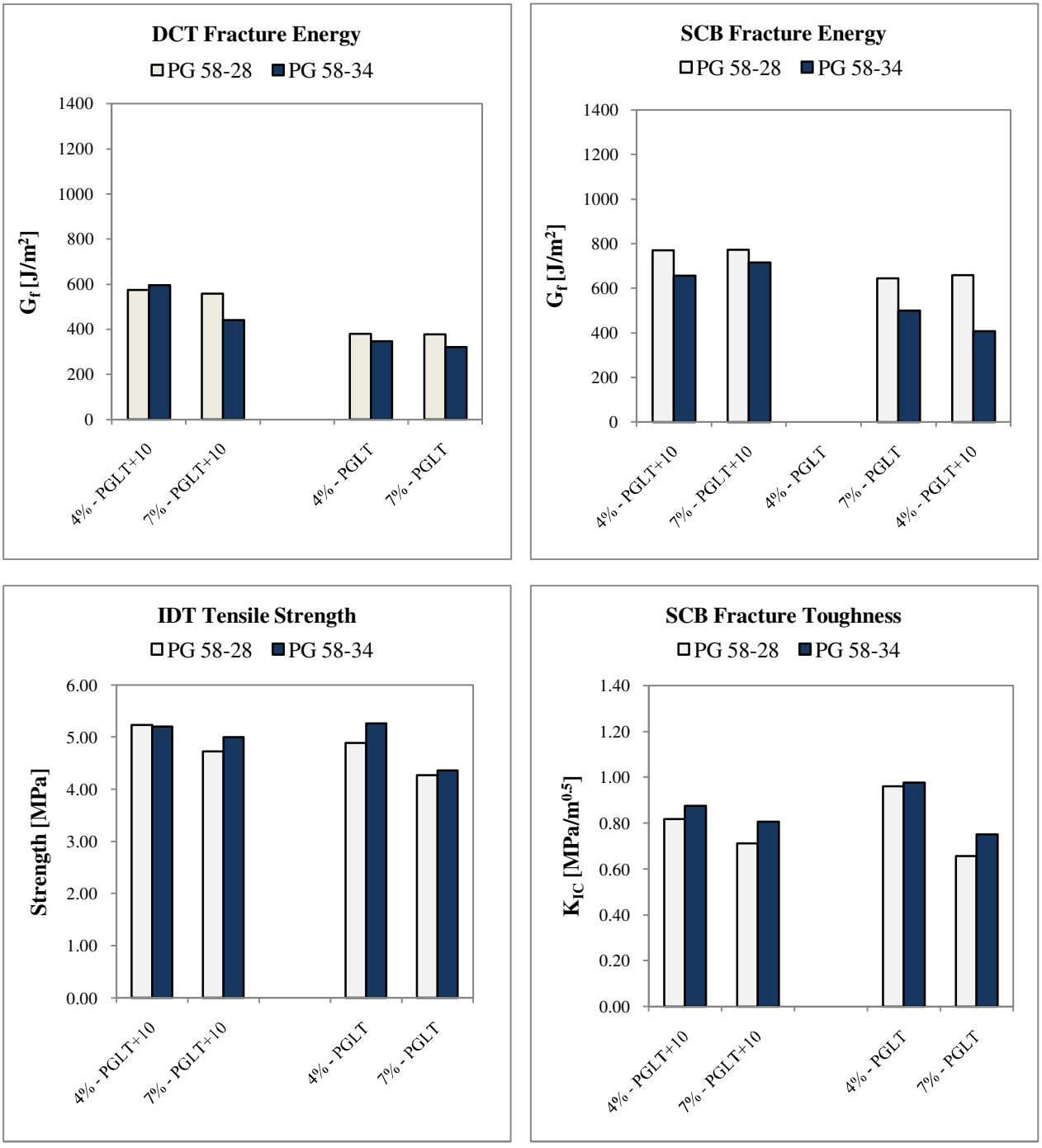

Figure 40. Effect of binder PG low limit on DCT, SCB, and IDT tensile strength

Table 45. ANOVA evaluating effects of PG low limit

Model for DCT fracture energy used is GF=(void+temp+pglt) SS are Type III sums of squares					
	DF	**SS**	**MS**	**F**	**P-value**
CONSTANT	1	4.5228e+06	4.5228e+06	1406.55719	< 1e-08
void	1	19284	19284	5.99730	0.024202
temp	1	1.7874e+05	1.7874e+05	55.58631	4.6964e-07
pglt	1	8041.7	8041.7	2.50092	0.13028
ERROR1	19	61094	3215.5		

Model used for SCB fracture energy is GF= void+temp+pglt SS are Type III sums of squares					
	DF	**SS**	**MS**	**F**	**P-value**
CONSTANT	1	8.4307e+06	8.4307e+06	547.48719	< 1e-08
void	1	856.44	856.44	0.05562	0.81638
temp	1	1.5919e+05	1.5919e+05	10.33771	0.0050783
pglt	1	1.0958e+05	1.0958e+05	7.11616	0.016235
ERROR1	17	2.6178e+05	15399		

Model used SCB fracture toughness is K_{IC}= void+temp+pglt					
	DF	**SS**	**MS**	**F**	**P-value**
CONSTANT	1	16.135	16.135	1443.09930	< 1e-08
void	1	0.18625	0.18625	16.65840	0.00058148
temp	1	0.0068323	0.0068323	0.61108	0.44354
pglt	1	0.026212	0.026212	2.34438	0.1414
ERROR1	20	0.22361	0.011181		

Model used IDT strength is Strength=(void+temp+pglt) SS are Type III sums of squares					
	DF	**SS**	**MS**	**F**	**P-value**
CONSTANT	1	461.84	461.84	6584.40138	< 1e-08
void	1	1.5581	1.5581	22.21350	0.00023446
temp	1	0.72916	0.72916	10.39559	0.0053008
pglt	1	0.18446	0.18446	2.62980	0.12441
ERROR1	16	1.1223	0.070141		

Effects of binder PG low limit on DCT, SCB and IDT for field mixtures

Figure 41 reports the change in the responses of the various test parameters due to varying PG low limit, for field cored samples.

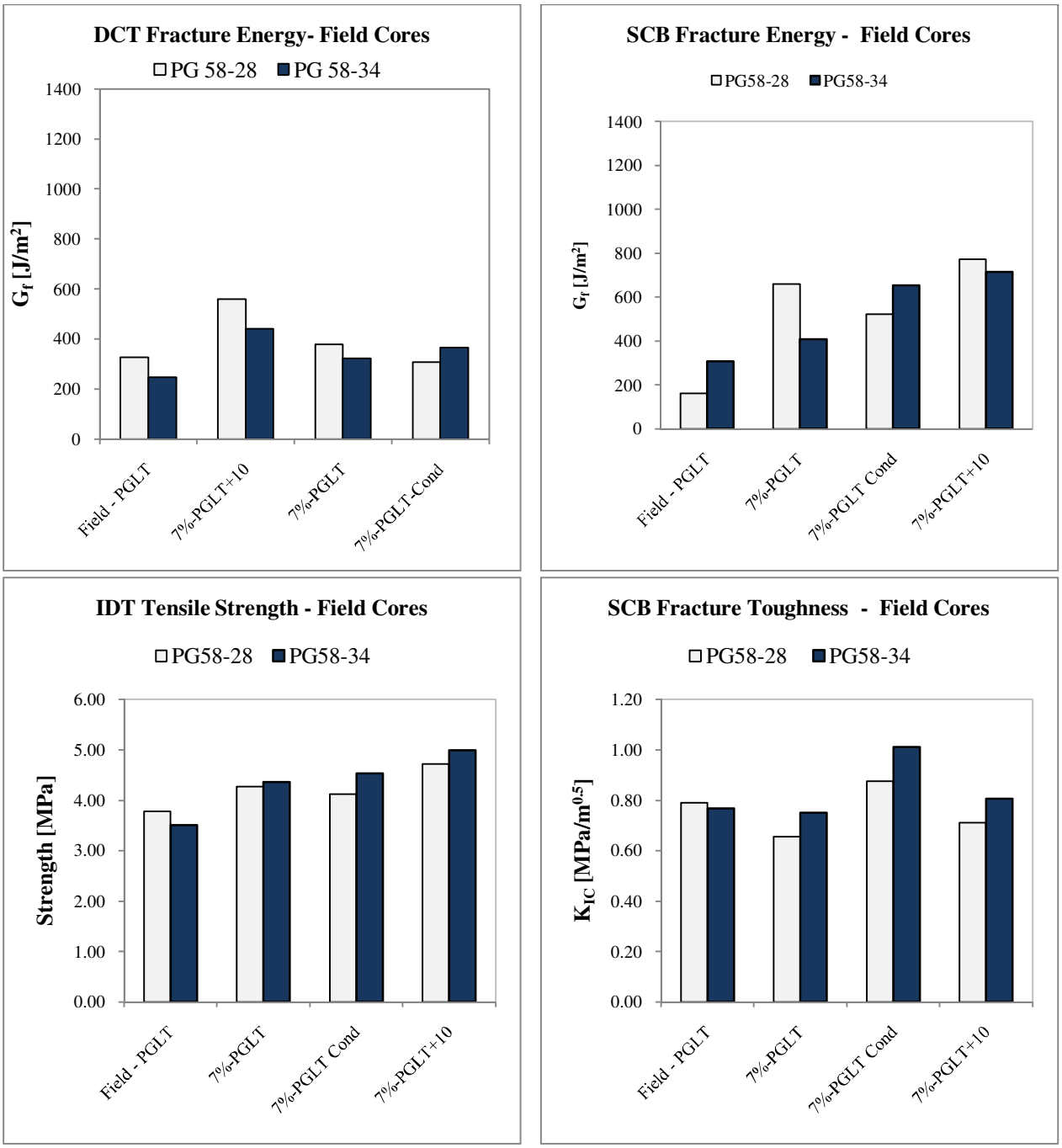

Figure 41. Effect of binder PG low limit on DCT, SCB, and IDT tensile strength -field

The plots appear to indicate mixed behavior for all test parameters. The ANOVA tables however, indicate the binder type is significant only for SCB fracture energy. Accordingly, mixtures with PG 58-34 have higher fracture energy than the PG 58-28 mixture.

Table 46. ANOVA evaluating effects of PG low limit – field

Model used for DCT fracture energy is GF=pglt					
	DF	SS	MS	F	P-value
CONSTANT	1	4.9307e+05	4.9307e+05	353.11530	4.7224e-05
pglt	1	9600	9600	6.87515	0.058673
ERROR1	4	5585.3	1396.3		

Model used for SCB fracture energy is log(GF) = pglt SS are Type III sums of squares					
	DF	**SS**	**MS**	**F**	**P-value**
CONSTANT	1	140.15	140.15	8813.16892	2.6644e-06
pglt	1	0.47425	0.47425	29.82347	0.012065
ERROR1	3	0.047705	0.015902		

Model used for SCB fracture toughness is K_{IC}= pglt					
	DF	**SS**	**MS**	**F**	**P-value**
CONSTANT	1	3.6432	3.6432	459.68121	2.7988e-05
pglt	1	0.00064424	0.00064424	0.08129	0.78971
ERROR1	4	0.031702	0.0079254		

Model used for IDT strength is Strength= pglt					
	DF	**SS**	**MS**	**F**	**P-value**
CONSTANT	1	79.605	79.605	991.10897	6.0673e-06
pglt	1	0.10928	0.10928	1.36061	0.30823
ERROR1	4	0.32127	0.080319		

Effects of binder PG low limit on IDT creep stiffness.

The IDT results are summarized in Figure 42. According to the plots, the stiffness measured at 60sec shows mixed response, while the stiffness at 500sec clearly indicates an increase in stiffness due to using PG 58-34. The increase observed for S(500s) is statically significant as reported in

Table 47.

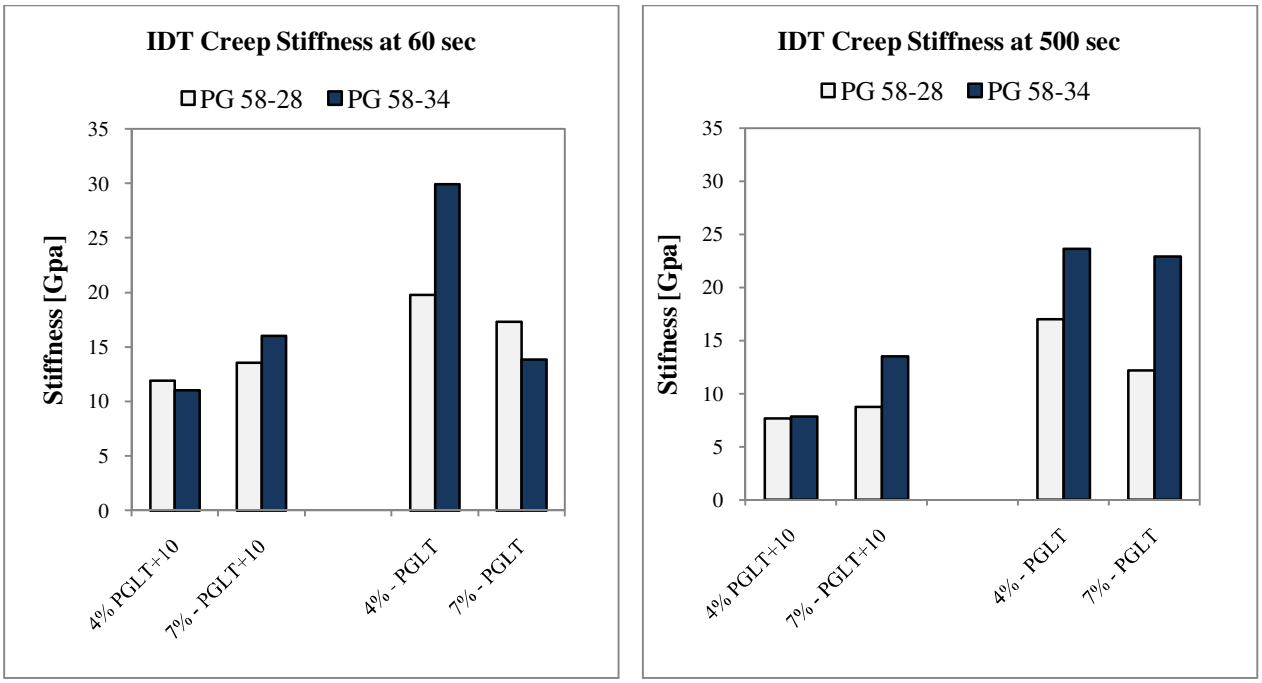

Figure 42. Effect of binder PG low limit on DCT, SCB, and IDT tensile strength

Table 47. ANOVA evaluating effects of PG low limit on IDT creep stiffness

Model used for IDT c.stiffness at 60 sec is log(S60)=(void+temp+pglt)

SS are Type III sums of squares

	DF	SS	MS	F	P-value
CONSTANT	1	142.07	142.07	2182.27402	< 1e-08
void	1	0.081652	0.081652	1.25422	0.28036
temp	1	0.87191	0.87191	13.39315	0.0023234
pglt	1	0.056713	0.056713	0.87115	0.36542
ERROR1	15	0.97652	0.065102		

Model used is for IDT c.stiffness at 500 sec log(S500)=(void+temp+pglt)

SS are Type III sums of squares

	DF	SS	MS	F	P-value
CONSTANT	1	134.42	134.42	2597.14112	< 1e-08
void	1	0.010533	0.010533	0.20351	0.6576
temp	1	2.3537	2.3537	45.47668	3.438e-06
pglt	1	0.83632	0.83632	16.15868	0.0008883
ERROR1	17	0.87987	0.051757		

Effects of binder PG low limit on IDT creep stiffness for field mixtures

Figure 43 summarizes the results for the field mixtures. Similar to the results of the laboratory compacted specimens, the stiffness of the mixtures increases considerably when

PG58-34 is used instead of PG 58-28. From ANOVA, the increase in stiffness at 500s is statistically significant.

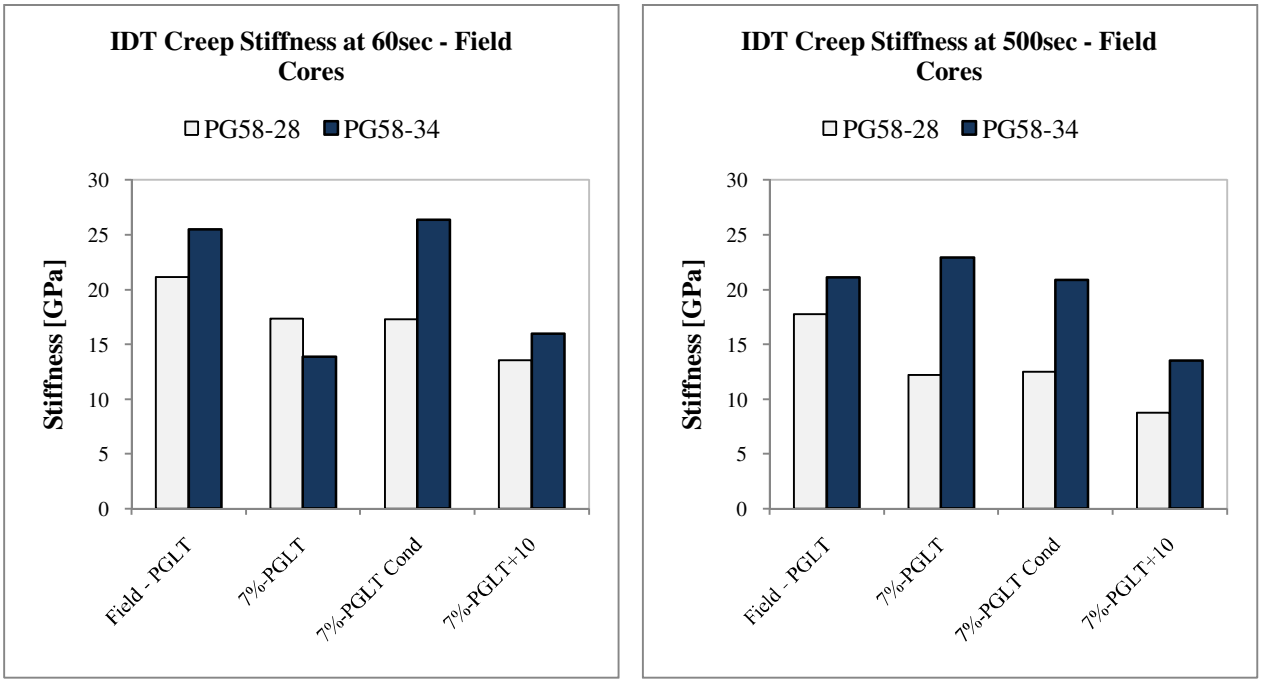

Figure 43. Effect of binder PG low limit on IDT creep stiffness

Table 48. ANOVA evaluating effects of PG low limit on IDT creep stiffness -firld

Model used for IDT c. stiffness at 60 sec is S60=pglt					
	DF	**SS**	**MS**	**F**	**P-value**
CONSTANT	1	3301.1	3301.1	726.12573	1.1276e-05
pglt	1	32.615	32.615	7.17417	0.055317
ERROR1	4	18.185	4.5462		

Model used is S500=pglt					
	DF	**SS**	**MS**	**F**	**P-value**
CONSTANT	1	2205.7	2205.7	1945.18569	1.5803e-06
pglt	1	11.714	11.714	10.33008	0.032464
ERROR1	4	4.5358	1.1339		

4. SUMMARY OF FINDINGS

The main objective of the research investigation was to characterize the low-temperature fracture properties of modified asphalt mixtures by means of traditional and newly developed experimental procedures. The set of mixtures included Recycled Asphalt Pavement (RAP) mixtures, Poly-Phosphoric Acid (PPA) modified mixtures, and polymer modified mixtures (SBS, and Elvaloy). Nine laboratory compacted asphalt mixtures were tested at low temperatures using Indirect Tensile (IDT), Semi-Circular Bend (SCB), and Disc-Shaped Compact Tension (DCT) test protocols. The effect of aging was also investigated by conditioning the mixtures for 5 days at 85˚C. In addition, field specimens cored from MnROAD test cells, were tested and compared to the laboratory asphalt mixtures.

A summary of the findings from the research performed in this task are presented next.

- For the unconditioned laboratory compacted mixtures, the DCT fracture energy values ranged from approximately 190 J/m^2 to 800 J/m^2. The values obtained at PGLT+10˚C were always larger than those obtained at PGLT, except for mixture '*Wisconsin*'. Overall, the effect of the air void content on DCT fracture energy appeared to be minimal.
- The SCB fracture energy values ranged between 300 and 1380 J/m^2. The SCB fracture energy values at PGLT+10˚C were always higher than those at PGLT. The SCB fracture energy decreases when air void content increases.
- The SCB fracture toughness values vary from 0.45 to 1.20 MPa/m$^{0.5}$. For specimens with 4% air void content, the SCB fracture toughness value increased when temperature decreases. Contrarily to fracture energy, the K_{IC} results suggest testing temperature has a minimal effect.
- The IDT tensile strength ranged from 2.30 to 7 MPa. The strength was higher for mixtures with lower air void content. In addition, except for a few mixtures, the strength values obtained at PGLT+10˚C were higher than the values obtained at PGLT. The NY mixture had a significantly higher IDT strength than all the other mixtures with 7% air voids. Please note that this is the mixture that could not be compacted to 4% air voids.
- Multiple comparisons, at 5% level of significance, were performed to compare and rank the laboratory mixtures, according the different test methods. The mixture in cell 35 scored the best and ranked in the first category for all test methods. The mixture from Wisconsin ranked the least favorable out of all mixtures tested (NY mixture was not included in the analysis since it could not be compacted to 4%).
- For field cores, except for the SCB fracture energy, the mixtures are statistically similar. For SCB fracture energy, the best performer was again the mixture from cell 35.
- A comparison between laboratory mixtures and field cores was performed by means of data correlation and correlation plots. The best match was observed for DCT fracture energy. For SCB fracture energy, on the other hand, significantly lower values were obtained for the cores.
- The limited comparison of the results obtained at UMN and UIUC laboratories, respectively, indicated significant differences for both the DCT and SCB test methods.
- Mix conditioning was found significant only for DCT fracture energy and SCB fracture toughness. DCT fracture energy decreased with mix conditioning, and SCB fracture toughness increased with mix conditioning.

- Asphalt modification had a significant effect on fracture properties of laboratory mixtures. A multiple comparison indicates that the SBS modified mixture (cell 35) ranked the best overall.
- For the field cores, however, asphalt modification was significant only for SCB fracture energy. The statistically significant higher fracture energy was again observed for cell 35 mixture.
- The effect of RAP fractioning in laboratory compacted asphalt mixtures was found statistically not significant except for the SCB fracture toughness. For the field cores, RAP fractioning was found insignificant for all test results.
- The effect of PG lower limit was found statistically significant only for SCB fracture energy. For the laboratory mixtures, the PG 58-28 mixture tested at PGLT had higher fracture energy compared to the PG 58-34mixture. The opposite was true for the field cores.

REFERENCES

1. AASHTO. (2002). Mixture Conditioning of Hot Mix Asphalt. Standard Specification for Transportation Materials and Methods of Sampling and Testing. *AASHTO R30-02 Part 1B. American Association of State Highway and Transportation Officials*.
2. Mugurel Turos;Ki Hoon Moon; Mihai Marasteanu. (2010). Air Voids Testing for MnROAD Cells. *St. Paul Minnesota: Minnesota Departement of Transportation*.
3. ASTM D7313-06. (2006). Standard Test Method for Determining Fracture Energy of Asphalt-Aggreagte Mixtures Using the Disk-Shaped Tension Geometry. *American Society for Testing and Materials, Philadelphia* .
4. Wagoner, M., Buttlar, W., & Paulino, G. (2005). Disk-shaped compact tension test for asphalt concrete fracture. *Experimental Mechanics, Vol. 45, No. 3* , 270-277.
5. Li, X., & Marasteanu, M. (2004). Evaluation of the Low Temperature Fracture Resistance of Asphalt Mixtures Using the Semi Circular Bend Test. *Association of Asphalt Paving Technologists, No. 73* , 401-426.
6. Marasteanu, M., Zofka, A., Turos, M., Li, X., Velasquez, R., Li, X., et al. (2007). National Pooled Fund Study 776 - Investigations of Low Temperature Cracking in Asphalt Pavements. *St. Paul, MN: Mn/DOT*.
7. AASHTO T322-03. (2003). Standard Method of Test for Determining the Creep Compliance and Strength of Hot-Mix Asphalt (HMA) Using Indirect Tensile Test Device. *American Association of State Highway and Trasportation Officials* .